Innate Immune Dysfunction as a Driver of Impaired Neurodevelopment

Catherine Rose Lammert
Glenburn, ME

B.S. Neuroscience, Stonehill College, 2012

A Dissertation presented to the Graduate Faculty of the University of Virginia Candidacy for the Degree of Doctor of Philosophy

Department of Neuroscience
University of Virginia

August, 2020

Dedication and Acknowledgements

Nothing is ever accomplished alone, and that is especially true in graduate school. A lot of people have contributed to getting me to the finish line of graduate school and I would like to acknowledge a few of them here.

First, to my mentor, **John Lukens.** Every success I have had in graduate school would not have been possible without you. Your kindness, generosity, intelligence, and empathy have made you such a great mentor. Thank you for believing in me, teaching me to be a better scientist, for your guidance and support these past five years, and for being the best role model. The road to a Ph.D. is a long one with many ups and downs, but throughout it all I have never once felt unsupported.

I would also like to acknowledge my committee: Drs. **Jonathan Kipnis**, **Sarah Kucenas**, **Javier Provencio**, and **Scott Zeitlin**. Thank you for all your support, insight, and for the fun and engaging scientific conversations. When I first started graduate school committee meetings were intimidating; however, leaving graduate school they are something I will miss.

To my lab members: thank you for your comradery, for your countless hours of help, and for the laughs; graduate school would have been a lot less fun without all of you. To past members **Celia McKee, Matthew Paysour, Mariah Hurt, Calli Bellinger,** and **Muhannah Hossain** thank you for all of your help moving my projects forward. To **Elizabeth Frost**, thank you for being my go-to lab person for laughs, cries, and everything in between, Thank you for your patience, never-ending support, and friendship. I am so glad I didn't have to go through graduate school without you. To **Ashley Bolte,** thank you for always being a calming presence in the lab; your hard work, intelligence, perspective, and friendship has kept me motivated and grounded. To **Hannah Ennerfelt** and **Kristine Zengeler** thank you for your friendship and support, and for always agreeing to edit, I am glad I was able to get to know and work with both of you.

To all the members of the **BIG center**, thank you for the sense of community. Thank you for your willingness to help and for always pushing me to be a better scientist and think more deeply. Being surrounding by such brilliant and motivated scientists has kept me inspired.

To the current and past directors of the NGP**: Manoj Patel, Chris Deppmann,** and **Alban Gaultier** and to **Nadia Cempre:** Thank you for the all your hard work and dedication to the trainees.

To my friends near and far. Thank your friendship and for making life outside of work full of adventure, fun, and laughter.

To my family: My dad and mom, **Steve and Mary Lammert.** Thank you for always believing in me, encouraging me, and supporting me. Thank you for your unconditional love, for teaching me to be independent, and for being incredible role models. You are the best parents and I would not be the person I am today without you. To my sisters and best friends: **Sara and Molly**. You are both brilliant, kind, and strong women who I have always looked up to. Thank you for your

friendship, love, and support. **To Silas**: Thank you for being a constant source of light, love, laughter, and adventure. Your perspective, joy, and patience has kept me going throughout graduate school. I love you all and dedicate this work to you.

Table of Contents

List of Figures

Chapter 1

Chapter 2

Chapter 3

Chapter 4

Chapter 5

Chapter 6

None.

Appendix 1

List of Abbreviations

Abbreviations	Definitions
Aβ	Amyloid beta
AD	Alzheimer's disease
AIM2	Absent in melanoma 2
ASC	Apoptosis-associated speck-like protein containing a CARD
ASD	Autism spectrum disorder
ATM	Ataxia-telangiectasia mutated
ATP	Adenosine triphosphate
ATR	Ataxia-telangiectasia and Rad3-related
CARD	Caspase recruitment domain
CNS	Central nervous system
CRS	Congenital rubella syndrome
CSF	Cerebrospinal fluid
DAMPs	Danger associated molecular patterns
DDR	DNA damage response
dsDNA	Double stranded DNA
EAE	Experimental autoimmune encephalomyelitis
EE	Environmental enrichment
GFAP	Glial fibrillary acidic protein
HFD	High fat diet
HR	Homologous recombination
IFI16	Interferon-inducible protein 16
IL-1α	Interleukin 1 alpha
IL-1β	Interleukin 1 beta
IL-1R	IL-1 receptor
IL-1R2	IL-1 receptor 2
IL-1RAP	IL-1 receptor accessory protein
IL-17	Interleukin 17
IL-6	Interleukin 6
IHC	Immunohistochemistry
LI	Latent inhibition
LPS	Lipopolysaccharide
LRR	Leucine rich repeat
LT	Lethal toxin
LTP	Long term potentiation
MAA	Maternal allergic asthma
MAPK	Mitogen-activated protein kinase
MHC-1	Major histocompatibility complex 1
MIA	Maternal immune activation
MRN	Mre11-Rad50-Nbs1
MYD88	Myeloid differentiation primary response protein
MS	Multiple sclerosis
NF-κB	Nuclear factor κB
NHEJ	Non-homologous end joining
NLRs	Nod like receptors

OVA	Ovalbumin
PAMPs	Pathogen associated molecular patterns
PD	Parkinson's disease
PDD-NOS	Pervasive developmental disorder not otherwise specified
Poly(I:C)	Polyinosinic:polycytidylic acid
PPI	Pre-pulse inhibition.
PRR	Pattern recognition receptors
PYD	Pyrin domain
PYHIN	Pyrin and HIN
PV	Parvalbumin
ROS	Reactive oxygen species
RPA	Replication protein A
SCI	Spinal cord injury
S1DZ	Primary somatosensory cortex dysgranular zone region
SNPs	Single nucleotide polymorphisms
TBI	Traumatic brain injury
TIR	Toll/IL-1
TLRs	Toll like receptors
TNF-α	Tumor necrosis factor alpha
TopBP1	Topoisomerase II binding protein 1

Chapter 1: Introduction

This thesis is the cumulation of my studies into how the innate immune system affects neurodevelopment. Throughout my graduate career, I have investigated both how lack of innate immune signaling and how overactive immune signaling are detrimental to neurodevelopment. As with most biological systems, neurodevelopment requires a careful balance of immune signaling in order to establish and maintain properly formed connections and functions.

In this chapter, I will introduce how the innate immune system is known to function in the central nervous system (CNS), particularly in response to injury and disease. I will then discuss the process of neurodevelopment and how faulty recognition and clearance of DNA damage can lead to cognitive disorders through overactive cell death and cytokine production. I will then focus on factors that contribute to autism spectrum disorder (ASD) with a focus on how a hyperinflammatory environment during pregnancy can contribute to abnormal neurodevelopment in offspring. Finally, I will provide a summary of these principles as rationale for my thesis work.

The innate immune system in the central nervous system

Science has taught us much about the ways in which the human body functions; however, we still lack a deep understanding of the brain. The brain is an essential organ that interprets information from the world to enable functions such as movement, emotion, and memory and also coordinates internal organ function. Being an essential organ, there are many defensive barriers that surround and protect the CNS from endogenous and exogenous threats. Studies performed in the mid-20th century gave rise to the idea that these protective layers result in the brain being an immune privileged site[1]. However, more recent studies have shown that immune functions in the CNS are important not just in response to pathogens, but also in homeostatic conditions[2]. As our knowledge about the delicate interaction between the immune system and

the CNS expands, it is becoming more apparent that immune functions within the CNS are important for maintaining CNS homeostasis; moreover, these immune pathways and molecules often function differently from peripheral tissues making the immune system within the CNS unique.

The body is protected from infectious agents and harmful toxins by a variety of cells and molecules that together make up the immune system. The immune system has evolved to detect certain structural features of pathogens that mark it as “non-self,” or different from host cells. The immune system is comprised of two general arms that recognize pathogen-derived, toxic, or allergenic structures: the innate and adaptive immune system.

On the frontlines of the broader immune response is the innate immune system. The innate immune system is a rapid coordinated cellular defense response to eliminate both sterile and infectious threats. The innate immune system recognizes these pathogenic agents through pattern recognition receptors (PRRs) that sense pathogen-associated molecular patterns (PAMPS) and danger-associated molecular patterns (DAMPS). PRRs in the CNS are mainly expressed by microglia, astrocytes, and infiltrating macrophages; however, other CNS resident cells such as endothelial cells, neurons, and oligodendrocytes have been reported to express these receptors[3, 4]. Toll-like receptors (TLRs) are membrane-bound PPRs that sense signals from the extracellular environment while Nod-like receptors (NLRs) are cytosolic receptors. A key feature in the initiation of many inflammatory responses is the activation of the inflammasome. Historically, inflammasomes have been mostly studied in the context of peripheral infection. However, accumulating studies point to the important roles of the immune system in the CNS, and these molecules have been implicated in CNS homeostasis, injury, and disease.

The second set of responses constitutes the adaptive immune response. Due to the fact that the adaptive system contains only small numbers of cells with a high specificity for an individual pathogen, toxin, or allergen, the responding cells must proliferate after encountering the antigen in order to mount an effective response. Thus, the adaptive response is generally fully activated after the innate response. Moreover, a key feature of the adaptive response is the ability to manifest memory as well as its ability to mount more rapid responses following a secondary encounter with cognate antigen. Despite the important role of the immune system in clearance of pathogens, excessive and/or dysregulated inflammation can cause damage to healthy tissues through production of cytokines, reactive oxygen species (ROS), and growth factors by both adaptive and innate immune cells[5].

Inflammasomes

Inflammasomes are large multi-protein complexes activated through both endogenous and exogenous danger signals that are recognized by certain receptors. Inflammasomes are assembled by the complexing of three main components: a cytosolic receptor, the enzyme Caspase-1, and the adaptor protein, apoptosis-associated speck-like protein containing a CARD (ASC), that enables the interaction between the two. Although some inflammasomes, such as NLRC4 and NLRP1b do not require ASC in order to assemble the complex, ASC is seen to contribute to optimal activation of Caspase-1 and cytokine release[6-8].

Upon inflammasome formation, Caspase-1 becomes active and cleaves the inactive forms of IL-18 and IL-1β into their biologically active forms. Activated Caspase-1 will also incite an inflammatory form of cell death, commonly referred to as pyroptosis, through its cleavage of Gasdermin-D (GSDMD). Upon cleavage, the N terminus of GSDMD oligomerizes and perforates the plasma membrane, resulting in cell swelling, lysis, and cytokine release[9, 10] (Figure

1.1). Released IL-1β and IL-1α both signal through receptors that contain an extracellular immunoglobulin domain and an intracellular/cytoplasmic Toll/IL-1 (TIR) domain. A response is induced when an IL-1 receptor binds a ligand and this interaction promotes the recruitment of a second receptor, the IL-1R accessory protein (IL-1RAP). The formation of this receptor heterodimer is what enables the recruitment of myeloid differentiation primary response protein (MYD88) and other signaling intermediates that ultimately result in the activation of nuclear factor-κB (NF-κB) and mitogen-activated protein kinase (MAPK) pathways[11]. Upon recognition of toxic stimuli, the mRNA expression levels of *Il1α* and *Il1β* are upregulated within minutes[12].

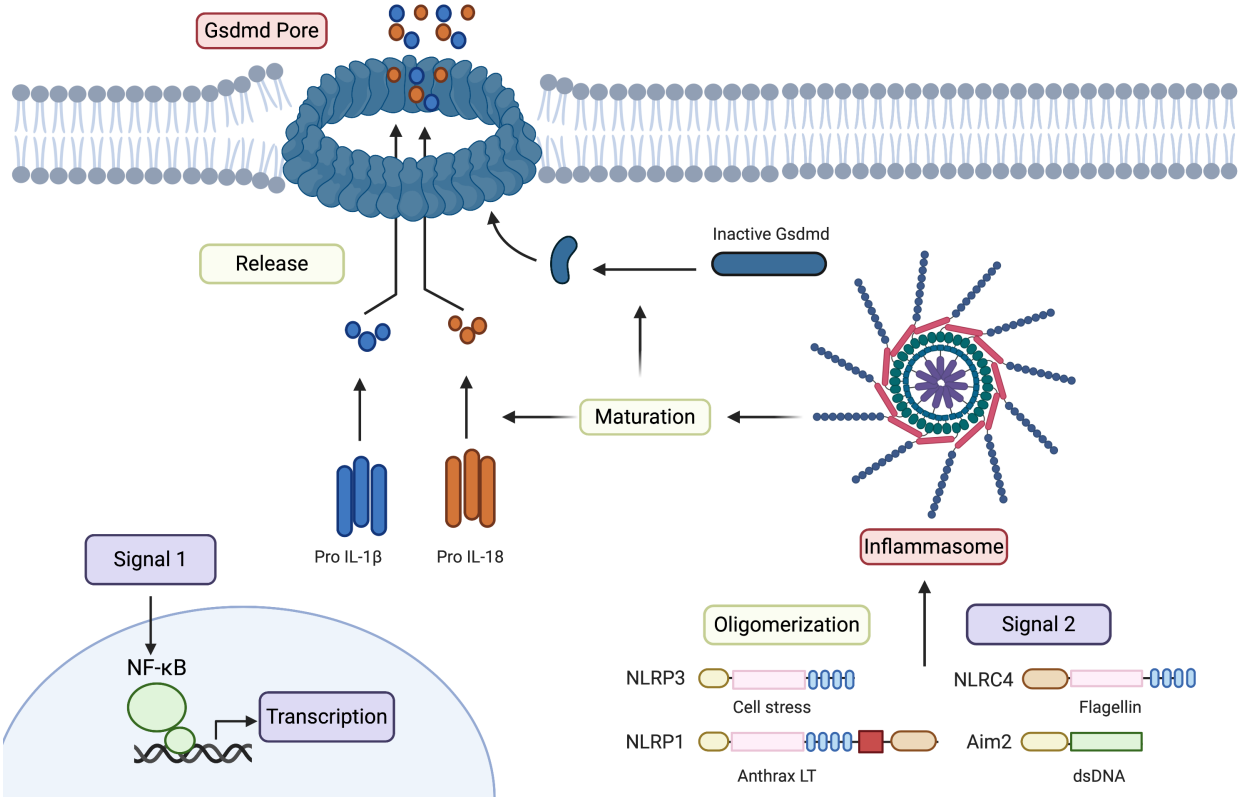

Figure 1.1. Inflammasome activation. Inflammasomes are assembled in response to host-derived insults or pathogens. Often preceding the assembly of the inflammsome complex is a priming stimulus (signal 1) which acts through the nuclear factor-κB (NF-κB) pathway to upregulate the expression of NLRP3 and pro-interleukin 1β (Pro-IL-1β). Upon activation of an upstream inflammasome sensor (signal 2), the cytosolic sensors oligomerize to form the inflammasome. Through its protease activity Caspase-1 cleaves Pro-IL-1β and Pro-IL-18 into their mature forms. Caspase-1 also cleaves inactive Gsdmd. Once activated, Gsdmd will form pores in the membrane of the cell, inciting a lytic form of cell death known as pyroptosis.

Although there are multiple sensors that can induce inflammasome activation they all belong to either the NLR family of proteins or the pyrin and HIN domain (PYHIN) family of proteins. The NLRs contain a carboxy-terminal leucine rich repeat (LLR) domain, a preserved NACHT domain, which is necessary for protein oligomerization and nucleotide-binding that enable the formation of multiprotein inflammasome complexes, as well as a variable amino-terminal domain that defines several NLR subfamilies. The PHYIN-containing inflammasomes comprise interferon-inducible protein 16 (IFI16) and absent in melanoma 2 (AIM2).

NLRP1 inflammasome

The NLRP1 inflammasome was the first to be identified; however, its function remains poorly understood due to uncertainty of a specific ligand, substantial divergence between human and mouse homologs, and the complexity of its domain structure[13]. The murine orthologues of human *NLRP1* are *Nlrp1a, Nlrp1b,* Nlrp1c[14]*.* Murine NLRP1 activation occurs in response to anthrax lethal toxin (LT) in *Bacillus anthracis* and is also thought to be activated in response to *Toxoplasma gondii* in rats, although the mechanism of this activation remains unclear[14, 15]. In addition to sensing microbial stimuli, NLRP1 activation in response to reductions in cellular ATP have also been proposed[16]. Although its ability to respond to anthrax LT has not been confirmed in humans, multiple gene association studies in humans have implicated that mutations in *Nlrp1* can result in an increased susceptibility to CNS disorders such as bacterial meningitis and Alzheimer's Disease (AD)[17, 18].

NLRC4 inflammasome

The NLRC4 inflammasome is activated in response to bacterial pathogens, such as *Salmonella typhimurium* and is able to bind both bacterial flagellin and PrgJ, a secreted

component of bacteria[19, 20]. *NLRC4* expression levels can be upregulated in response to pro-inflammatory stimuli as well as p53 activation mediated by genotoxic stress[21, 22]. A unique aspect of the NLRC4 inflammasome is its ability to complex directly with Caspase-1, where as other major inflammasome sensors require ASC to activate Caspase-1. Accumulating evidence demonstrates the NLRC4 inflammasome to be a critical component in the body's defense against both systemic and enteric pathogens. The NLRC4 inflammasome has also been shown to drive human diseases such as an autoinflammatory disease known as Macrophage activation syndrome through gain-of-function mutations[23-26]. In the CNS, the NLRC4 inflammasome has been mostly studied in the context of pathogens that infect microglia. These pathogens, such as *Legionella pneumophila* and *L. monocytogenes,* result in meningitis and encephalitis[23].

NLRP3 inflammasome

The NLRP3 inflammasome is the most widely studied regulator of Caspase-1 activation. This sensor can be activated by a broad array of endogenous and exogenous stimuli including viral, fungal, and bacterial components; endogenous danger signals such as extracellular adenosine triphosphate (ATP), amyloid-β (Aβ), and uric acid crystals; and environmental microparticles[27-31]. In addition, physiological events such as ion fluxes, ROS production, and endosomal rupture can also trigger activation of the NLRP3 inflammasome[32-34]. The ability of NLRP3 to be activated in response to such a diverse range of stimuli enables this inflammasome to be a general sensor of cellular damage and stress. NLRP3 activation requires a two-step activation process: a priming signal, such as lipopolysaccharide (LPS), that initiates the transcription and translation of pro-IL-1β and NLRP3, and a secondary signal, such as ATP, which is required to trigger the formation of the inflammasome complex.

Due to the fact that various stimuli can lead to the activation of the NLRP3 inflammasome, it is the most widely studied inflammasome in neurological diseases. Most studies to date have focused on NLRP3 function in microglia and have shown that molecules present in neurological diseases, such as Aβ and α-synuclein, can activate this inflammasome[35, 36]. In addition, NLRP3 inflammasome activation has been demonstrated in response to ATP released in the context of neurological damage resulting from infection or injury.

AIM2 inflammasome

Unlike NLRP3, which is activated in response to a variety of endogenous and exogenous danger signals, AIM2 has only been shown to be activated in response to double-stranded DNA. AIM2 consists of two major domains, a C-terminal DNA-binding HIN domain and an N-terminal PYD domain that mediates homotypic interactions with ASC. Through its HIN domain, AIM2 binds and senses dsDNA, either self or foreign, that is present in the cytoplasm. Upon binding DNA, an auto-inhibitory interaction between the HIN and PYD domains is lifted, leading to the formation of a complex of AIM2 molecules binding along the DNA strand which results in the recruitment of ASC and Caspase-1.

AIM2 inflammasomes have been reported to be activated in neurons in response to injury and stroke and has also been described to regulate neuronal morphology under homeostatic conditions[37].

Inflammasomes in neurological disease

Inflammasome activation in response to neurological disease and injury is currently a topic of investigation and has been linked to a variety of CNS infections, injury, and neurodegenerative disease. Most research on the contributions of inflammasomes to

neurodegenerative diseases has focused on the importance of the NLRP3 inflammasome, yet other inflammasomes are activated in the CNS in response to injury and infection, as well as in neurodegenerative disease. High levels of the inflammasome associated cytokines, IL-1β and IL-18, are hallmarks of many neurodegenerative conditions and are considered to be crucial for the establishment of a chronic inflammatory environment, leading to neuronal dysfunction and eventually neurodegeneration. In addition, pyroptotic cell death of CNS cells in response to injury or disease contributes to inflammasome driven pathology through the expulsion of DAMPs and other inflammatory signals.

CNS injury

In recent years, mounting evidence using clinical and animal models of brain injury have implicated dysregulated immune signaling in the progression of neurological dysfunction and CNS pathology[38]. Clinical studies demonstrating increased levels of inflammasome components, such as ASC, Caspase-1, NLRP1, and NLRP3 in the cerebrospinal fluid (CSF) after traumatic brain injury (TBI) has resulted in increased efforts to identify the inflammasome-associated signaling events that are engaged in response to brain injury[39, 40]. Additional insights into the timing and importance of inflammasome activation in CNS injury have been gained through mouse models of TBI. For instance, NLRP3-deficient mice have improved recovery post-TBI, and it has been demonstrated that TBI results in an upregulation of inflammasome associated proteins (i.e. NLRP3, ASC, and Caspase-1) and these proteins remain elevated 7 days post-injury[41].

Inflammasome induced cytokines are also upregulated after TBI with levels of IL-1β peaking around 6 hours post-injury and IL-18 levels remaining elevated 7 days after injury[42].

These data suggest that early inflammasome production of IL-1β may be involved in acute inflammation and tissue damage, while inflammasome-driven IL-18 may contribute to the perpetuation of TBI-induced inflammation.

Murine models of other forms of CNS injury have uncovered inflammasome activation as a main driver of inflammatory responses following tissue damage in the CNS. For instance, following spinal cord injury (SCI), spinal neurons increase levels of NLRP1 components and inflammasome assembly. Additionally, blocking the inflammasome through a neutralizing anti-ASC antibody treatment was found to improve histopathological and functional outcomes following SCI[43]. In models of stroke *Nlrp3*$^{-/-}$, *Asc*$^{-/-}$, *Nlrc4*$^{-/-}$, and *Aim2*$^{-/-}$ mice display improved functional recovery[44].

Demyelinating Disease

Multiple sclerosis (MS) is a chronic neuroinflammatory disease. MS is characterized by immune cell infiltration from the periphery into the CNS which promotes inflammation, demyelination, and neurodegeneration. Symptoms of MS can vary from patient to patient but often include fatigue, loss of vision, pain, and impaired coordination. The inflammasome components Caspase-1, IL-18, and IL-1β are reported to be upregulated in both the CSF and blood of MS patients[45, 46]. In addition, *Casp1* expression was shown to be elevated within demyelinating lesions.[47]

MS is modeled in rodents using experimental autoimmune encephalomyelitis (EAE). Studies using both *Nlrp3* and *Asc* knockout mice have indicated that the induction of EAE is dependent on the NLRP3 inflammasome[48, 49]. However, protection against EAE disease progression in these knockout mice was only seen in mild forms of EAE, whereas more

aggressive forms of EAE are not NLRP3 inflammasome-dependent, indicating a complex role for the NLRP3 inflammasome in EAE[46]. Loss of the NLRP3 inflammasome and it's downstream inflammatory cytokines, IL-1β and IL-18, ameliorates the EAE disease course through the reduction of T cell priming and T cell trafficking into the CNS.

Another common method used to study demyelinating disease is the cuprizone model. In this model, demyelination in the corpus callosum is accomplished through oligodendrocyte cell death as a result of mice being fed with the copper chelator, cuprizone. *Nlrp3*-deficient mice that we put on a cuprizone diet showed a delay in the onset of demyelination, oligodendrocyte loss, and neuroinflammation[50]. This protection was also recapitulated in *Casp1* and *Il18* knockout mice. Conversely, *Il1b* knockout mice showed no difference in disease progression comparted to wild type mice but had slower remyelination. These results indicate that the NLRP3 inflammasome and the downstream cytokine signaling impact disease progression and recovery.

Alzheimer's disease

Alzheimer's disease is the most prevalent neurodegenerative disease and is characterized by cognitive impairments and progressive memory loss. Although there is evidence that attributes improper accumulation of both Tau and Aβ to AD to pathology, neuroinflammation is becoming increasingly considered to be another key component of AD progression[51, 52]. Increased levels of pro-inflammatory cytokines are found in the blood and cerebrospinal fluid (CSF) of AD patients, suggesting a critical role for them in disease pathogenesis. Neuroinflammation associated with AD is predominately driven by microglia, whose activation and inflammation can impact other CNS resident cells ultimately leading to

neuronal damage and synaptic loss[53]. Recent clinical studies of AD patients indicate that increased levels of the inflammasome induced cytokine, IL-1β, are found in microglia that are directly surrounding AD plaques[54, 55]. Additionally, gene analysis of AD patients revealed increased expression of the inflammasome-mediated cytokines (IL-1β and IL-18), NLRP3, Caspase-1, and ASC[56].

Accumulating evidence suggests a detrimental role for microglial inflammasome activation in AD. In particular, the NLRP3 inflammasome has been identified as an important contributor to AD pathogenesis. *In vitro* studies have shown that microglial phagocytosis of fibrillar Aβ induces NLRP3 inflammasome activation and IL-1β release[35]. *In vivo,* pharmacological inhibition of Caspase-1 results in reduced Aβ accumulation, CNS inflammation, and cognitive impairment. NLRP3 was recently shown to promote Tau aggregation hyperphosphorylation[57]. The loss of the NLRP3 inflammasome in APP/PS1 mice attenuates long term potentiation (LTP) deficits and spatial memory loss. Deletion of the NLRP3 inflammasome also resulted in decreased Aβ burden, in both the hippocampus and the cortex, as well as reduction in levels of pro-inflammatory cytokines[58]. Accordingly, pharmacological inhibition the NLRP3 inflammasome in APP/PS1 mice promotes Aβ clearance and improved cognitive outcome[59].

Extracellular ASC, released from microglia, has also been shown to seed Aβ oligomers and contribute to worsened disease. NLRP3 activation in response to AD pathology results in the release of ASC specks from microglia into the extracellular environment. This extracellular ASC can then act as a danger signal to macrophages or physically bind to Aβ. This ASC-Aβ

interaction promotes misfolded protein aggregation which results in the spread of Aβ pathology in a prion-like manner[60].

Although most research has focused on a role for the NLRP3 inflammasome in AD, other inflammasomes are also known to contribute to AD pathology. *Aim2*-deficient 5xFAD AD mice have decreased Aβ plaque load but rescue memory deficits[61]. In addition, *Nlrp1* knockdown in the APP/PS1 murine AD model was shown to significantly protect against neuronal cell death and cognitive decline[62].

Parkinson's disease

Parkinson's disease (PD) is a neurodegenerative disorder that is triggered by the death of dopaminergic neurons in the substantia nigra. Lewy bodies are pathological hallmarks of PD and predominantly consist of fibrillar α-synuclein aggregates in neurons[63]. Clinical studies from the serum of PD patients have revealed increased levels of inflammasome components such as IL-1β and Caspase-1[64]. In addition, elevated levels of IL-1β have been observed both in the brains PD patients and murine models of PD[65]. Delivery of a recombinant adenovirus expressing IL-1β into the substantia nigra of rats was sufficient to induce the death of dopaminergic neurons and subsequent motor impairment[66]. In agreement, injection of the Caspase-1 inhibitor Ac-YVAD-CMK resulted in reduced levels of NLPR3 inflammasome proteins and an increase in the number of dopaminergic neurons[67]. Caspase-1 was also recently shown to cleave α-synuclein *in vitro*, resulting in an aggregation prone protein that was toxic to cultured neurons[68].

Neurodevelopment

The human brain is wired with approximately 86 billion neurons, all of which are interconnected and function to receive input from the outside world to generate an appropriate output[69, 70]. The coordination of these connections through the stages of neurodevelopment requires an array of highly complex and dynamic processes that ensure the proper formation of the brain that will be maintained throughout the lifetime of the organism. Due to the long-lived nature of neurons and glia, neurodevelopment must function to ensure that proper connections are made, the correct number of cells are incorporated into the mature CNS, and that these cells are healthy and functional. Perturbations in any of these processes can lead to improper neurodevelopment and result in neurodevelopmental disorders; therefore, the brain must also be poised to recognize and respond to damage that is generated throughout the entirety of neurodevelopment.

DNA damage in the CNS

Damage to the human genome is believed to occur upwards of 10,000 times per day as a result of replicative and oxidative stress, transcriptional disruptions, and exposure to genotoxic environmental agents (e.g., UV radiation, DNA damaging chemicals) [71-76]. The long-lived nature of neurons and glia, coupled with their exposure to high levels of replicative stress during neurodevelopment, makes the CNS especially vulnerable to DNA damage-induced dysfunction and pathology[74, 76]. The extent to which DNA damage impacts neural function is seen in several key stages of neurodevelopment including proliferation, migration, differentiation, and maturation. Genome maintenance is therefore needed for not only CNS development, but also throughout CNS homeostasis. Indeed, DNA damage buildup in the CNS has been implicated in many neurodevelopmental, psychiatric, and degenerative diseases[72-83].

DNA damage repair

Due to the high levels of damage generated during neurogenesis, the CNS is equipped with an arsenal of tools to recognize and repair DNA damage to ensure genome integrity. This critical role of initiating DNA damage signaling in the CNS is accomplished by the DNA damage activated kinases ATM and ATR. These kinases function throughout the process of neurodevelopment to ensure genome stability[84].

Double-stranded DNA breaks are first detected by PARP1, which recruits the MRN complex and leads to activation of ATM[84-86]. Once recruited, ATM will amplify the DNA damage response (DDR) pathway through its phosphorylation of several downstream targets, such as the histone variant H_2AX, resulting in cell cycle arrest to allow for DNA repair or cell death. The ATR kinase plays a central role in preventing DNA damage accumulation during replication and is therefore essential in proliferating cells. ATR is activated in response to replication protein A (RPA)-coated portions of single-stranded DNA during stalled replication forks[87]. Topoisomerase II binding protein 1 (TopBP1), which binds to RPA, is the best-characterized activator of ATR, and once activated, ATR will stall or arrest cell cycle progression to allow for stabilization of the replication fork, DNA repair, or if the damage is too extensive, programmed cell death.

Different types of dsDNA breaks will activate different repair pathways or programmed cell death. Double-stranded DNA breaks can be repaired through either non-homologous end joining (NHEJ) or homologous recombination (HR). NHEJ is an error-prone repair mechanism that facilitates the rejoining of broken DNA ends while HR is an error-free repair process that uses a sister chromatid as a template to precisely repair DNA.

DNA damage in neurodevelopment

CNS cells are particularly vulnerable to DNA damage throughout the process of neurodevelopment. An early source of DNA damage in neurodevelopment is replication induced DNA damage during neurogenesis[74, 84, 88]. Neural progenitor cells that undergo massive amounts of proliferation during the process of neurogenesis are vulnerable to replication-induced DNA damage during early stages of neurodevelopment. In non-cycling neural cells, dsDNA breaks can occur through oxidative damage that is generated as cells differentiate. Even in mature, differentiated neuronal and glial cells, DNA damage can arise as a result of neuronal firing or free radicals produced through cellular metabolism[74, 88]. Moreover, the types of DNA damage that occur as the brain matures change, thus changing how the cells respond. For example, mutations in an essential gene for maintaining DNA integrity during replication, *TopBP1,* during early cortical development was shown to result in widespread cell death and neurodevelopmental abnormalities[89, 90]. In contrast, if *TopBP1* is deleted in later stages of cortical development then the loss of progenitor cells is markedly reduced[84]. These data suggest that earlier-born progenitors have enhanced susceptibility to DNA damage after TopBP1 loss. Enhanced susceptibility to DNA damage in progenitors during early stages of neurodevelopment might also indicate a lower threshold for cell death compared to progenitors that are generated in later phases of neurodevelopment. Indeed, cell death is the preferred mechanism to maintain genome integrity during neurogenesis as not to allow for progenitor expansion with damaged or unrepaired DNA[91].

Disorders associated with DNA damage

DNA damage repair is essential for maintaining CNS health as genetic mutations in many of the repair pathways are associated with neurodevelopmental and neurodegenerative disorders.

For example, mutations in DNA damage repair and removal pathways have been linked to Alzheimer's disease, Parkinson's disease, ataxia, schizophrenia, autism, and multiple psychiatric disorders [72-83, 92, 93]. Specific mutations in DNA damage response pathway genes, such as *MRN* and *ATM*, can lead to the childhood neurodegenerative disorder, ataxia telangiectasia and microcephaly[74, 86, 94, 95]. Mutations in *ATR* have also been shown to lead to a neurodevelopmental syndrome known as ATR-Seckel syndrome[96, 97]. These correlations point to a critical role for DNA damage surveillance within the central nervous system and suggest that faulty DNA damage repair might be a common link in many neurodevelopmental and neurodegenerative disorders.

Cytokines in neurodevelopment

Cytokines are small proteins that are most commonly thought of as immune modulators but have recently been found to mediate a more diverse array of functions in nonimmune tissues, including having profound roles in the central nervous system (CNS). Cytokines have been demonstrated to have important roles during all stages of neurodevelopment including the induction of the neuroepithelium, renewal of radial glia cells, gliogenesis, migration, axon pathfinding, fate specification, differentiation, cell survival, and likely more[98-100]. Expression of the pro-inflammatory cytokine IL-6 during neurodevelopment has been shown to protect against cytotoxicity, influence neurotransmitter phenotype, and regulate neuronal morphology through dendritic growth (383-391). Other cytokines, such as IL-1β, have been shown to contribute to various neurodevelopmental processes including neurite growth, neuronal migration, and axon pathfinding[101-104]. The role of cytokines during neurodevelopment is extremely complex, with the effects of individual cytokines likely being impacted by cell type, brain region, microenvironment, timepoint, and convergence with other signaling cascades.

Although cytokines primarily act locally, they can also have endocrine effects. Thus, cytokine induction in response to maternal infection or fetal injury may adversely affect neurodevelopment. Indeed, epidemiological evidence points to maternal infection as a cause of neurodevelopmental abnormalities that increase the risk for schizophrenia, cerebral palsy, and autism in the offspring.

Autism Spectrum Disorder

Autism is one of the most prevalent childhood disorders, affecting one in every 54 children in the U.S. Since its original description in 1943 by Kanner[105], the disease has since been characterized into a broader classification of autism spectrum disorders (ASD) which includes Asperger syndrome, childhood disintegrative disorder, and pervasive developmental disorder not otherwise specified (PDD-NOS), highlighting the heterogeneity within the disorder[106]. Typical symptoms associated with ASD are impaired social interactions and communication in addition to repetitive/stereotyped behaviors. However, beyond this unifying definition there is extreme clinical heterogeneity between those diagnosed with ASD. Despite the increasing prevalence of ASD, the etiology remains unknown and treatment options that target the root cause of ASD do not exist.

Genetics in ASD

Family and twin studies were the first to conclusively describe autism as having a genetic component. Concordance rates of autism in monozygotic twins range from 82-92% compared with only about 10% in dizygotic twins[107]. In recent years, many genetic mutations have been identified that are associated with an increased risk for ASD diagnosis. Included in these are mutations in many proteins that are critical for certain aspects of neurodevelopment including

synaptic scaffolding, neurotransmission, synapse formation, and secreted proteins involved in neuronal migration[108]. One such gene that has been associated with severe cognitive deficits and ASD is *SHANK3*, located on chromosome 22[109]. SHANK3 is scaffolding protein found in excitatory synapses that regulates the structure of dendritic spines. Durand *et al.* (2006) found that heterozygous mutation of *SHANK3* can result in language and social deficits. In addition, the authors found that partial trisomy of chromosome 22 resulted in social abnormalities that are more closely associated with Asperger syndrome. They conclude that the correct dosage of *SHANK3* is important for the development of language and social skills.

Another common mutation in ASD is a mutation on chromosome 7 where the *RELN* gene is located[108]. *RELN* encodes reelin, a large secreted glycoprotein that is essential for proper neural migration during development. It has been observed that there are decreased levels of *RELN* transcript and encoded protein in some ASD patients, particularly in the cerebellum and the frontal cortex[110, 111]. Reelin is also important for the migration and positioning of Purkinje cells in the cerebellum, a cell type and area commonly affected in ASD[112]. Interestingly, *RELN* expression has been shown to be particularly sensitive to maternal stressors[113]. More specifically, maternal exposure to the viral mimetic Poly(I:C) at E9 was sufficient to alter the number of reelin positive cells in the hippocampus[114]. These results support the emerging idea that gene-environment interactions are likely at play in many ASD cases.

Importantly, several ASD-associated genes encode specific immune components[115]. One of these highly associated genes is *MET*, which encodes the receptor for hepatocyte growth factor that promotes differentiation and proliferation of hematopoietic cells in embryogenesis. In the CNS, *MET* mediates critical aspects of neurodevelopment including the migration of neuronal precursors and the formation of excitatory synapses[108]. Decreased *MET* expression has been reported in the temporal lobes of post-mortem brains from individuals diagnosed with

ASD[116]. Loss-of-function mutations in genes that encode proteins involved in the formation of the IL-1 receptor have also been associated with ASD. Recent exome sequencing studies have found that single nucleotide polymorphisms (SNPs) in the gene that encodes the IL-1 decoy receptor, IL-1 receptor type 2 (IL-1R2), and IL-1RAP have been reported in patients with ASD[117, 118].

Despite obvious genetic components, only about 20% of diagnoses are 'syndromic' or derived from a known genetic mutation[116]. For the vast majority of patients, the origin of 'non-syndromic' or 'idiopathic' ASD is unknown. Therefore, new research should also be focused on identifying environmental factors that contribute to autism pathogenesis.

Environmental contributors to ASD

Due to the lack of etiologic knowledge, there have been increasing efforts to understand the environmental components that contribute to ASD pathogenesis. Although there are many diverse environmental factors that can contribute to ASD, many converge on alterations in immune responses during pregnancy. Environmental factors such as parental age, maternal infection during pregnancy, diet, pollutants, and maternal obesity have been correlated with an increased risk of developing autism and also have been shown to alter the maternal immune environment[112, 119-122]. The maternal-fetal environment has become increasingly studied as epidemiological links have been discovered between an inflammatory response in the maternal environment during pregnancy and the development of autism in the offspring.

Immune dysfunction

ASD was first linked to maternal immune dysregulation during the rubella epidemic in 1964. In the aftermath of the outbreak, Chess *et al.* examined children with congenital rubella

syndrome (CRS) and found a marked increase in children displaying some degree of autism, identifying 18 cases of 243 examined and suggesting an incidence of 741 autism diagnoses per 10,000 children. Since this original observation, others have identified similar connections between maternal infection and autism[123-125]. Maternal infection with influenza [126], measles and mumps[125], and bacterial infection[119] have all demonstrated links to autism. More recently, a Danish study that involved over one million children demonstrated that maternal infection resulting in hospitalization increased the incidence of their children developing ASD by threefold[119]. The range of infectious agents linked to neurodevelopmental disorders suggests that immune activation during gestation, rather than a specific pathogen, underlies the link with ASD. These studies strongly implicate a correlation between activation of the maternal immune response and altered neurodevelopment in the offspring and can result in a variety of neurodevelopmental disorders including autism and schizophrenia. In addition, these studies suggest that the timing of the maternal immune activation, the type of immune response, and the duration of the response may determine which type of neurodevelopmental disorder the offspring develop.

Maternal immune activation

The animal model of maternal immune activation (MIA) has provided some of the strongest support for maternal immune dysregulation as a contributor to neurodevelopmental abnormalities including schizophrenia and autism. Originally developed as a model for schizophrenia, it was first used to establish a link between maternal immune dysfunction and altered neurodevelopment in the offspring. Zuckerman *et al.* tested if prenatal immune activation with Poly(I:C), a synthetic viral mimic and prototypical trigger of innate-driven inflammation, at E15 would lead to a loss of latent inhibition (LI), a key deficit seen in schizophrenic patients that

involves the inability to ignore irrelevant stimuli[127, 128]. Zuckerman *et al.* found that immune activation during pregnancy can lead to the development of abnormal behaviors in the offspring including disrupted LI as well as increased anxiety.

More recently, MIA has been adopted as an experimental model to study the relationship between hyperactive maternal immune responses and an increased risk of ASD in the offspring. Minor modifications in the timing of Poly(I:C) administration, as well as the downstream behavioral assays, has enabled this model to be adapted to study ASD. MIA is a model of autism in which immune-mediated inflammation in pregnant mothers promotes the acquisition of permanent autistic-like behaviors in offspring. MIA-mediated autism can be induced by treating pregnant mice with Poly(I:C) at E12.5[129]. Importantly, mice that mature in this inflammatory maternal environment develop the three core symptoms used to diagnose ASD. Namely, MIA causes communicative impairments, defects in social interactions, and repetitive and stereotyped behaviors in the male offspring[129]. A seminal study in the field demonstrated that the maternal immune response, rather than viral infection, contributes to the neurodevelopmental abnormalities in the fetus and their subsequent irregular behavior[126]. This was tested by injecting pregnant dams with either influenza virus or Poly(I:C). Behavior abnormalities, consistent with the core symptoms of ASD, were observed in the offspring born from both groups and therefore are likely a result of inflammation rather than fetal infection[126].

The Poly(I:C) maternal activation model was adapted into rhesus macaques which demonstrated the efficacy of the model as offspring showed many of the same behavioral abnormalities seen in rodent MIA offspring[130]. Pregnant monkeys were injected with Poly(I:C) at gestational day 43, 44, and 46 to mimic the first trimester or at 100, 101, and 103 to mimic the second trimester and their offspring were monitored for 2 years[130]. Offspring of the Poly(I:C)-

injected mothers displayed atypical phenotypes associated with ASD including abnormal vocalizations, social interaction, and repetitive behaviors. Further experiments concluded that this phenomenon is not solely limited to viral infection. For instance, other inflammatory triggers in the mothers, such as the bacterial stimulus LPS, have been shown to have similar negative effects on the neurodevelopment of the offspring[131].

The MIA model also recapitulates many of the impaired neuronal circuitry and associated comorbidities seen in ASD. Post-mortem studies of autistic brains show various neurodevelopmental alterations such as an increase in the number of cells, altered cell migration, abnormal cell differentiation, and altered synaptogenesis[132]. Synaptic deficits can also be seen in the brains of rodent MIA offspring when compared to saline controls. For instance, Coiro *et al.* find that offspring of Poly(I:C)-injected mothers have a decreased dendritic spine density that persists into adulthood when compared to their saline-injected controls[133]. In addition, this study found that these dendritic spines were less dynamic and that MIA offspring had a decrease in the total number of excitatory inputs. The authors also demonstrated that MIA offspring had increased levels of major histocompatibility complex I (MHCI) which is known to be a negative regulator of synapse formation[134, 135].

Traditionally, the cerebral cortex has been the focus of neurological abnormalities in ASD[136]. However, recent evidence suggests that the cerebellum may also be an important determinant in ASD[137]. Abnormalities in the cerebellum, including Purkinje cell loss, are found in the majority of autistic patients in both autopsy and MRI studies. The rodent model of MIA-induced autism also results in cerebellar neuropathology as demonstrated by reductions in Purkinje cell numbers[138]. Moreover, Reith *et al.* (2013) demonstrated that a loss of Purkinje cells was sufficient to promote autistic-like behaviors including decreased communication, altered

social behavior, and increases in repetitive behaviors[139].

A number of the MIA rodent studies have also replicated the observation of altered microglia in the brains of autistic individuals. Autopsies of brains from autistic individuals showed significantly increased densities of microglia throughout the cerebral cortex [140, 141]. One study, using the MIA model of autism, demonstrated increased expression of glial fibrillary acidic protein (GFAP) and an increased number of activated microglia, specifically in the hippocampus[142]. However, this result is not consistent within the literature, as Hsiao *et al.* did not uncover overt alterations in microglial biology in the Poly(I:C) MIA model[143].

Obesity and diet

Recently, it has been revealed that obesity is associated with low levels of chronic systemic inflammation, driven by innate immune cell-mediated release of pro-inflammatory cytokines such as tumor necrosis factor-α (TNFα), IL-6, and activated IL-1β mentioned earlier. The main source of pro-inflammatory cytokines is the infiltrating macrophages in the adipose tissue[144]. It has become increasingly important to understand the mechanism by which maternal obesity can influence the developing brain in the offspring, as data from 2006 shows that 35.3% of women are obese[145]. Moreover, there have been a number of recent studies that link maternal obesity and high fat diet (HFD) to the development of autistic like behaviors in the offspring. For instance, a recent murine study showed that offspring born to mothers that were fed a HFD showed decreased stress calls and increased anxiety when compared to their controls[146]. In addition, offspring of dams fed HFD compared to their normal diet controls show decreased social interaction[120].

Hsiao *et al.* also showed that maternal Poly(I:C) injection is sufficient to induce similar changes in the offspring that were observed in maternal HFD models. Furthermore, offspring of Poly(I:C)-injected mice show increased gut dysbiosis and significant decreases in genes associated with intestinal barrier integrity. This study also demonstrated an important role for the microbiome in the development of autistic-like behaviors by showing that when the microbiome was supplemented with *Bacteroides fragilis*, many behavioral phenotypes were also restored[147]. Dysbiosis and gastrointestinal dysfunction, perhaps primed by maternal microflora, are common in ASD and may modulate immune and neurological dysfunction[148]. These studies point toward a critical gut-immune-brain connection that is disrupted in ASD and may be influenced by MIA.

Autoimmune diseases

Estimates indicate that there is up to a 50% increase of an ASD diagnosis among children who have a parent who has been diagnosed with an autoimmune disorder[149]. Keil *et al.* showed that, collectively, autoimmune disease increased the risk of having a child diagnosed with ASD and that certain autoimmune diseases, including type I diabetes and rheumatoid arthritis, are more correlated with this increased risk.

Allergy

During pregnancy, exposure to other inducers of inflammation have also been identified as risk factors for development of ASD in the offspring including maternal exposure to allergens. Allergens are thought to impact fetal neurodevelopment through alterations of the mother's immune profile toward a T_H2-mediated response. Using the maternal allergic asthma (MAA) model, in which female mice are sensitized to ovalbumin (OVA) and then subsequently exposed to aerosolized OVA at E9.5, E12.5, and E17.5, Schwartzer *et al.* demonstrated that an

inflammatory response to allergens in the mother is sufficient to alter behavior in the offspring[122]. Although offspring behaviors did not mimic those seen in the classic Poly(I:C) model of MIA, this suggests that fetal exposure to different inflammatory conditions can potentially alter neurodevelopment in a variety of ways, thus affecting the downstream behaviors.

Cytokines

Due to the epidemiological connections between a diversity of maternal infections that show a connection to ASD, in addition to the evidence from the MIA model that the immune response, specifically cytokines, to infection rather than infection itself may lead to autism-like behaviors, a possible common etiology may be the influence of the immune system on neurodevelopment.

A key mediator in the development of MIA-induced autism is IL-6. Smith *et al*. found that maternal injection of IL-6 alone is sufficient to drive the development of behavioral abnormalities in the offspring, including decreases in pre-pulse inhibition (PPI) and latent inhibition[150]. In addition, when Smith *et al*. injected an IL-6 neutralizing antibody alongside a Poly(I:C) injection, they found that IL-6 neutralization completely ameliorated the behavioral deficits previously seen in LI, PPI, and social preference. To demonstrate that this was specific to IL-6, they also injected a neutralizing antibody to IFN-γ and saw that it was not sufficient to rescue the phenotypes.

In the follow-up study, Hsiao and Patterson sought to examine the mechanism through which IL-6 influences fetal development. They found that IL-6 protein and mRNA was significantly increased in the placenta up to 24 hours after Poly(I:C) injection[151]. Moreover, they found that the increase in placental IL-6 is maternally-derived. Since IL-6 signals through STAT3, the authors performed histological staining for phosphorylated STAT3 (pSTAT3) in the

trophoblast layer (the layer of the placenta comprised of fetal trophoblast cells). They saw that IL-6 heterozygous mothers (*IL-6*$^{+/-}$) injected with Poly(I:C) had increased pSTAT3 staining in the trophoblast layer compared to saline controls. However, when they looked at *Il6r*-deficient mothers, they observed no pSTAT3 positive cells in the trophoblast layer, confirming their conclusion that maternal IL-6 drives pSTAT3 activation in the placenta. To further understand the role of IL-6 in the placenta, Wu *et al.* created trophoblast-specific *Il6ra* knockouts (*Cyp*19-*Cre; Il6ra*$^{fl/fl}$)[138]. When these pregnant mice were subjected to Poly(I:C) injection, there was a marked decrease in *Il6* mRNA in the brain, protection from the loss of Purkinje cells when compared to WT Poly(I:C) controls, and normal social and repetitive behaviors. Despite these findings, much remains unknown about the mechanisms in which inflammation in the mother and placenta can alter neurodevelopment in the fetus.

Recent studies demonstrate a key role for IL-17 in the MIA pathway. Poly(I:C) injections in pregnant dams results in increases in the serum levels of IL-6 3 hours post-injection with later increases in IL-17 at 2 days post-injection[152]. Increases in IL-6 and IL-17a in the maternal serum were absent in *Il6* knockout mothers; moreover, injection of IL-6 into a pregnant dam also resulted in increased IL-17 production in the mother. These results indicate that IL-6 can lead to increases in maternal IL-17 production.

Using the MIA model, this study also showed that IL-17a promotes abnormal cortical development and ASD-like phenotypes. Mice injected with Poly(I:C) and an IL-17a neutralizing antibody were rescued from both cortical abnormalities and ASD-associated behaviors. The authors then narrowed down the source of IL-17a to *RORγt*-expressing T cells, which include T_H17 cells, when they found that offspring of Poly(I:C)-injected *RORγt* T cell knock out (TKO) mothers (*CD4*^{Cre}*;RORγt*$^{fl/fl}$) were protected from cortical deficits and autistic-like behaviors. Choi *et al.* determined that maternally-derived IL-17a acts directly on receptors in the fetal brain to

result in ASD-associated phenotypes through the injection of IL-17a or PBS directly into the ventricles of fetal brains at E14.5. Injections of IL-17a alone were sufficient to lead to cortical disorganization, enhanced communication, social deficits, and increased repetitive behaviors in a similar manner to those observed in MIA-exposed offspring.

Although alterations in behavior and neurodevelopment in the MIA model of autism and other models of altered maternal immune system have been fairly well established, less well understood are the mechanistic details of how maternal immune activation impairs neurodevelopment in the offspring. Recent publications are beginning to uncover more mechanistic details driving MIA and demonstrate that MIA offspring harbor atypical cortical patches that localize highly to the dysgranular zone region of the primary somatosensory cortex (S1DZ). Moreover, this study showed that the size of these patches correlates with behavioral abnormalities. These patches contain fewer PV^+ interneurons, which corresponds to hyperactivation in the region. Hyperactive S1DZ projections to the striatum and temporal association cortex accounted for abnormal repetitive and social behaviors, respectively[153]. Further elucidation of the biologic underpinnings of the role of the immune system in neurodevelopment will likely shed light on homeostatic functions of immunity in the nervous system as well as reveal potential treatment strategies for cases of dysfunction.

Thesis rationale

Accumulating evidence points to a clear role for the innate immune system, particularly the inflammasome, in response to both CNS injury and neurodegenerative disease. However, less clearly defined are the contributions of the inflammasome to CNS homeostasis. While CNS cells are equipped with inflammasome components, whether or not they utilize this innate

immune signaling tool during neurodevelopment and under normal conditions remains poorly studied. **The overarching question my thesis aims to answer is: how does the innate immune system, in particular the inflammasome, impact neurodevelopment?**

Detailed in the following chapters will be our work published in detailing the role of the AIM2 inflammasome in neurodevelopment (chapter 2). This work describes a novel role for the AIM2 inflammasome in the removal of genetically compromised cells in neurodevelopment via Gasdermin-D-mediated pyroptosis. Previously, it was believed that massive periods cellular dieback that are characteristic of neurodevelopment solely occur through the process of apoptosis. Our studies demonstrate that CNS cells harboring irreparable DNA can also be eliminated through Gasdermin-D-mediated pyroptosis, suggesting that the CNS has multiple removal mechanisms in place to dispose of genetically compromised cells.

The following chapters will also cover our unpublished work describing the role of IL-1β in the maternal immune activation (MIA) model of ASD (chapter 3). Several key cytokines have been previously implicated in this model, including IL-6 and IL-17[138, 150, 152]. However, the upstream signaling pathways have not been extensively studied. Our studies demonstrate that IL-1β signaling is both sufficient and necessary to induce behavioral abnormalities that are often associated with ASD.

Finally, I will discuss our published work describing the role of the maternal microbiome in the MIA model of ASD (chapter 4). Studies from our lab, and others, have demonstrated that the gut microbiome plays a key role in amplifying the immune response in the dam when subjected to Poly(I:C)[154, 155]. We find that key microbes present in Taconic, but not Jackson, mice infer susceptibility of developing ASD associated behavioral abnormalities through

amplification of an IL-17 immune response. We show that co-housing mice to transfer the microbiome will induce ASD-associated behaviors in Jackson MIA offspring who are normally protected against the development of MIA-induced behavioral abnormalities.

Chapter 2: *AIM2* inflammasome surveillance of DNA damage shapes neurodevelopment

Abstract

Neurodevelopment is characterized by rapid rates of neural cell proliferation and differentiation followed by a period of massive cell death where over half of all recently generated brain cells are pruned back. Large amounts of DNA damage, cellular debris, and byproducts of cellular stress are generated during these neurodevelopmental events, all of which can potentially activate immune signaling. How the immune response to this collateral damage influences brain maturation and function currently remains poorly understood. Here we show that the AIM2 inflammasome contributes to proper brain development and that disruptions in this immune sensor of genotoxic stress lead to behavioral abnormalities. The AIM2 inflammasome has been most extensively studied in the context of infection, where its activation in response to double-stranded DNA (dsDNA) is known to trigger cytokine production as well as a Gasdermin-D-mediated form of cell death commonly referred to as pyroptosis[156-159]. We observe pronounced AIM2 inflammasome activation in neurodevelopment and find that defects in this DNA damage surveillance sensor result in anxiety-related behaviors. We further show that the AIM2 inflammasome contributes to central nervous system (CNS) homeostasis specifically through its regulation of the cell death executioner Gasdermin-D, and not via its involvement in IL-1 and/or IL-18 production. Consistent with a role for this sensor of genomic stress in the purging of genetically compromised CNS cells, we find that defective AIM2 inflammasome signaling results in decreased neural cell death both in response to DNA damage-inducing agents and during neurodevelopment. Moreover, we report that disruptions in DNA damage surveillance by the AIM2 inflammasome lead to excessive DNA damage accumulation in neurons as well as increased numbers of neurons that incorporate into the adult brain. Our findings identify the inflammasome as a critical player in establishing a properly formed CNS through its role in the removal of genetically compromised cells.

Introduction

Maintenance of genomic integrity is essential for (CNS) health and mounting evidence indicates that DNA damage accumulation in the brain centrally contributes to a number of neurodevelopmental, psychiatric, and neurodegenerative disorders[72-83]. Damage to the human genome is believed to occur upwards of 10,000 times per day as a result of replicative and oxidative stress, transcriptional disruptions, and exposure to genotoxic environmental agents (e.g., UV radiation, DNA damaging chemicals)[71-76]. The long-lived nature of neurons and glia, coupled with their exposure to high levels of replicative stress during neurodevelopment, makes the CNS especially vulnerable to DNA damage-induced dysfunction and pathology[74, 76]. Indeed, DNA damage buildup in the CNS has been implicated in many neurodevelopmental, psychiatric, and degenerative diseases[72-83]. For example, mutations in DNA damage repair and removal pathways have been linked to Alzheimer's disease, Parkinson's disease, ataxia, schizophrenia, autism, and multiple psychiatric disorders[72-83, 92, 93]. Currently, the nature of the DNA damage response pathways that promote the neuroinflammation and CNS pathology underlying these disorders remains poorly understood. In recent years, great strides have been made in characterizing the types of processes and molecular pathways that are capable of generating DNA damage in the CNS. Although there is growing appreciation for the roles of DNA damage in driving neurological dysfunction and pathology, little is currently known about the specific molecular pathways that the brain relies on to safeguard itself from DNA insults or how altered regulation of these pathways leads to neurological disease. In recently published studies, we recently found that DNA damage surveillance by the AIM2 inflammasome is required for normal brain maturation and function[160]. The AIM2 inflammasome has been most extensively studied in the context of infection, where its activation in response to double-stranded DNA (dsDNA) insults

is known to trigger production of the inflammatory cytokines IL-1 and IL-18, as well as a Gasdermin-D-mediated form of cell death commonly referred to as pyroptosis[156, 157, 159, 161]. Although AIM2 is highly expressed in the CNS[162], its function there is largely unknown. We found that defective AIM2 inflammasome signaling results in excessive DNA damage accumulation in the brain and abnormal brain maturation that is highlighted by cerebellar disorganization, elevated Purkinje cell numbers, and astrogliosis throughout the brain. Disruption in genotoxic stress sensing by the AIM2 inflammasome also promoted the development of anxiety-related behaviors, impaired motor function, and communicative deficits.

Here we asked whether the damage signals generated during neurodevelopment trigger activation of the innate immune response and, if so, how this immune activation shapes neurodevelopment and behavior. The high levels of replicative stress and cell death that occur during brain maturation are known to generate a number of damage/danger signals such as DNA damage, ATP, and mitochondrial stress, all of which are capable of triggering inflammasome activation.

Results

ASC specks form in neurodevelopment

Since both cytokine production and cell death have been shown to be pivotal modulators of neurodevelopment[4, 12, 152, 163-169], along with the fact that key inflammasome components are highly expressed during development. (Fig. 2.1 a-c), we were interested in determining if inflammasome activation influences brain maturation and CNS function. We first asked if inflammasome activation is observed during neurodevelopment. To test this, we utilized ASC reporter mice to track the development of ASC specks, which are prototypical markers of inflammasome activation[170]. When we looked in the developing brain at postnatal day 5 (p5), a

time point characterized by high levels of DNA damage and cell death[77, 171], we observed surprisingly high levels of ASC speck formation throughout the brain (Fig. 2.2 a-b and Fig. 2.3 a). In comparison, we were barely able to detect any ASC specks in fully matured lymphoid organs such as the lymph nodes (LNs) (Fig. 2.2 b and Fig. 2.3 b-c).

Inflammasomes influence behavior

We next wanted to assess the importance of inflammasome activation in setting up a properly functioning CNS. To accomplish this, we performed a battery of behavioral tests on Caspase-1/11-deficient mice (also referred to as *Ice*$^{-/-}$ mice*).* We found that genetic ablation of the inflammasome results in profound anxiety-like behaviors in the elevated plus maze and in open field testing (Fig. 2.2 c-g). More specifically, we observed that *Ice*$^{-/-}$ mice spent significantly less time exploring the open arm of the elevated plus maze (Fig. 2.2 c-d). Moreover, in open field testing, *Ice*$^{-/-}$ mice explored the center significantly less than WT mice, urinated more frequently, and produced more fecal pellets (Fig. 2.2 e-g and Fig. 2.4 a-b). To ensure that impaired vision and/or locomotor activity did not underlie the poor performance of inflammasome-deficient mice in our behavioral tests, we evaluated their ability to find a visible escape platform in the Morris water maze (MWM). In these studies, deletion of the inflammasome was not found to negatively impact the ability of mice to reach the visual platform indicating that neither impaired vision nor motor deficits likely contribute to the differences in performance seen in our elevated plus and open field tests (Fig. 2.2 h). Genetic ablation of inflammasome signaling in Caspase-1/11-deficient mice also did not result in global behavioral abnormalities as *Ice*$^{-/-}$ mice were found to perform normally in the tail suspension and sucrose preference tests (Fig. 2.4 c-d), both of which are commonly used to assess depressive

behaviors. Collectively these results indicate that impaired inflammasome activation leads to behavioral abnormalities that include the development of pronounced anxiety-like behaviors.

The immune system is equipped with a repertoire of intracellular receptors that enable the host to coordinate inflammasome activation in response to a diverse array of pathogens and endogenous damage/danger signals. We first turned our attention to a potential role for NLRP3 in our model, as NLRP3 is known to incite inflammasome activation in response to a diverse array of damage/danger-associated molecular patterns (DAMPs) that are likely generated during normal brain maturation (e.g., ATP, damaged mitochondria, reactive oxygen species, etc.)[159]. To our initial surprise, we found that *Nlrp3*$^{-/-}$ mice performed similar to WT mice in the elevated plus maze, open field, visual platform test, and depressive assays (Fig. 2.2 c-h, Fig. 2.4). These results suggest that NLRP3 is not coordinating the inflammasome activation needed to prevent the development of anxiety-like behaviors in mice.

The AIM2 inflammasome affects behavior

Maintenance of genomic integrity is essential for CNS health and mounting evidence suggests that inability to control genotoxic stress centrally contributes to a number of neurodevelopmental, psychiatric, and neurodegenerative disorders[74, 88]. In the majority of cases, DNA damage is quickly remediated by repair pathways. However, DNA insults can persist as a result of unsuccessful repair attempts and/or impaired DNA damage removal[172, 173]. Recent studies conducted in peripheral immune cells have shown that sensing of DNA damage by AIM2 can trigger inflammasome activation[174]. In addition, emerging work has described roles for AIM2 in models of CNS injury[175, 176] and also has begun to characterize how deletion of AIM2 can alter neuronal morphology and influence behavior[37]. However, it still remains to be determined whether the AIM2 inflammasome is activated during neurodevelopment and, if so, how this

impacts brain maturation and behavior. When we tested AIM2-deficient mice for anxiety-like behaviors we found that *Aim2*$^{-/-}$ mice phenocopied *Ice*$^{-/-}$ mice and displayed anxiety-like behaviors in both the elevated plus maze and the open field test (Fig. 2.2 c-g, Fig. 2.4 a-b). Like *Ice*$^{-/-}$ mice, AIM2-deficient mice reached the visual platform in the MWM in similar times as their WT controls (Fig. 2.2 h) and performed normally in both the tail suspension and sucrose preference tests (Fig. 2.4 c-d).

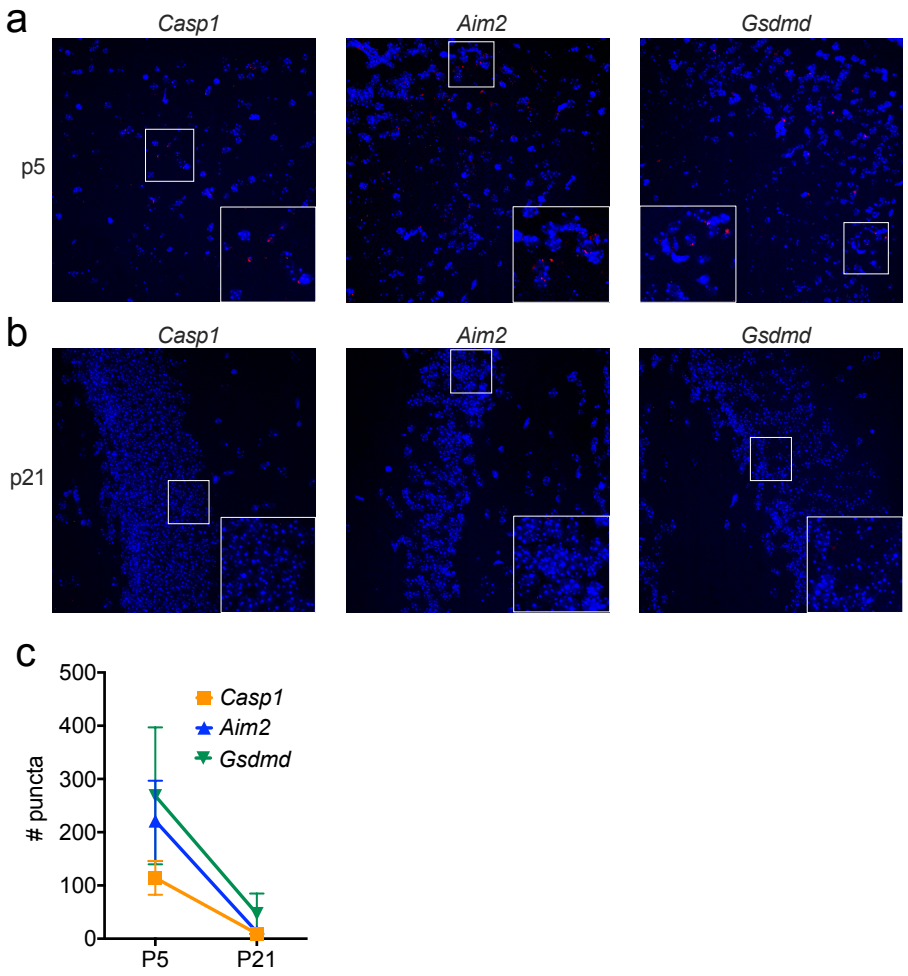

Figure 2.1 Molecular components of the AIM2 inflammasome are abundantly expressed in the brain during neurodevelopment. (a-c) Brains from (a) p5 and (b) p21 WT mice were evaluated for the mRNA expression of inflammasome component genes (red) *Casp1* (p5 *n*=4, p21 *n*=2) , *Aim2* (p5 *n*=3, p21 *n*=2), and *Gsdmd* (p5 *n*=3, p21 *n*=2) using RNA scope. (c) Quantification of *Casp1* (p5 *n*=4, p21 *n*=2) , *Aim2* (p5 *n*=3, p21 *n*=2), and *Gsdmd* (p5 *n*=3, p21 *n*=2) mRNA puncta in the hippocampus per 40X image; from 1 experiment. Error bars depict mean ± s.e.m. *n* values refer to biological replicates.

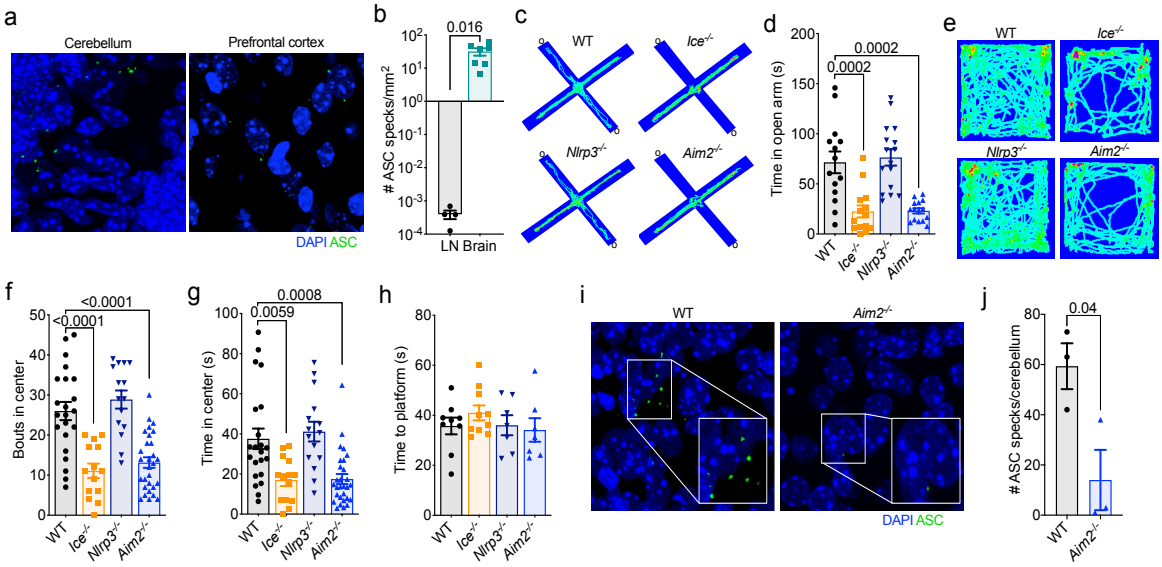

Figure 2.2. Inflammasome activation occurs in the CNS during neurodevelopment and disruption of the AIM2 inflammasome results in anxiety-related behaviors. (a) Brains from postnatal day 5 (p5) ASC-Citrine reporter mice were analyzed for the presence of ASC specks (green). Representative images from 3 independent experiments with similar results. (b) Number of ASC specks formed in the brain at p5 (*n*=7; from 3 independent experiments) and the adult (8-16 weeks old) deep cervical lymph nodes (DCLN) (*n*=4; representative data from 2 independent experiments). (c-h) Wild-type (WT), *Ice*$^{-/-}$, *Nlrp3*$^{-/-}$, and *Aim2*$^{-/-}$ mice (8-12 weeks old) were assessed for behavioral abnormalities. (c-g) Anxiety behaviors were assessed using the elevated plus maze and the open field test. (c) Representative elevated plus maze heat maps; open arms (o); from 6 independent experiments with similar results. (d) Quantification of time spent in the open arms of the elevated plus maze (WT *n=14,* *Ice*$^{-/-}$ *n*=14, *Nlrp3*$^{-/-}$ *n*=16, *Aim2*$^{-/-}$ *n*=15; from 3 independent experiments). (e) Representative open field arena heat maps; from 6 independent experiments with similar results. (f-g) Quantification of (f) bouts into and (g) time spent in the center of the open field arena (WT *n=22,* *Ice*$^{-/-}$ *n*=14, *Nlrp3*$^{-/-}$ *n*=15, *Aim2*$^{-/-}$ *n*=29; from 5 independent experiments). (h) Visual platform test of the Morris water maze (WT *n=9,* *Ice*$^{-/-}$ *n*=10, *Nlrp3*$^{-/-}$ *n*=7, *Aim2*$^{-/-}$*n*=7; from 2 independent experiments). (i-j) Cerebellar ASC speck formation in p5 WT and *Aim2*$^{-/-}$mice. (i) Representative images from 2 independent experiments with similar results. (j) Quantification of cerebellar ASC speck formation in WT *n*=3 and *Aim2*$^{-/-}$ *n*=3 mice; representative data from 2 independent experiments. All *n* values refer to the number of mice used. Error bars depict mean ± s.e.m. Statistics calculated by unpaired two-tailed Student's *t*-test (b,j) or one-way ANOVA with Tukey's post hoc tests (d,f,g,h).

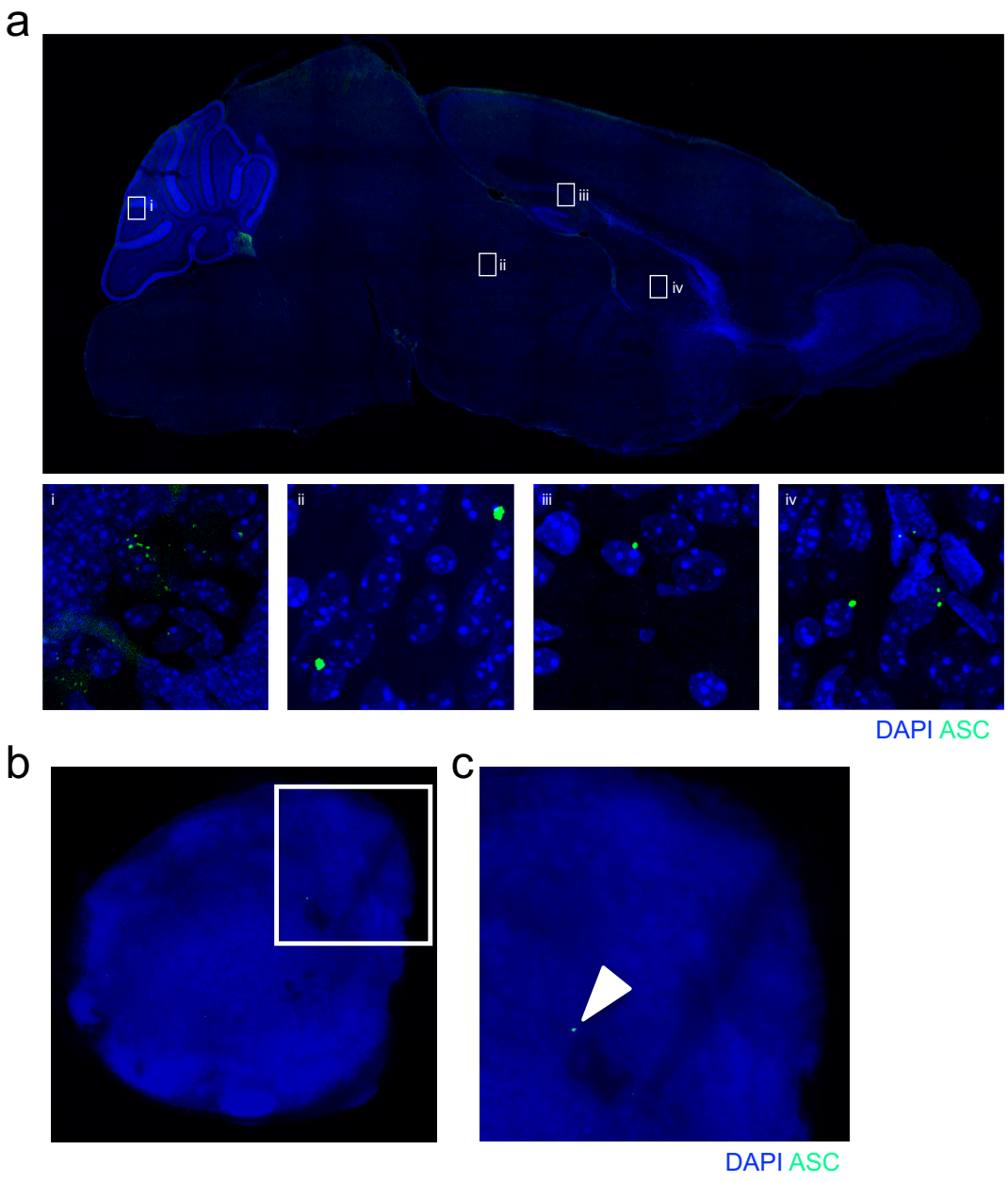

Figure 2.3 ASC speck formation routinely occurs in the developing brain but is rare in mature lymph nodes under steady-state conditions. (a) 10X sagittal image of ASC speck formation (green) in the brain of p5 ASC-Citrine reporter mice. ASC specks are detected throughout the brain using a 40X objective including in the (i) cerebellum, (ii) midbrain, (iii) hippocampus, and (iv) thalamus. Representative images from 3 independent experiments with similar results. (b-c) Adult (8-12 weeks old) ASC-citrine reporter mice were evaluated for peripheral inflammasome activation based on (b) ASC speck formation (green) in the deep cervical lymph node (DCLN) using confocal microscopy with a 10X objective. (c) Arrow shows zoomed in image of ASC speck (green) formed in DCLN. Representative images from 2 independent experiments with similar results.

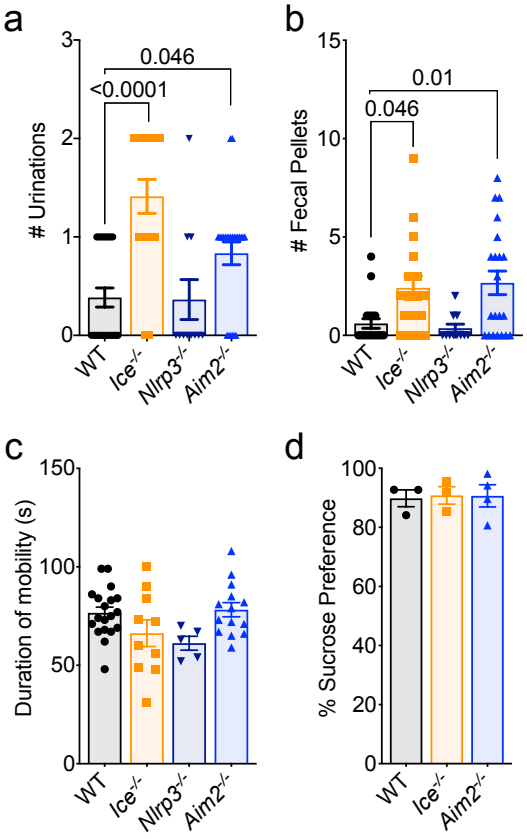

Figure 2.4. Lack of AIM2 inflammasome signaling results in an increase in anxiety-related behaviors but not depressive-related behaviors. Adult (8-12 weeks old) WT, *Ice*$^{-/-}$, *Aim2*$^{-/-}$, and *Nlrp3*$^{-/-}$ mice were assessed for behavioral abnormalities. (a) Number of urinations (WT *n*=26, *Ice*$^{-/-}$ *n*=17, *Nlrp3*$^{-/-}$ *n*=11, *Aim2*$^{-/-}$ *n*=24; from 3 independent experiments) and (b) number of fecal pellets (WT *n*=20, *Ice*$^{-/-}$ *n*=17, *Nlrp3*$^{-/-}$ *n*=11, *Aim2*$^{-/-}$ *n*=21; from 3 independent experiments) were measured during 10 minutes of open field-testing. Depressive behaviors were evaluated in adult male mice using the (c) tail suspension test for escape behavior (WT *n*=19, *Ice*$^{-/-}$ *n*=10, *Nlrp3*$^{-/-}$ *n*=5, *Aim2*$^{-/-}$ *n*=14; from 2 independent experiments) and (d) sucrose preference test (WT *n*=3, *Ice*$^{-/-}$ *n*=3, *Aim2*$^{-/-}$ *n*=4; from 1 independent experiment). All *n* values refer to the number of mice used. Error bars depict mean ± s.e.m. Statistics calculated by one-way ANOVA with Tukey's post hoc tests.

DNA damage and AIM2 promote ASC specks

Since key AIM2 inflammasome-associated genes are abundantly expressed during neurodevelopment (Fig. 2.1) and dsDNA is known to activate AIM2, we were next interested in elucidating whether the DNA damage that normally arises during neurodevelopment can trigger AIM2 inflammasome activation in the developing brain. As a first approach, we explored if the inflammasome activation observed during neurodevelopment occurs in close proximity to cells harboring DNA damage. To this end, we evaluated the spatial localization of ASC specks in relation to cells that co-stain for the DNA damage markers γH2AX and 53BP1. Many of the ASC specks formed in the developing brain were identified to be in the vicinity of cells that co-stained for the DNA damage markers γH2AX and 53BP1 (Fig. 2.5 a). Moreover, we found that the bulk of this inflammasome activation at p5 in neurodevelopment is dependent on AIM2 surveillance, as genetic abrogation of AIM2 greatly decreased the number of ASC specks detected in the developing cerebellum (Fig. 2.2 i-j). To further interrogate whether the AIM2 inflammasome can be activated in the developing brain in response to DNA damage, we induced overt DNA damage at p5 in the brains of WT and AIM2-deficient mice by exposing them to ionizing radiation (IR). We found that exposure to ionizing radiation results in increased expression of DNA damage markers in WT mice (i.e. γH2AX staining) and that this corresponds with concomitant increases in inflammasome activation (ASC speck formation) (Fig. 2.5 b-e). We observed a corresponding increase in γH2AX staining in ionizing radiation-treated AIM2-deficient mice (Fig. 2.5 b-c). However, ASC speck formation was substantially blunted in the absence of AIM2 (Fig. 2.5 d-e). Taken together, these findings suggest that AIM2 inflammasome activation occurs during neurodevelopment likely in response to DNA damage and that disruptions in this pathway can lead to behavioral abnormalities.

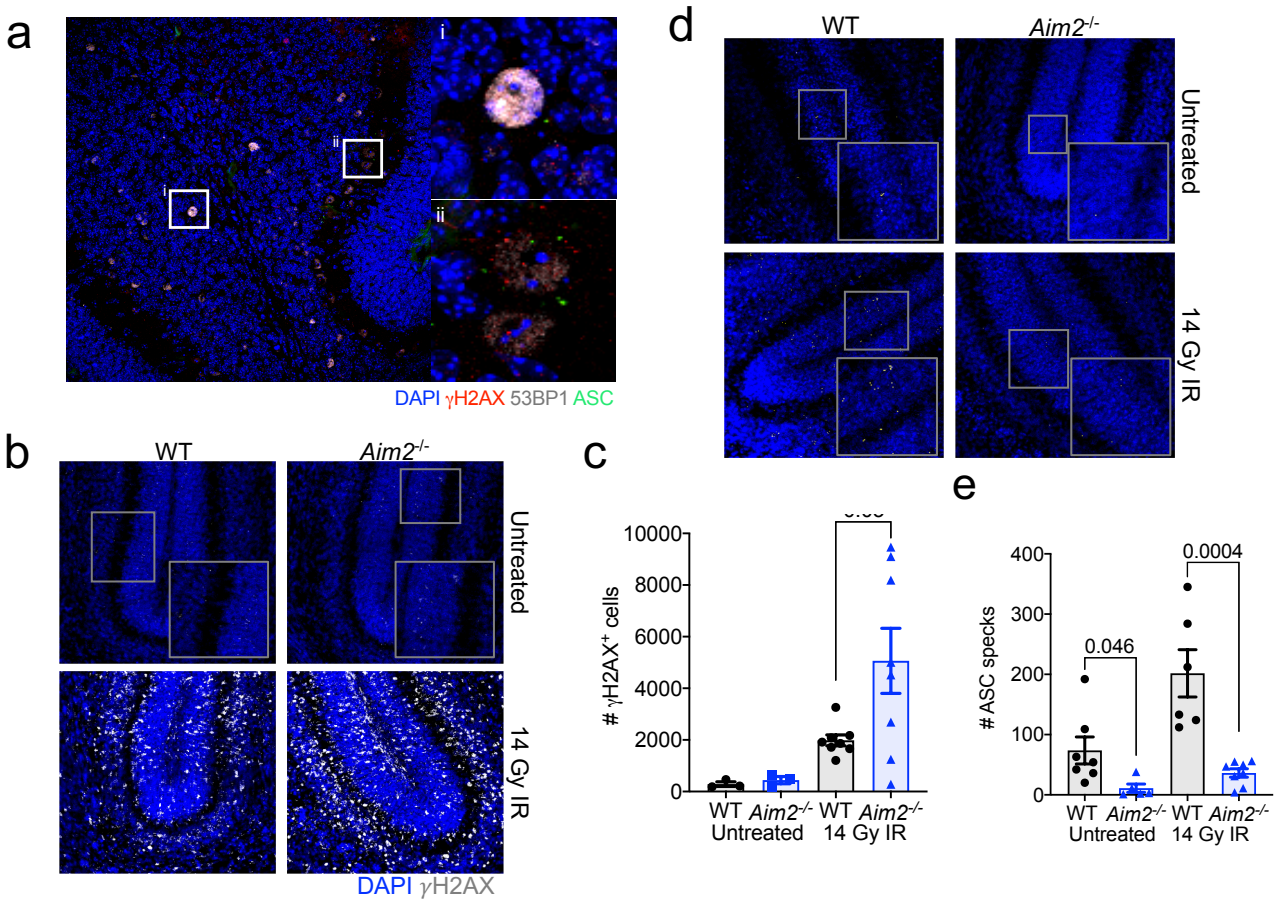

Figure 2.5. ASC specks form in response to DNA damage in the developing brain. (a) Brains from p5 WT mice were evaluated for localization of ASC specks (green) in relation to DAPI^{+} nuclei (blue) harboring DNA damage (γH2AX (red), 53BP1 (grey)) in the cerebellum. (i, ii) Zoomed in regions of 40X images showing ASC specks formed in close proximity to nuclei harboring DNA damage. Representative images from 4 mice with similar results from 1 experiment. Differences in nuclei size likely reflect specific stages in replication, DNA repair, differentiation, or cell death the individual cells are in as well as differences seen across CNS cell types. (b-e) Postnatal day 5 (p5) WT and *Aim2*$^{-/-}$ mice received either control treatment or 14 Grays (14 Gy) of ionizing radiation (IR) to induce DNA damage. Brains were harvested 6 hrs later and then immunostaining was conducted to measure DNA damage induction (γH2AX staining) and inflammasome activation (ASC speck formation) in the cerebellum. (b) Representative 20X cerebellar images of γH2AX staining; from 2 independent experiments with similar results. (c) Quantification of γH2AX staining in the cerebellum (Untreated: WT *n*=3, *Aim2*$^{-/-}$ *n*=3; IR treated: WT *n*=8, *Aim2*$^{-/-}$ *n*=8; from 2 independent experiments). (d) Representative 20X cerebellar images of ASC speck formation; from 2 independent experiments with similar results. (e) Quantification of ASC speck formation in the cerebellum (Untreated: WT *n*=7, *Aim2*$^{-/-}$ *n*=5; IR treated: WT *n*=6, *Aim2*$^{-/-}$ *n*=8; from 2 independent experiments). All *n* values refer to the number of mice used. Error bars depict mean ± s.e.m. Statistics calculated by unpaired two-tailed Student's *t*-test.

Gasdermin-D shapes behavior

Inflammasome activation can lead to IL-1 and IL-18 secretion, as well as a Gasdermin-D-mediated form of cell death, both of which can potentially impact neurodevelopment and behavior. Cytokines have been shown to be pivotal modulators of neurodevelopment, CNS function, and behavior[4, 12, 152, 164, 165]. In particular, the inflammasome-derived cytokines IL-1 and IL-18 have been reported to have especially prominent effects on the CNS[4, 12, 164, 165]. Therefore, we were interested in discerning whether the observed behavioral abnormalities in AIM2 inflammasome-deficient mice were caused by disruptions in AIM2 inflammasome-mediated production of IL-1 and/or IL-18. Surprisingly, abrogation of IL-1 or IL-18 signaling were not found to promote anxiety-related phenotypes (Fig. 2.6 a-b, Fig. 2.7 a-c). To interrogate whether IL-1 and IL-18 can play compensatory roles in shaping behavior, we also evaluated anxiety-related phenotypes in mice that lack MYD88, which is an essential adaptor molecule required for both IL-1R and IL-18R signaling. However, abrogation of MYD88 signaling was not observed to influence performance in tests measuring anxiety-related behaviors (Fig. 2.6 a-b, Fig. 2.7 a-e).

In addition to orchestrating IL-1 and IL-18 production, AIM2 inflammasome activation can also incite a Gasdermin-D-mediated form of cell death. To explore the role that Gasdermin-D plays in driving anxiety-like phenotypes, we assessed the performance of Gasdermin-D knockout mice in the elevated plus maze. Similar to *Ice*$^{-/-}$ and *Aim2*$^{-/-}$ mice (Fig. 2.2 c-d), Gasdermin-D-deficient mice spent less time exploring the open arm of the elevated plus maze (Fig. 2.6 c-d). Caspase-11, like Caspase-1, is also to known to orchestrate Gasdermin-D activation through noncanonical inflammasome signaling[9]. Nevertheless, Caspase-11-deficient mice were found to perform similarly to WT mice in both elevated-plus maze and open field testing (Fig. 2.6 c-d, Fig. 2.7 f-h). Taken together, these results suggest that the behavioral

abnormalities observed in AIM2 inflammasome-deficient mice are likely not due to defects in Caspase-1-mediated production of IL-1 and/or IL-18, but rather result from impaired Gasdermin-D signaling.

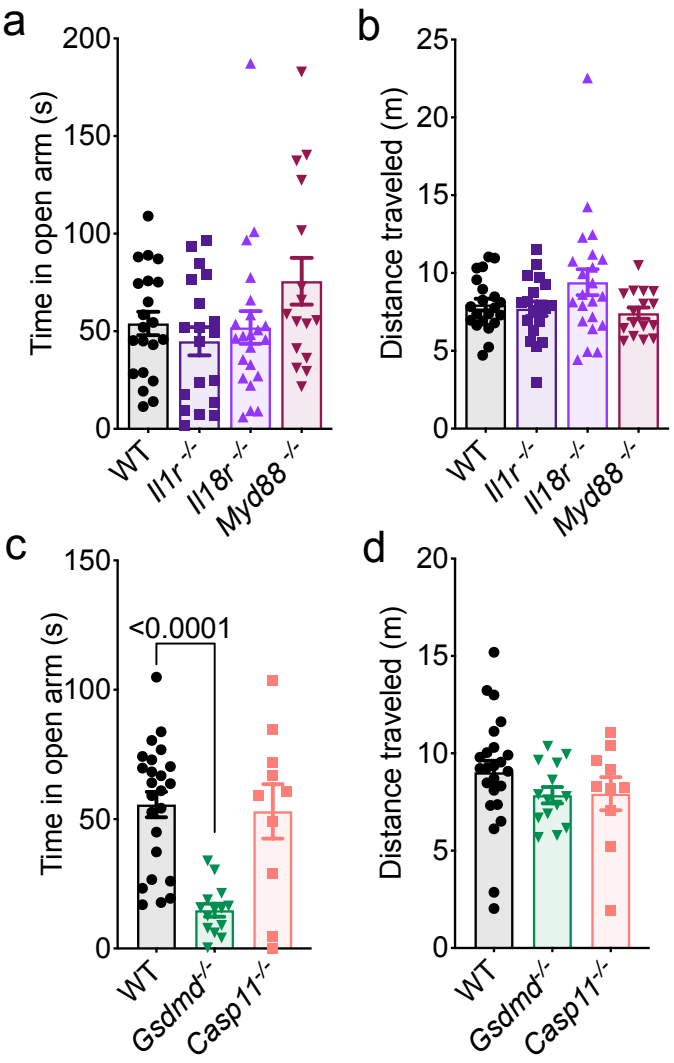

Figure 2.6. Lack of Gasdermin-D activation drives anxiety-like behaviors in mice. (a-d) Anxiety-related behaviors were assessed in adult (8-12 weeks old) WT, *Il1r*$^{-/-}$, *Il18r*$^{-/-}$, *Myd88*$^{-/-}$, *Gsdmd*$^{-/-}$, and *Casp11*$^{-/-}$ mice using the elevated plus maze. (a-b) Quantification of (a) time spent in the open arms (o) and (b) distance traveled (WT *n*=21, *Il1r*$^{-/-}$*n*=19, *Il18r*$^{-/-}$ *n*=22, *Myd88*$^{-/-}$*n*=16; from 4 independent experiments). (c) Time spent in the open arms of the elevated plus maze and (d) total distance traveled during testing (WT *n*=24, *Gsdmd*$^{-/-}$*n*=14, *Casp11*$^{-/-}$*n*=10; from 2 independent experiments). All *n* values refer to the number of mice used. Error bars depict mean ± s.e.m. Statistics calculated by one-way ANOVA with Tukey's post hoc tests.

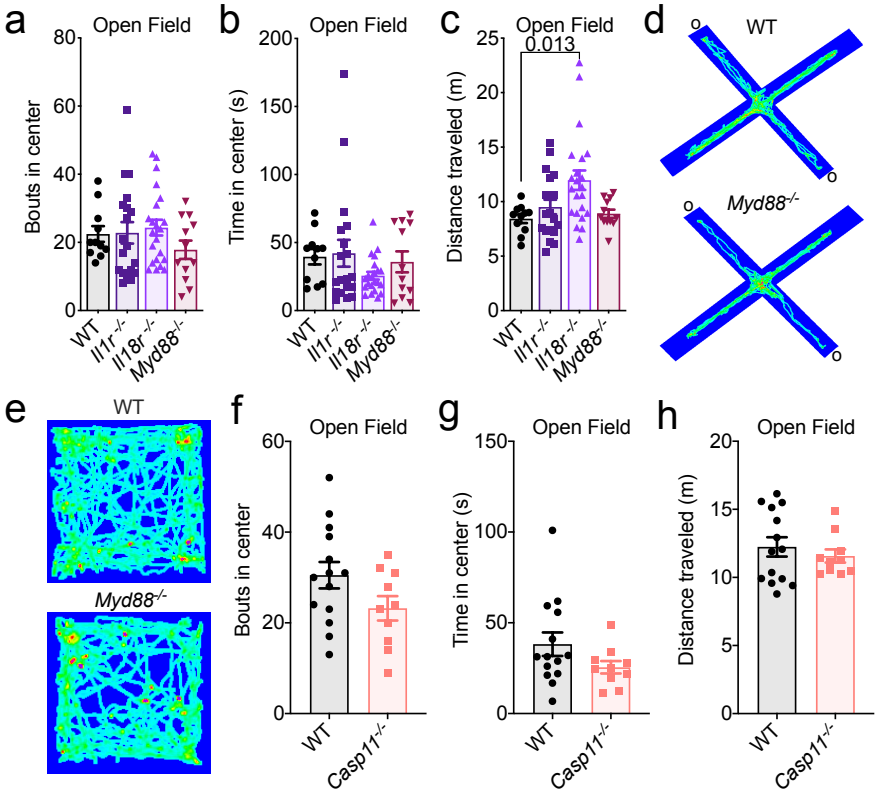

Figure 2.7. Anxiety phenotypes do not develop in mice that lack IL-1R, IL-18R, MYD88, or Caspase-11. All behavioral testing was conducted on adult (8-12 weeks old) mice. (a-c) Behaviors for anxiety were evaluated by (a) bouts into and (b) time spent in the center of the open field arena with (c) total distance traveled (WT *n*=11, Il1r$^{-/-}$ n=19, *Il18r*$^{-/-}$ *n*=22, *Myd88*$^{-/-}$ *n*=12; from 3 independent experiments). (d) Anxiety-related behaviors were assessed in WT and *Myd88*$^{-/-}$ mice using the elevated plus maze. Representative heat maps from 4 independent experiments with similar results depicting path of travel through open arms (o) and closed arms of the maze. (e) Representative heat maps from 4 independent experiments with similar results of the path traveled by adult WT and *Myd88*$^{-/-}$ mice in the open field arena. (f-h) Quantification of (f) bouts into and (g) time in center of the open field arena with (h) distance traveled (WT *n*=14, *Casp11*$^{-/-}$ *n*=10; from 2 independent experiments). All *n* values refer to the number of mice used. Error bars depict mean ± s.e.m. Statistical analysis by (a-c) one-way ANOVA with Tukey's post hoc tests or (f-h) unpaired two-tailed Student's *t*-test showed no statistically significant differences.

AIM2 coordinates neural cell death

It is believed that upwards of half of all neural cells are eliminated during neurodevelopment[166]. This process of neural cell pruning plays beneficial roles in the sculpting of strong connections in the brain and, consistent with this idea, disruptions in CNS cell death during development have been shown to cause neurological dysfunction[166-169]. Neuronal dieback is thought to occur solely through apoptotic cell death; however, this requires revisiting with the recent discovery of other forms of programmed cell death that include pyroptosis, necroptosis, and autophagic cell death[177]. Given our data indicating that the cell death executioner Gasdermin-D and the DNA damage sensor AIM2 both play key roles in limiting neurological dysfunction, we speculated that AIM2 inflammasome-induced cell death may help to prevent genetically compromised cells from being incorporated into the mature brain. To explore this possibility, we first evaluated if AIM2 inflammasome signaling is involved in CNS cell turnover in response to endogenous DNA damage. To this end, mixed cortical neural cells from WT, *Aim2*$^{-/-}$, *Ice*$^{-/-}$, and *Gsdmd*$^{-/-}$ mice were either transfected with dsDNA (PolydA:dT) as a positive control or treated with ionizing radiation or the topoisomerase II inhibitor, etoposide, to induce endogenous DNA damage. We detected a substantial reduction in DNA damage-induced cell death in CNS cells lacking AIM2, Caspase-1/11, or Gasdermin-D (Fig. 2.8 a-b, Fig. 2.9 a-b).

To investigate whether the AIM2 inflammasome plays a role in coordinating neural cell dieback *in vivo*, we evaluated cell death in the cerebellum of WT and AIM2 inflammasome-deficient mice at p5, as this region of the brain has been previously reported to undergo DNA damage-induced cell death at this timepoint in neurodevelopment[77, 171]. We find that genetic ablation of AIM2 leads to reduced levels of cell death as indicated by a decrease in TUNEL and propidium iodide (PI)-positive cell staining in the cerebellums of p5 *Aim2*$^{-/-}$ mice (Fig. 2.8 c, Fig.

2.10 a-c). A reduction in cell death was also seen in *Casp1/11*$^{-/-}$ and *Gsdmd*$^{-/-}$ p5 cerebellums, indicating that the AIM2 inflammasome and Gasdermin-D are involved in orchestrating cell death at p5 in the developing brain (Fig. 2.8 c, Fig. 2.10 a). Notably, disruptions in AIM2 inflammasome signaling were not found to completely abrogate levels of CNS cell death at this timepoint, suggesting that other forms of cell death including apoptosis are also contributing to CNS cell pruning in AIM2 inflammasome-deficient mice. To further test our working model, which proposes that AIM2 inflammasome signaling coordinates the removal of DNA damage harboring CNS cells, we induced overt DNA damage in the developing brains of WT and AIM2-deficient mice by exposing them to ionizing radiation. We found that exposure to ionizing radiation results in increased TUNEL staining in WT and *Aim2*$^{-/-}$ mice; however, IR-induced cell death was substantially blunted in the absence of AIM2 (Fig. 2.10 d-e). These findings suggest that AIM2 is capable of executing cell death in response to IR-driven DNA damage.

AIM2 limits DNA damage levels in the CNS

If the AIM2 inflammasome does indeed function in the purging of genetically compromised cells from the brain, we would then expect that disruptions in this pathway would cause greater incorporation of cells into the adult brain as well as increased levels of DNA damage. Consistent with this idea, we observed increased numbers of calbindin^{+} Purkinje neurons in the brains of mice lacking either AIM2, Caspase-1/11, or Gasdermin-D (Fig. 2.8 d, Fig. 2.11). Furthermore, we also detected markedly enhanced staining of the DNA damage marker γH2AX in the brains of *Aim2*$^{-/-}$ mice (Fig. 2.8 e-h). This increase in DNA damage was seen throughout the brain including in regions that have been linked to fear and anxiety, such as the amygdala (Fig. 2.8 g-h). We also examined levels of DNA damage in the adult cortex using single-cell gel electrophoresis ('comet assay'). These studies confirmed our previous

γH2AX results and showed that deficits in AIM2 lead to substantially increased DNA damage accumulation as indicated by the higher comet tail moment in the brains of AIM2-deficient mice (Fig. 2.8 i-j). Likewise, we also observed increased levels of γH2AX staining in brains of *Ice*$^{-/-}$ and *Gsdmd*$^{-/-}$ mice (Fig. 2.8 k). Although the nature and timing of these dsDNA breaks remains to be determined, it is evident that deficits in AIM2 inflammasome signaling result in elevated accumulation of DNA damage in the brain. Collectively, these findings suggest that the AIM2 inflammasome and Gasdermin-D aid in the removal of DNA damage harboring cells from the brain.

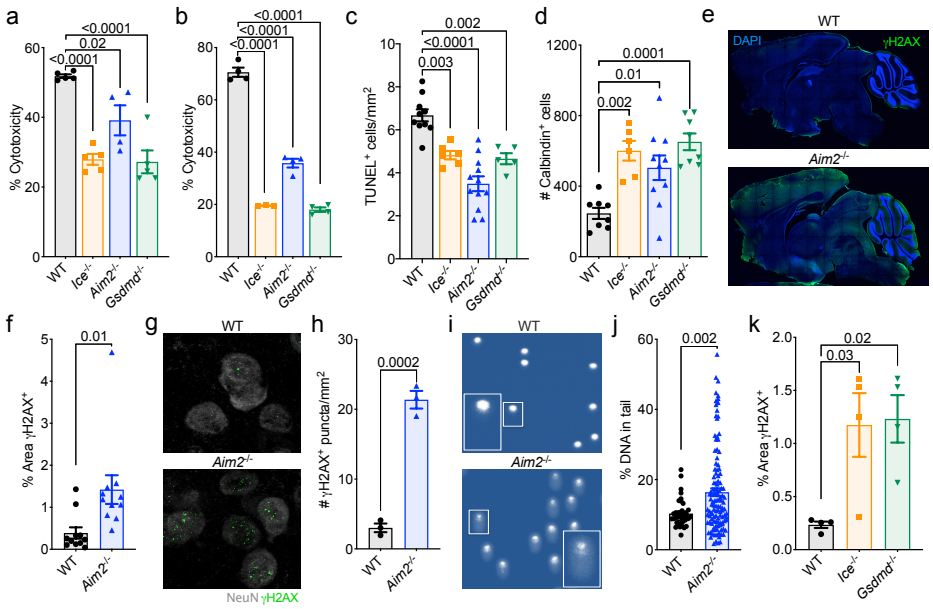

Figure 2.8. Activation of the AIM2 inflammasome in response to DNA damage coordinates CNS cell death and limits the accumulation of DNA damage in the brain. (a-b) Postnatal day 0 (p0) mixed neural cultures were primed with LPS for 4 hrs followed by overnight treatment with either (a) 40 Gy ionizing radiation (WT *n*=5, *Ice*$^{-/-}$ *n*=5, *Aim2*$^{-/-}$ *n*=4, and *Gsdmd*$^{-/-}$ *n*=5) or (b) 100 μM etoposide (WT *n*=4, *Ice*$^{-/-}$ *n*=3, *Aim2*$^{-/-}$ *n*=4, and *Gsdmd*$^{-/-}$ *n*=4). Cell death was measured by LDH release. Representative data from 3 independent experiments. (c) Quantification of cerebellar TUNEL staining in p5 mice (WT *n*=10, *Ice*$^{-/-}$ *n*=6, *Aim2*$^{-/-}$ *n*=12, and *Gsdmd*$^{-/-}$ *n*=5 mice; from 3 independent experiments). (d) Enumeration of cerebellar calbindin^{+} Purkinje neurons in adult (8-12 weeks old) mice (WT *n*=8, *Ice*$^{-/-}$ *n*=6, *Aim2*$^{-/-}$ *n*=10, and *Gsdmd*$^{-/-}$ *n*=8 mice; from 3 independent experiments). (e-f) Adult brains were evaluated for levels of DNA damage (γH2AX, green). (e) Representative images from 3 independent experiments with similar results. (f) Quantification of γH2AX staining in adult mice (WT *n*=11, *Aim2*$^{-/-}$*n*=11; from 3 independent experiments). (g-h) Adult brains were evaluated for γH2AX staining in NeuN-expressing neurons in the amygdala. (g) Representative images from 2 independent experiments with similar results. (h) Enumeration of γH2AX puncta in the amygdala (WT *n*=3, *Aim2*$^{-/-}$ *n*=3; representative data from 2 independent experiments). (i-j) DNA damage was evaluated in the cortex of 10-week-old WT and *Aim2*$^{-/-}$ mice by comet assay. (i) Representative images of single cell electrophoresis gels from 3 independent experiments with similar results. (j) Quantification of percent DNA in tail (WT *n*=38, *Aim2*$^{-/-}$ *n*=120; from 3 independent experiments). (k) Quantification of γH2AX staining in sagittal brain sections from WT *n*=4, *Ice*$^{-/-}$ *n*=4, and *Gsdmd*$^{-/-}$ *n*=4 mice; from 2 independent experiments. Error bars depict mean ± s.e.m. Statistics calculated by (a-d,k) one-way ANOVA with Tukey's post hoc tests and (f,h,j) unpaired two-tailed Student's *t*-test. (a-b,j) *n* values refer to biological replicates from representative experiments. (c-d,f,h,k) *n* values refer to the number of mice used.

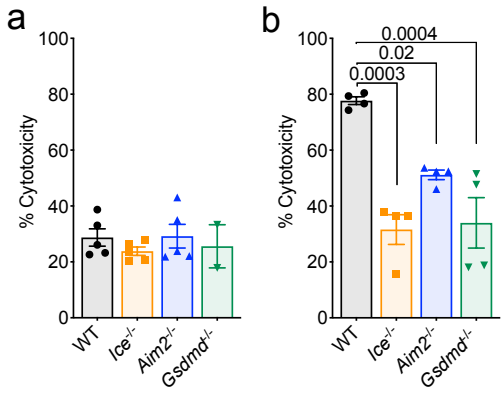

Figure 2.9. Genetic ablation of the AIM2 inflammasome or Gasdermin-D in CNS cells limits cell death in response to DNA insults. Mixed neural cultures were generated from postnatal day 0 (p0) WT, *Ice*$^{-/-}$, *Aim2*$^{-/-}$, and *Gsdmd*$^{-/-}$ mice. (a) Mixed neural cell cultures were left untreated to test for baseline differences in cytotoxicity (WT *n*=5, *Ice*$^{-/-}$ *n*=5, *Aim2*$^{-/-}$ *n*=5, and *Gsdmd*$^{-/-}$ *n*=2). (b) Mixed neural cell cultures were primed with LPS for 4 hrs followed by transfection with PolydA:dT (WT *n*=4, *Ice*$^{-/-}$ *n*=4, *Aim2*$^{-/-}$ *n*=4, and *Gsdmd*$^{-/-}$ *n*=4). Cell death was measured by LDH release after overnight stimulation. Representative data from 3 independent experiments. All *n* values refer to biological replicates from one representative experiment. Error bars depict mean ± s.e.m. Statistics calculated by one-way ANOVA with Tukey's post hoc tests.

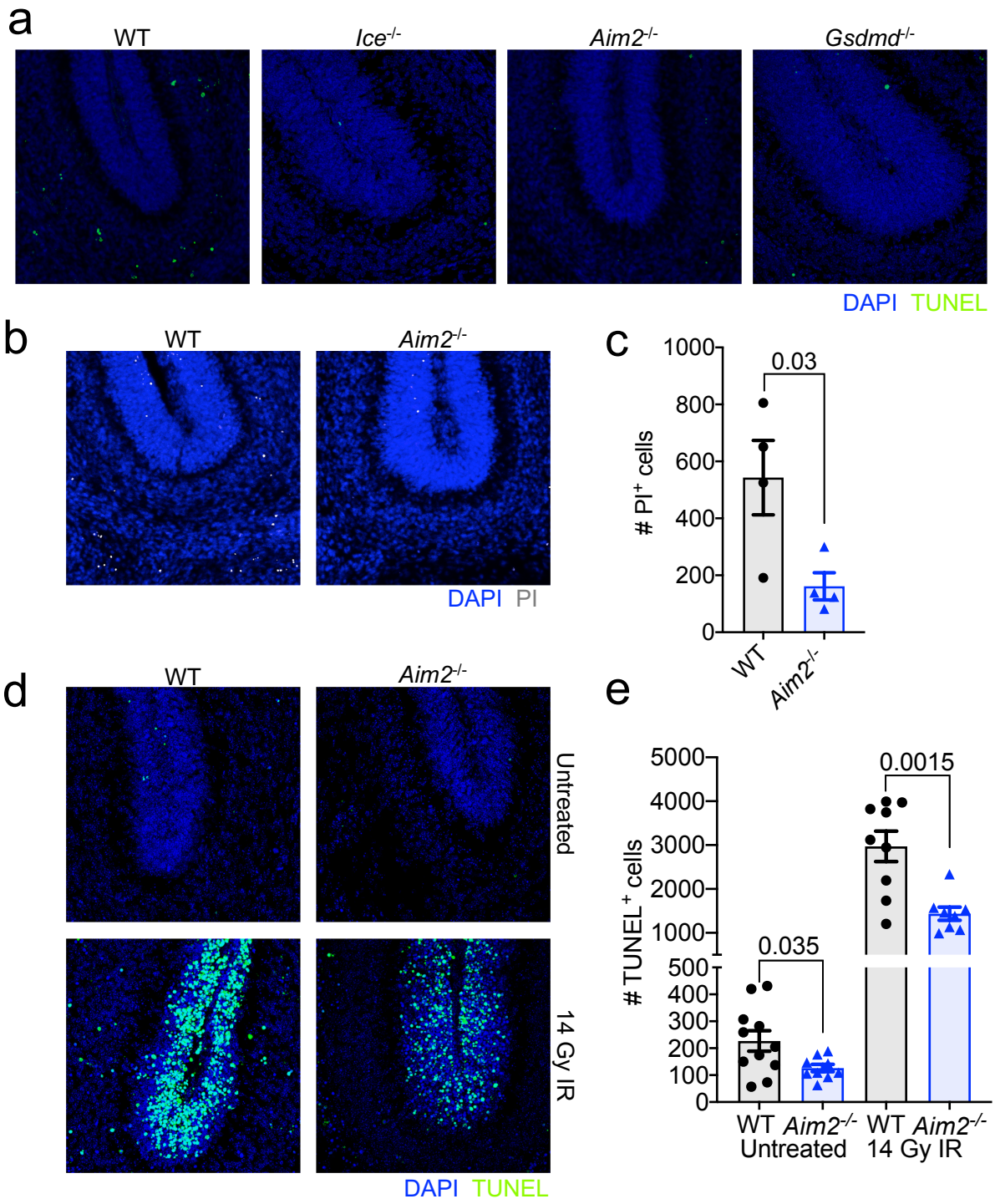
a
WT
Ice-/-
Aim2-/-
Gsdmd-/-
DAPI TUNEL
b
WT
Aim2-/-
DAPI PI
c
PI+ cells
1000
800
600
400
200
0
0.03
WT
Aim2-/-
d
WT
Aim2-/-
Untreated
14 Gy IR
DAPI TUNEL
e
TUNEL+ cells
5000
4000
3000
2000
1000
500
400
300
200
100
0
0.035
0.0015
WT Aim2-/-
Untreated
WT Aim2-/-
14 Gy IR

Figure 2.10. AIM2 contributes to CNS cell death during neurodevelopment and in response to ionizing radiation. (a) Representative 20X images from p5 WT, *Ice*$^{-/-}$, *Aim2*$^{-/-}$, and *Gsdmd*$^{-/-}$ mice showing TUNEL^{+} cells (green) in the cerebellum. Images are representative from 2 independent experiments with similar results. (b) Representative images of additional markers of cell death (propidium iodide (PI), grey) in p5 WT and *Aim2*$^{-/-}$ mice. (c) Quantification of PI^{+} cells in the cerebellum of p5 WT *n*=4 and *Aim2*$^{-/-}$ *n*=4 mice; from 1 independent experiment. (d-e) p5 WT and *Aim2*$^{-/-}$mice received either control treatment or 14 Grays (14 Gy) of ionizing radiation (IR) to induce DNA damage. Brains were harvested 6 hrs later and then TUNEL assay staining was conducted on cerebellar sections to evaluate cell death. (d) Representative 20X images showing TUNEL staining in the cerebellum of untreated and irradiated p5 WT and *Aim2*$^{-/-}$mice; from 3 independent experiments with similar results. (e) Quantification of number of TUNEL^{+} cells in the cerebellums of untreated and irradiated WT (*n*=11 untreated; *n*=9 IR) and *Aim2*$^{-/-}$ (*n*=9 untreated; *n*=8 IR) mice; from 3 independent experiments. All *n* values refer to the number of mice used. Error bars depict mean ± s.e.m. Statistics calculated by unpaired two-tailed Student's *t*-test.

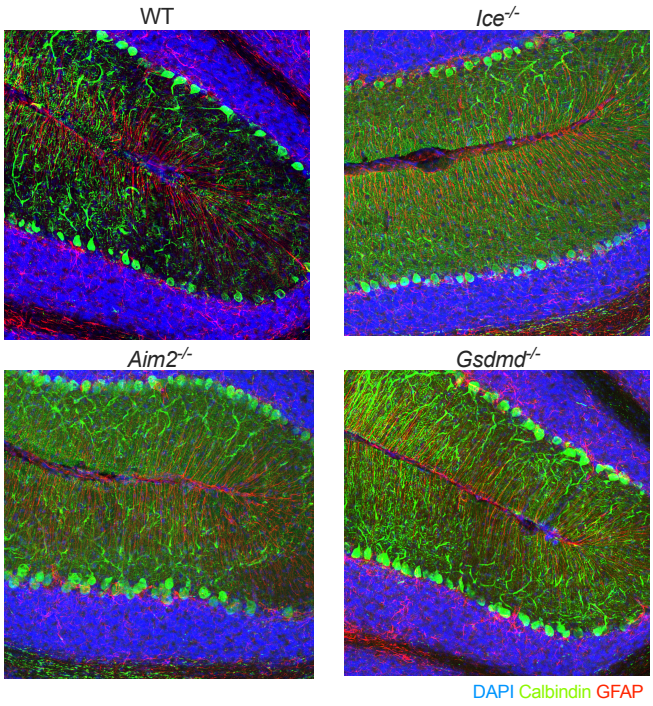

Figure 2.11. Lack of AIM2 inflammasome components increases the number of Purkinje neurons that are incorporated into the adult brain. Representative 20X images of cerebellums from adult (8-12 weeks old) WT, *Ice*$^{-/-}$, *Aim2*$^{-/-}$, and *Gsdmd*$^{+/-}$ mice showing an increase in number of Purkinje cells (calbindin^{+} cells) in mice lacking inflammasome components. Representative images from 3 independent experiments with similar results.

Local inflammasome activation within the CNS impacts behavior

Mounting evidence suggests that immune activation in the periphery can have profound effects on brain maturation and behavior[178]. Therefore, it is feasible that inflammasome signaling can shape behavior and neurodevelopment both through its local actions in the brain and also via its functions in the periphery. To investigate this in greater detail, we first sought to identify what CNS-derived cell types express *Aim2* during neurodevelopment. Using fluorescent in situ hybridization, we found that *Aim2* is appreciably expressed by microglia, astrocytes, and neurons in the developing brain (Fig. 2.12 a-b). Microglia are the innate immune sentinels of the brain and recent work suggests that microglia-coordinated innate immune responses can greatly impact brain development and function[179]. To our surprise, we found that deletion of Caspase-1 in CX3CR1-expressing cells, which includes microglia, does not result in the development of anxiety-related behaviors in either the open field or elevated plus maze tests (Fig. 2.13 a-c). In contrast, we found that conditional ablation of Caspase-1 from Nestin-expressing CNS cells (i.e. neurons, astrocytes, and oligodendrocyte lineage cells) in *Casp1*$^{fl/fl}$*Nestin*^{Cre} mice leads to anxiety-related behaviors and the accumulation of DNA damage in the brain (Fig. 2.14 a-g). These data indicate a specific role for Caspase-1 within the CNS in driving the observed behavioral phenotypes and preventing DNA damage accumulation.

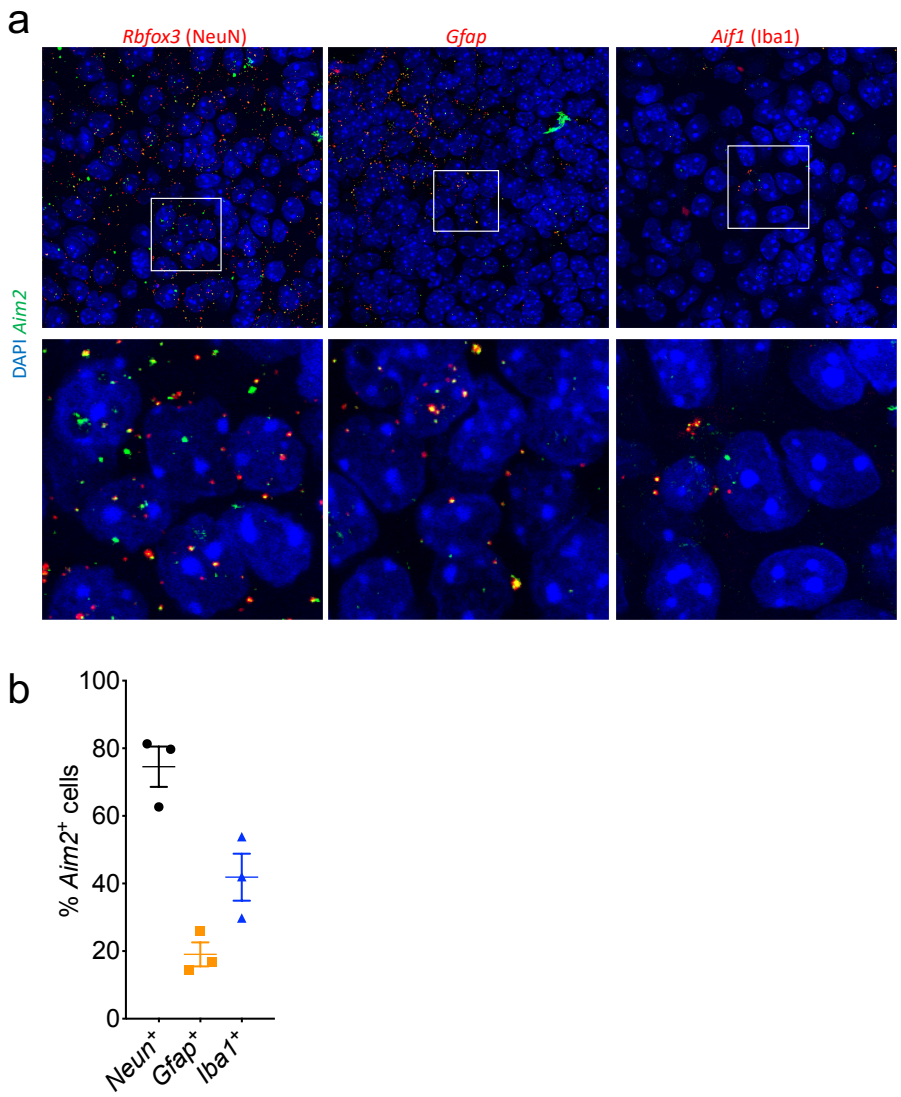

Figure 2.12. *Aim2* is expressed by neurons, astrocytes, and microglia in the developing brain. Brains from p5 WT mice (*n*=3; from 1 experiment) were evaluated for expression of *Aim2* using RNA scope. (a) Images showing co-expression of *Aim2* (green) and CNS cell-specific genes *Rbfox3*: NeuN (red), *Gfap*: GFAP (red), and *Aif1*: Iba1 (red) in the hippocampus. (b) Quantification showing percentage of CNS cells in 40X images that are positive for *Aim2.* Error bars depict mean ± s.e.m. *n* values refer to biological replicates.

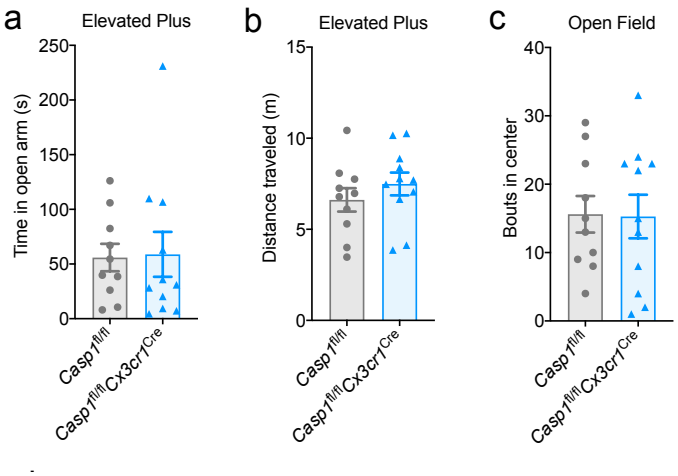

Figure 2.13. Deletion of Caspase-1 in CX3CR1-expressing cells does not result in the development of anxiety-related behaviors. Adult (8-12 weeks old) *Casp1*$^{fl/fl}$ *n*=10 and *Casp1* $^{fl/fl}$ *Cx3cr1*^{Cre} *n*=11 mice were evaluated for anxiety-related behaviors using (a) time in open arms and (b) distance traveled in the elevated plus maze along with (c) total bouts into the center of the open field arena; from 2 independent experiments. All *n* values refer to the number of mice used. Error bars depict mean ± s.e.m. Statistical analysis by unpaired two-tailed Student's *t*-test showed no statistically significant differences.

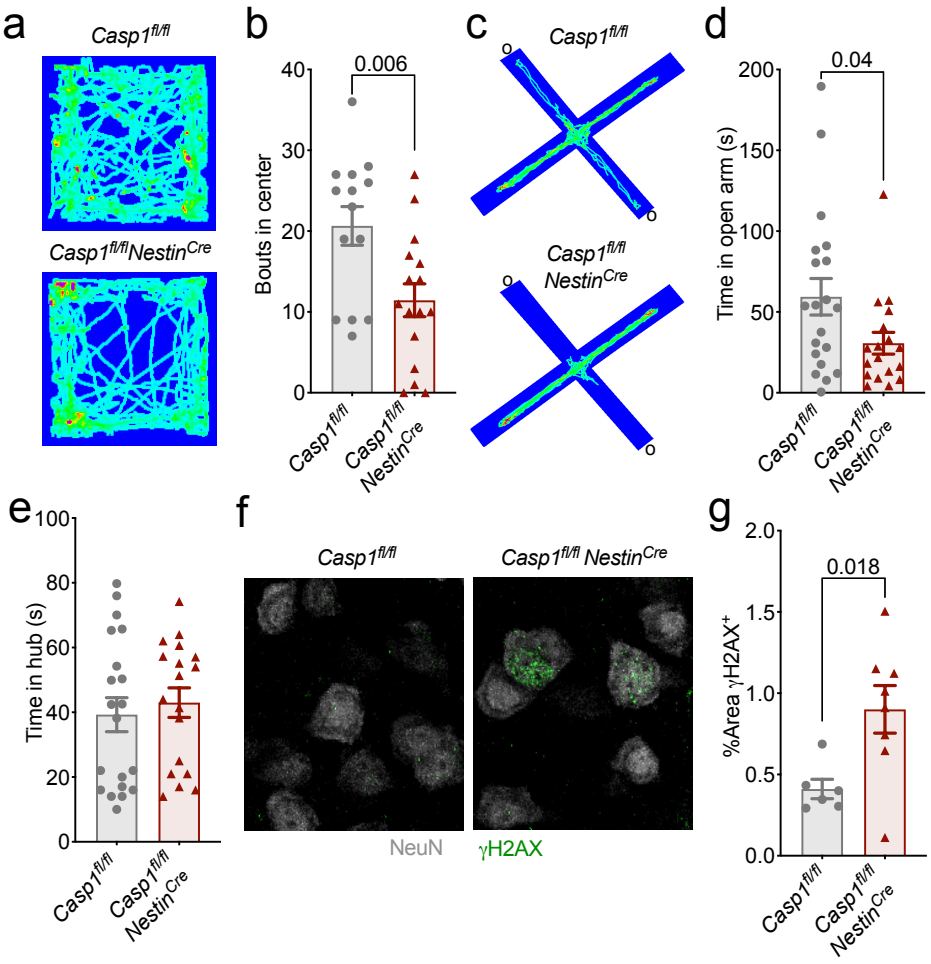

Figure 2.14. CNS-specific deletion of Caspase-1 results in anxiety-like behaviors and DNA damage accumulation in the brain. (a-e) Anxiety-associated behaviors were assessed in adult (8-12 weeks old) *Casp1*$^{fl/fl}$ and *Casp1* $^{fl/fl}$ *Nestin* ^{Cre} mice**.** (a) Representative heat maps of the path mice traveled in the open field arena; from 3 independent experiments with similar results. (b) Quantification of bouts into the center of the open field arena (*Casp1* $^{fl/fl}$ *n=14, Casp1* $^{fl/fl}$*Nestin* ^{Cre} *n*=16; from 3 independent experiments). (c) Representative heat maps depicting path of travel through open arms (o) and closed arms of the elevated plus maze; from 4 independent experiments with similar results. (d) Quantification of time spent in the open arms of the elevated plus maze and (e) time in the hub (*Casp1* $^{fl/fl}$ *n=20, Casp1* $^{fl/fl}$ *Nestin* ^{Cre} *n*=18; from 4 independent experiments). (f-g) Adult brains were evaluated for levels of DNA damage (γH2AX, green) in NeuN-expressing neurons. (f) Representative cortex images from 2 independent experiments with similar results. (g) Quantification of γH2AX staining in cortical brain sections (*Casp1* $^{fl/fl}$ *n*=6 and *Casp1* $^{fl/fl}$ *Nestin* ^{Cre} *n*=8; from 2 independent experiments). All *n* values refer to the number of mice used. Error bars depict mean ± s.e.m. Statistics calculated by unpaired two-tailed Student's *t*-test.

Discussion

Our results underscore how deficits in the immune response to DNA insults can lead to impaired CNS development and neurological disease. The long-lived nature of neurons and glia, coupled with their exposure to high levels of replicative stress during neurodevelopment, makes the CNS especially vulnerable to DNA damage-induced dysfunction and pathology[72, 74]. Yet, how the brain protects itself from genotoxic stress remains incompletely understood. Here we demonstrate that DNA damage surveillance by the AIM2 inflammasome is required for normal brain development and function. We found that the AIM2 inflammasome and downstream Gasdermin-D-mediated cell death contribute to the elimination of genetically compromised CNS cells. Furthermore, we report that disruptions in this pathway lead to the development of anxiety-related behaviors, DNA damage accumulation in the CNS, and increased numbers of neurons in the adult brain (Fig. 2.15). It is commonly assumed that CNS dieback relies solely on apoptosis as a cell death pathway to remove unwanted cells. Yet, this assumption was made at a time when it was thought that there were only two forms of cell death (i.e. apoptosis and necrosis). Our findings demonstrating decreased CNS cell death and greater incorporation of neurons into the brains of Gasdermin-D-deficient mice implicate the involvement of another form of cell death, namely pyroptosis, in the sculpting of the brain. Further elucidation of the functional consequence of DNA damage sensing by the innate immune system may offer novel strategies to treat a wide range of neurological disorders that are perpetuated by genotoxic stress.

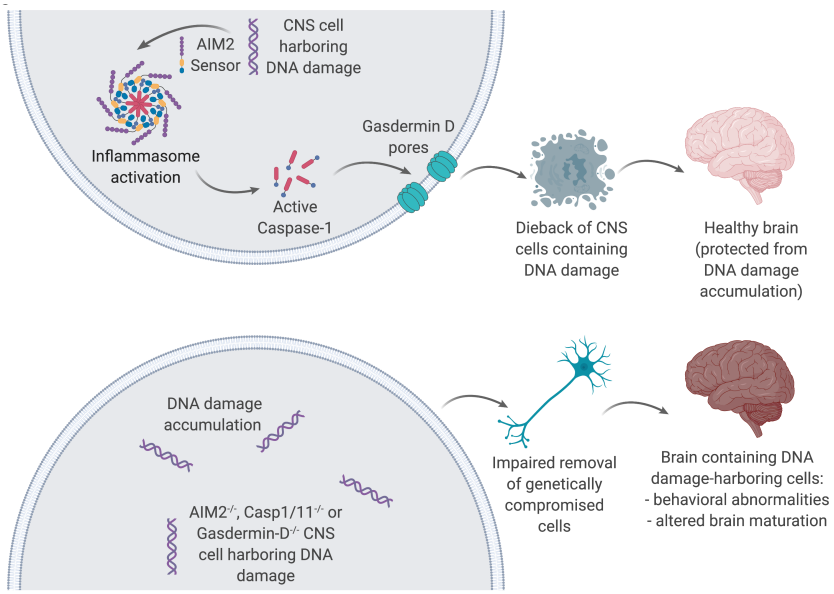

Figure 2.15. Graphical Abstract Schematic of the proposed role that DNA damage surveillance by the AIM2 inflammasome plays in neurodevelopment.

Chapter 3: IL-1β is sufficient to induce behavioral phenotypes associated with MIA

Abstract

Although aberrant inflammatory responses have been widely speculated to be involved in autism pathogenesis, the specific immune pathways that lead to abnormal neurodevelopment still remain elusive. The proinflammatory cytokine interleukin-1 (IL-1) has been reported to perturb various aspects of CNS function and development. IL-1 is also one of the most highly expressed inflammatory mediators in autistic individuals. However, whether dysregulated IL-1 production is a cause or consequence of ASD has not been formally investigated. In preliminary experiments, we show injection of IL-1β into a pregnant dam is sufficient to induce autism like phenotypes in male offspring.

Introduction

Despite certain cytokines being identified as key regulators of neurodevelopmental diseases, it is not known how these molecules mechanistically affect neurodevelopment. Despite the fact that increased levels of a variety of cytokines are seen in the brains and cerebral spinal fluid (CSF) of autistic individuals and experimental models of ASD, how these cytokines influence various aspects of neurodevelopment such as astrogliosis, neurogenesis, and/or microglial pruning remains unknown. It is important to elucidate the pathways both upstream and downstream of IL-6 and IL-17a in order to gain a better understanding of the mechanisms through which maternal inflammation can contribute to the development of neurodevelopmental disorders such as ASD. In addition, a better understanding of these pathways could provide important therapeutic insights and developments.

One of the most potent cytokines of the innate immune response is interleukin-1 (IL-1). IL-1 affects virtually all cells and organs including the central nervous system (CNS), where it has been shown to induce fever, alter both glia and neuronal biology, and contribute to

neuropathology. Moreover, IL-1 is a major pathogenic mediator of autoimmune, infectious, neurodegenerative, and auto-inflammatory diseases[180]. IL-1 is also known to be a pivotal regulator of cytokines that have been implicated in ASD, including IL-6 and IL-17a. For instance, signaling through the IL-1 receptor (IL-1R) induces the production of secondary inflammatory cytokines, including IL-6[181]. Moreover, IL-1 has also been shown to perpetuate T cell induction of pathogenic cytokines, such as IL-17a and IFN-γ[182].

IL-1 exists in two forms: IL-1α and IL-1β. IL-1α and IL-1β signal through the same receptor complex and therefore have similar biological functions; however, the two cytokines differ in a few ways. IL-1α is constitutively expressed in the epithelial layers of many organs and has a nuclear localization signal that brings IL-1α to the nucleus where it functions as a component of transcription[11, 183]. Unlike IL-1β, IL-1α is biologically active in its pro-form and can function as an alarmin. IL-1β, on the other hand, is produced by hematopoietic cells such as blood monocytes, tissue macrophages, and dendritic cells. IL-1β is not active as a precursor and must undergo cleavage by caspase-1 to become biologically active. In order to produce the active form of IL-1β, caspase-1 must first undergo activation-induced cleavage in inflammasome complexes.

There is some evidence that IL-1β plays a key role in aspects of neurodevelopment. One study showed that ectopic delivery of IL-1β into a spinal cord of a chick during embryonic development results in an increase in proliferating cells, suggesting a potential role for IL-1 during development[184]. Giard *et al.* also demonstrated blocking IL-1 signaling can protect against the adverse effects that LPS has on fetal development[185]. Autistic individuals also have been reported to have significantly elevated levels of IL-1 in their serum, brain, and CSF [186, 187]. Moreover, heightened serum levels of IL-1β have been correlated with severe impairments in

communication and aberrant behaviors in autistic individuals[188]. Due to these significant correlations between human samples and established pathogenic cytokines, IL-1 is a target for autism research and has thus far been unexplored. In preliminary studies using the MIA model of autism, we found that IL-1-dependent signaling is critically involved in promoting the development of certain autistic behaviors.

Results

Maternal Immune Activation results in ASD associated behaviors

First, we established the model of MIA-induced autism in our lab (Figure 3.1). We found that the offspring of pregnant dams exposed to 20 mg/kg Poly(I:C) at E11.5 and 12.5 showed abnormal behaviors reminiscent of core ASD phenotypes compared to the saline injected controls. These behaviors include a decrease in communication, impaired social behavior, and increased repetitive behaviors (Fig. 3.2). Communication was measured by quantifying the number of ultrasonic vocalizations made by p10 pups following separation from their mother. The offspring of Poly(I:C) injected females called significantly less than the saline injected controls (Fig. 3.2 a-b). To measure social anxiety, a three-chamber sociability test was performed. At 8 weeks of age, experimental mice were placed into a neutral chamber and allowed to freely roam between a chamber containing a novel mouse and a chamber containing a novel object. Mice are normally social and would therefore choose to spend time with a mouse rather than an object, as seen in the saline injected offspring (Fig. 3.2 c). However, offspring of mothers injected with Poly(I:C) did not prefer to spend more time with the mouse, demonstrating decreased social interaction as is seen with many ASD patients (Fig. 3.2 c). Repetitive or stereotyped behaviors are the third phenotypic hallmark of ASD behaviors. In order to test these behaviors in mice, a marble-burying assay was performed in which mice were introduced to 20

marbles for 15 minutes. The number of marbles buried was then enumerated and mice that bury more marbles are said to demonstrate repetitive behaviors. Offspring of Poly(I:C) injected mothers buried significantly more marbles than saline controls (Fig. 3.2 d). These three behavioral assays confirm MIA-induced autism can be modeled in our lab.

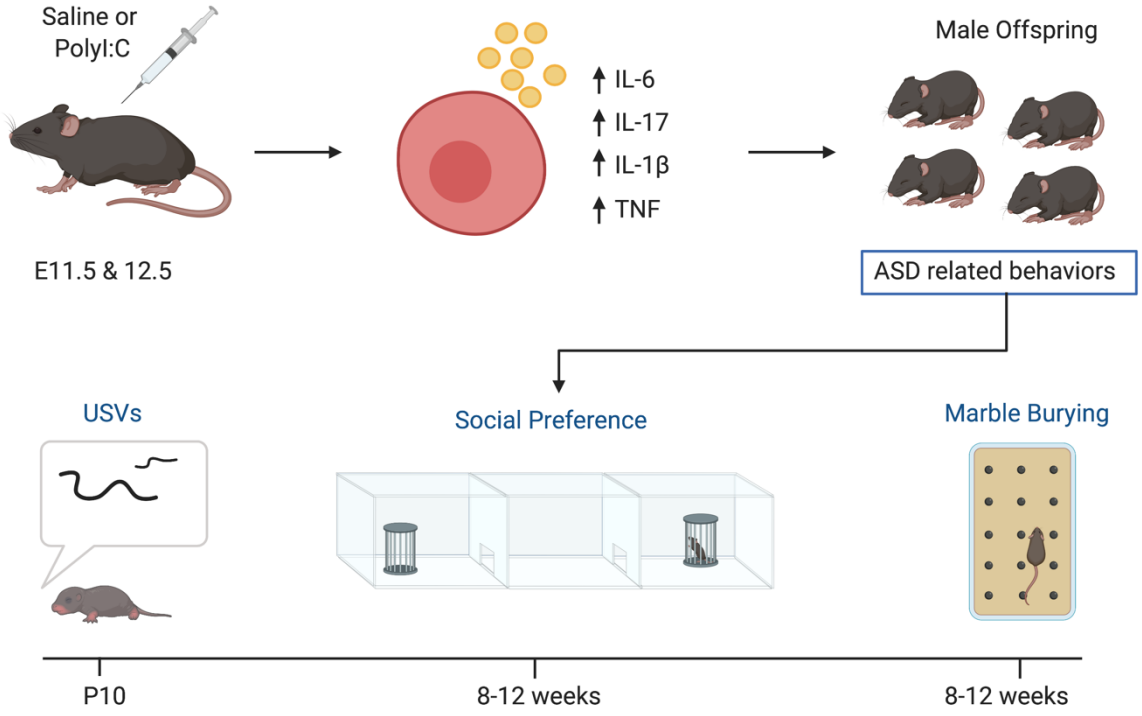

Figure 3.1. Maternal Immune activation timeline. Timeline depicting key stages of the MIA model of autism.

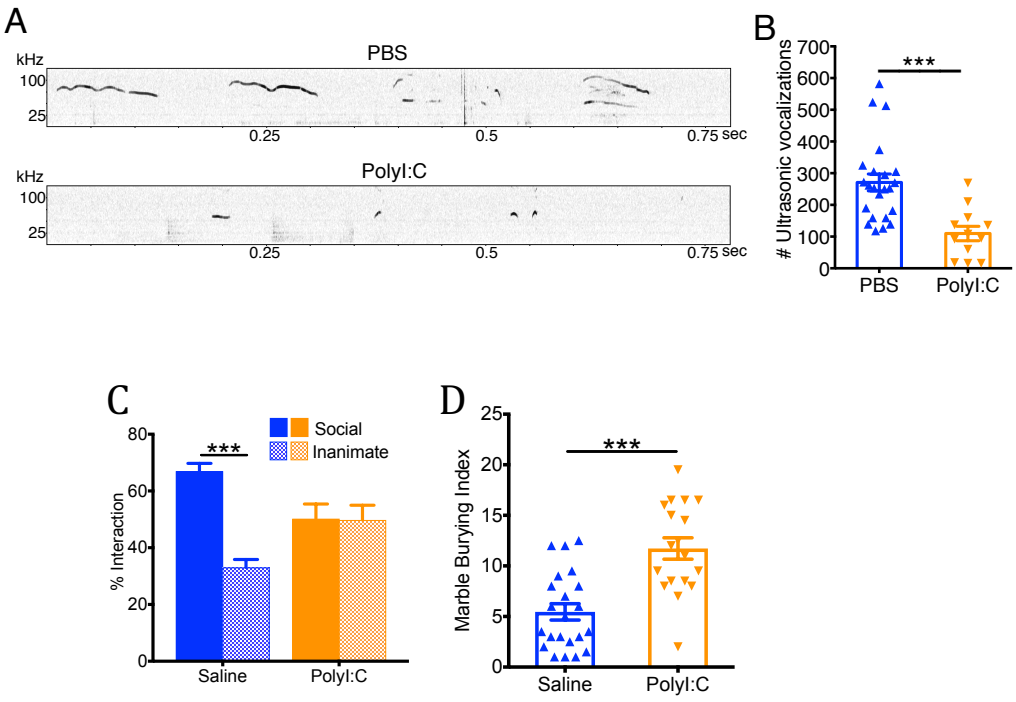

Figure 3.2. Behavioral abnormalities observed in MIA offspring. Pregnant C57BL/6 mice were treated with either saline or 20 mg/kg Poly(I:C) at embryonic days 11.5 (E11.5) and 12.5 (E12.5). (A-B) Communicative deficits in 10-day old pups were evaluated through recording of ultrasonic vocalizations (USVs). (A) Representative USV detection plots. (B) Total number of USVs emitted during 3 minutes of recording. (C) 8wk old mice were evaluated for social behavior using the three chamber preference test. Graph depicts percent interaction with a novel mouse (social) and object (inanimate). (D) 8wk old mice were evaluated for repetitive behaviors using a Marble burying test. Graph represents marble burying index. ***$P < 0.001$ calculated by Student's t-test.

IL-1β is sufficient to induce the behavioral abnormalities associated with MIA

In order to determine the extent to which IL-1 signaling contributes to neurodevelopmental abnormalities and ASD-associated phenotypes, we injected pregnant dams at E11.5 and E12.5 with 1.5 ug of bioactive murine IL-1β. The offspring were then analyzed for typical ASD phenotypes using the behavioral assays described in detail above. We found that IL-1β injection during pregnancy is sufficient to drive offspring to develop abnormalities in communication (Fig. 3.3 a), social interaction (Fig. 3.3 b), and repetitive/stereotyped behaviors (Fig 3.3 c) to the same degree as seen in the classical Poly(I:C)-induced model of autism.

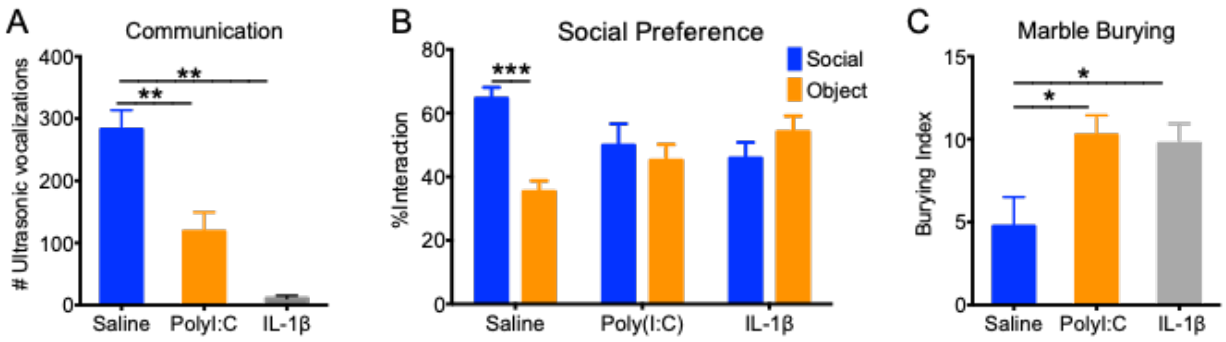

Figure 3.3. IL-1β is sufficient to induce behavioral abnormalities associated with MIA. Pregnant C57BL/6 mice were treated with either saline, 20 mg/kg Poly(I:C), or 1.5μg IL-1β at embryonic days 11.5 (E11.5) and 12.5 (E12.5). (A) Communicative deficits in 10-day old pups were evaluated through recording of ultrasonic vocalizations (USVs). Graph depicts total number of USVs emitted during 3 minutes of recording. (B) 8wk old mice were evaluated for social behavior using the three chamber preference test. Graph depicts percent interaction with a novel mouse (social) and object (inanimate). (D) 8wk old mice were evaluated for repetitive behaviors using a Marble burying test. Graph represents marble burying index.

Blocking IL-1 signaling protects against MIA-associated behavioral abnormalities

Lastly, we wanted to investigate if neutralization of IL-1β signaling both prior to and post Poly(I:C) injections would be sufficient to protect the offspring from developing ASD associated behavioral abnormalities. To accomplish this, we injected pregnant dams at E11.5 and 12.5 first with a IL-1 blocking antibody, Anakinra, followed a by Poly(I:C) or saline injection. We continued to dose the pregnant females with Anakinra until E16.5 in order to ensure that IL-1 signaling was blocked until the inflammatory response from Poly(I:C) was diminished (Figure 3.4). Behavioral analysis of the male offspring indicated that blocking IL-1 signaling during MIA was sufficient to protect against MIA-associated behavioral abnormalities. Male offspring from mothers who were given anakinra displayed normal levels of communication and social interaction (Figure 3.4).

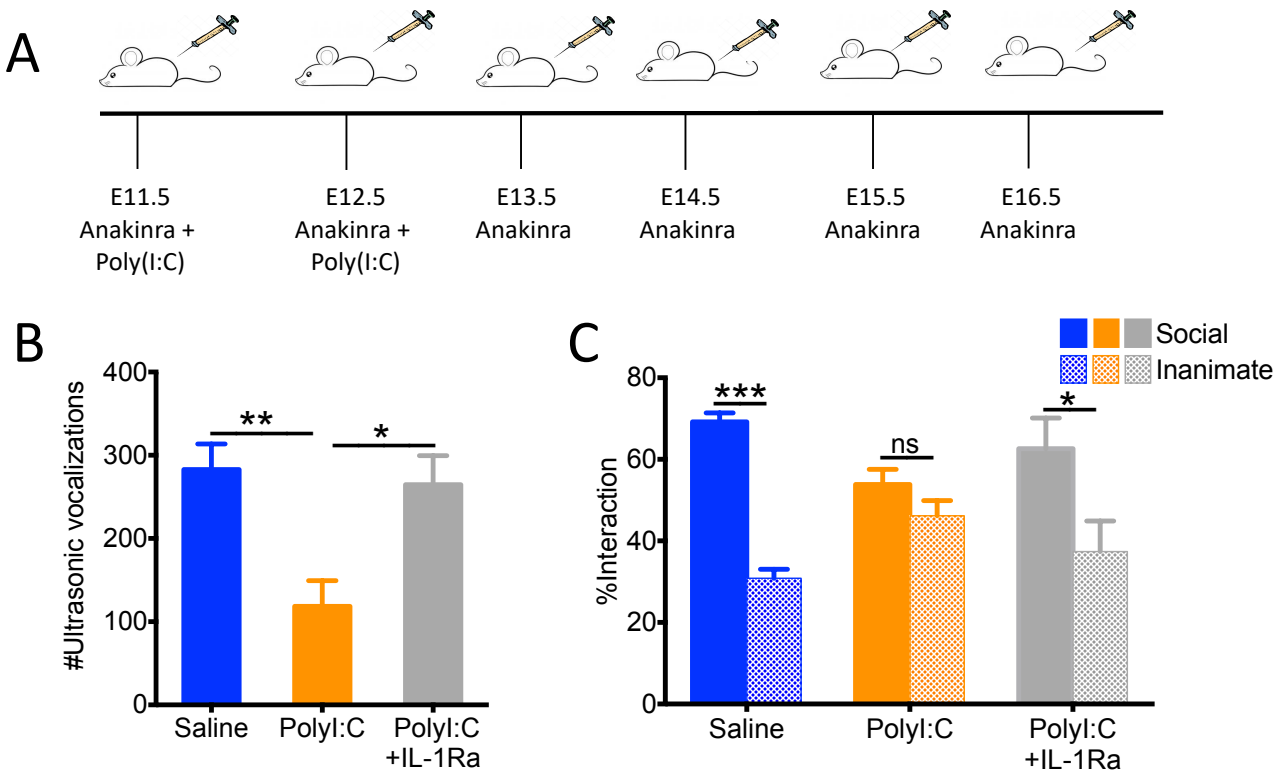

Figure 3.4. Blocking IL-1 signaling protects against MIA-associated behavioral abnormalities. (A) Pregnant C57BL/6 mice were treated with either saline or 20 mg/kg Poly(I:C), at embryonic days 11.5 (E11.5) and 12.5 (E12.5) as well as Anakinra from E11.5-E16.5. (B) Communicative deficits in 10-day old pups were evaluated through recording of ultrasonic vocalizations (USVs). (C) 8wk old mice were evaluated for social behavior using the three-chamber preference test. Graph depicts percent interaction with a novel mouse (social) and object (inanimate).

Discussion

Collectively, these results identify IL-1 as a novel mediator in the pathogenesis of MIA-driven autism and suggest that aberrant IL-1 signaling is sufficient to promote the development of autistic behaviors. We demonstrate that injection of IL-1β alone is sufficient to induce the behavioral abnormalities seen with the more traditional MIA activator, Poly(I:C). We find injection with either Poly(I:C) or IL-1β results in ASD-associated behaviors including decreases in communication and social interaction as well as an increase in repetitive/stereotyped behaviors. Moreover, we find that blocking IL-1β signaling induced by Poly(I:C) protects against the development of behavioral abnormalities commonly associated with ASD. Key future experiments will be aimed to investigate the mechanism by which IL-1 signaling is impacting fetal neurodevelopment. It will be important to uncover where IL-1 is acting, whether in the mother or in the fetus, to drive abnormal behaviors. Other open questions that are important to investigate are the cellular targets of IL-1 signaling and the timepoints in which aberrant IL-1 signaling results in altered neurodevelopment and behavior.

Chapter 4: Critical Roles for Microbiota-Mediated Regulation of the Immune System in a Prenatal Immune Activation Model of Autism

Abstract

Recent studies suggest that autism is often associated with dysregulated immune responses and altered microbiota composition. This has led to growing speculation of potential roles for hyperactive immune responses and the microbiome in autism. Yet, how microbiome-immune crosstalk contributes to neurodevelopmental disorders currently remains poorly understood. Herein, we report critical roles for prenatal microbiota composition in the development of behavioral abnormalities in a maternal immune activation (MIA) model of autism that is driven by the viral mimetic poly(I:C). We show that microbiota transplantation can transfer susceptibility to MIA-associated neurodevelopmental disease and that this is associated with modulation of the maternal immune response. Furthermore, we find that ablation of IL-17a signaling provides protection against the development of neurodevelopmental abnormalities in MIA offspring. Our findings suggest that microbiota landscape can influence MIA-induced neurodevelopmental disease pathogenesis and that this occurs as a result of microflora-associated calibration of gestational IL-17a responses.

Introduction

The etiology of autism spectrum disorder (ASD) currently remains poorly understood; however, emerging clinical and experimental evidence suggests central roles for immune dysregulation in autism pathogenesis[150, 188, 189]. Our understanding of the immunological processes underlying neurodevelopmental abnormalities in the MIA model is still limited. Recent evidence indicates roles for IL-17a and IL-6 in promoting MIA-induced neurodevelopmental disease [150, 152-154]; however, there are likely other immune pathways that contribute to altered neurodevelopment. In addition to immune dysfunction, autism in humans has also been associated with dysbiosis and gastrointestinal inflammation [148, 190, 191], which has led to

increasing speculation of a role for the microbiome in ASD. Furthermore, recent studies have identified pivotal roles for the microbiome in the regulation of neurological disease progression, brain function, and neurodevelopment [147, 192]. Given the extensive clinical evidence of dysbiosis in autism [148, 190] and emerging data implicating key roles for the microbiome-gut-brain axis in neurological disorders [147, 192], we were interested in determining whether differences in maternal microbiota composition affect the induction of ASD-related phenotypes in the MIA model. To investigate this, we capitalized on the well-described differences in intestinal microbial landscape that exist between C57BL/6 mice originating from The Jackson Laboratories (Jax) and Taconic Biosciences (Tac) [193, 194]. Studies show that C57BL/6 mice from these vendors harbor distinct intestinal microflora and that these differences in microbiota landscape uniquely modify aspects of the immune response [193, 194]. A well-described example of this is the skewing of T cell responses towards IL-17a production by the commensal segmented filamentous bacteria (SFB) in Taconic mice[193].

Herein, we report that microflora landscape dictates neurodevelopmental disease susceptibility in a gestational inflammation-based model of autism. Moreover, we identify the microbiome as a pivotal modulator of maternal immune responses and demonstrate that blockade of IL-17a signaling during gestation ameliorates the development of neurodevelopmental abnormalities in MIA offspring.

Results

MIA preferentially induces the development of autism-related phenotypes in Taconic C57BL/6 mice

To better understand how alterations in maternal microbiota diversity impact the development of autism-related phenotypes, we treated C57BL/6 Jackson and Taconic mice with

either Poly(I:C) to induce prenatal MIA or saline as a control at E11.5 and E12.5. Offspring from Poly(I:C)-treated mothers develop many of the defining features of ASD including abnormalities in social preference, communicative impairments, and repetitive/stereotyped behaviors. We first assessed communicative irregularities by recording ultrasonic vocalizations (USVs) in control and MIA pups following separation from their mothers. Offspring from Poly(I:C)-treated Taconic dams made substantially fewer calls and vocalized for shorter total durations than pups from saline-treated Taconic mothers (Fig. 4.1 a-b). On the other hand, MIA offspring from Jackson dams did not display communicative deficits and vocalized as frequently and for the same duration of time as control offspring from both Jackson and Taconic mothers (Fig. 4.1 a-b). Next, we evaluated the development of ASD-related abnormalities in social behavior using the three-chamber social preference test. Adult offspring from Poly(I:C)-treated Taconic dams exhibited irregular social behavior as indicated by the lack of preference for the novel mouse over the novel object in this test (Fig. 4.1 c-d). In contrast, prenatal exposure to MIA did not appreciably influence sociability in Jackson mice (Fig. 4.1 c-d). Distance traveled in the sociability test was similar between all groups (Fig. 4.1 e**)**, suggesting that the abnormal social behavior detected in MIA offspring from Taconic dams was likely not due to differences in overall activity or arousal. Repetitive and stereotyped behaviors are also hallmarks of autism; therefore, we next assessed repetitive/stereotyped behaviors in our experimental mice using the marble-burying test. In these studies, we found that Taconic MIA mice exhibited excessive repetitive behaviors and buried significantly more marbles than control offspring from saline-treated mothers (Fig. 4.1 f). In contrast, no significant differences in marble burying behavior were detected between MIA and control Jackson offspring (Fig. 4.1 f). Taken together, these findings indicate that vendor-specific differences in C57BL/6 mouse colonies prominently influence the development of autism-related behaviors in the MIA mouse model of ASD.

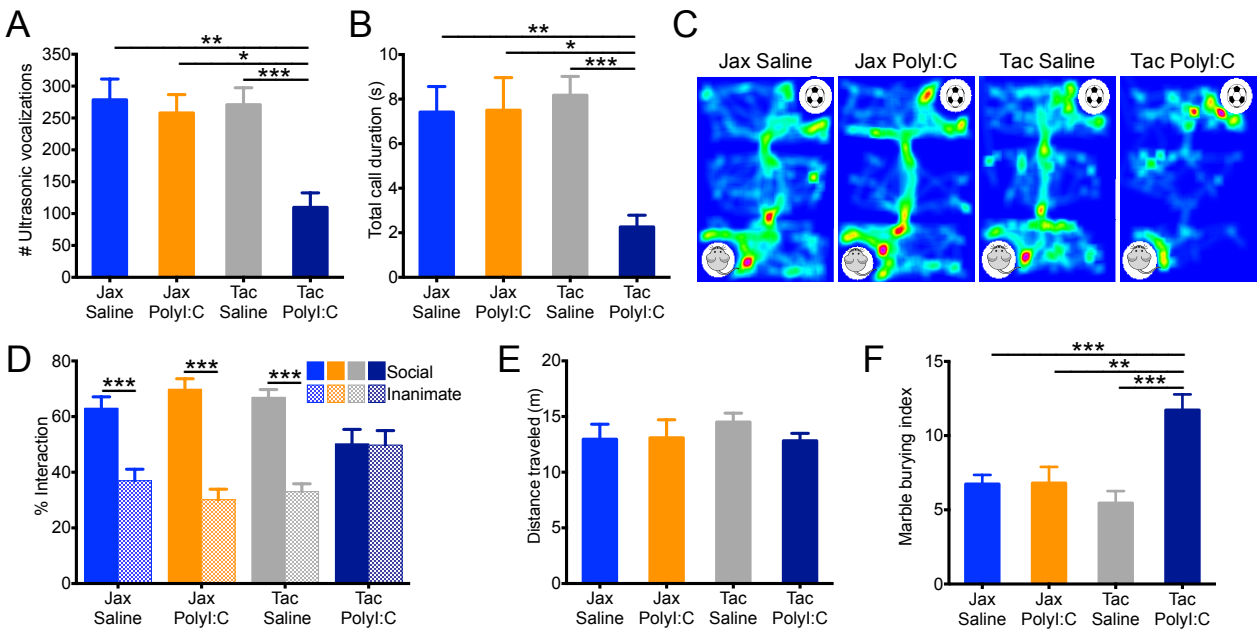

Figure 4.1. Differential susceptibility to MIA-induced neurodevelopmental disease between Taconic and Jackson C57BL/6 mice. Pregnant C57BL/6 mice from The Jackson Laboratories (Jax) or Taconic Biosciences (Tac) were treated with either saline or 20 mg/kg Poly(I:C) at embryonic days 11.5 (E11.5) and 12.5 (E12.5). (A-B) Communicative deficits in 10-day-old pups were evaluated through recording of ultrasonic vocalizations (USVs) (Jax Saline *n*=13, Jax Poly(I:C) *n*=11, Tac Saline *n*=23, Tac Poly(I:C) *n*=12; 4-6 independent experiments). (A) Number of USVs. (B) Total duration of vocalization. (C-E) Social preference was evaluated by a three-chamber sociability test in adult MIA offspring (Jax Saline *n*=13, Jax Poly(I:C) *n*=13, Tac Saline *n*=18, Tac Poly(I:C) *n*=17; 3-5 independent experiments). (C) Representative heat maps depicting time spent interacting with a novel mouse (bottom chamber) or a novel object (top chamber). (D) Percent interaction with the novel mouse (social) and object (inanimate). (E) Total distance traveled by MIA offspring during the three-chamber sociability test. (F) Repetitive/stereotyped behavior in adult MIA offspring was assessed in the marble burying test (Jax Saline *n*=17, Jax Poly(I:C) *n*=10, Tac Saline *n*=22, Tac Poly(I:C) *n*=18; 4-6 independent experiments). Error bars depict mean ± s.e.m. **P* < 0.05, ***P* < 0.01, ****P* < 0.001 calculated by two-way ANOVA with Tukey (A-B & E-F) or Sidak (D) post hoc tests.

Microbiota composition influences the development of autism-related phenotypes in the MIA model

We were next interested in ascertaining whether the observed differences in MIA-induced neurodevelopmental disorder susceptibility between Taconic and Jackson C57BL/6 mice were indeed due to differences in microbiota diversity and not the potential effects of genetic drift. To this end, we performed fecal transplantation studies in which Jackson mice were exposed to the Taconic microbiome for at least two weeks prior to MIA induction. Following fecal transplantation of Taconic microbiota into Jackson mice, MIA was induced with gestational Poly(I:C) treatment and then the development of ASD-related phenotypes including social preference abnormalities and communicative deficits were evaluated in the offspring. Interestingly, MIA offspring from Jackson dams that were previously co-housed with Taconic microbiota (Co Jax mice) exhibited abnormalities in social preference, whereas MIA did not promote social interaction deficits in conventionally raised Jackson mice (Fig. 4.2 a-b). Distance traveled during the sociability test was similar between all experimental groups, which suggests that the effects of fecal transplantation on autism-like behaviors were not due to altered mobility or arousal (Fig. 4.2 c). Likewise, co-housing Jackson mice with Taconic microbiota before Poly(I:C) treatment was sufficient to confer communicative defects in MIA Jackson offspring Fig. 4.2 a-b). Notably, we observed reduced numbers and duration of ultrasonic vocalizations in MIA offspring from Jackson mice supplemented with Taconic microbiota (Fig. 4.2 d-e). Collectively, these findings indicate key roles for the prenatal microbiome in shaping the development of autism-associated behaviors in the MIA model.

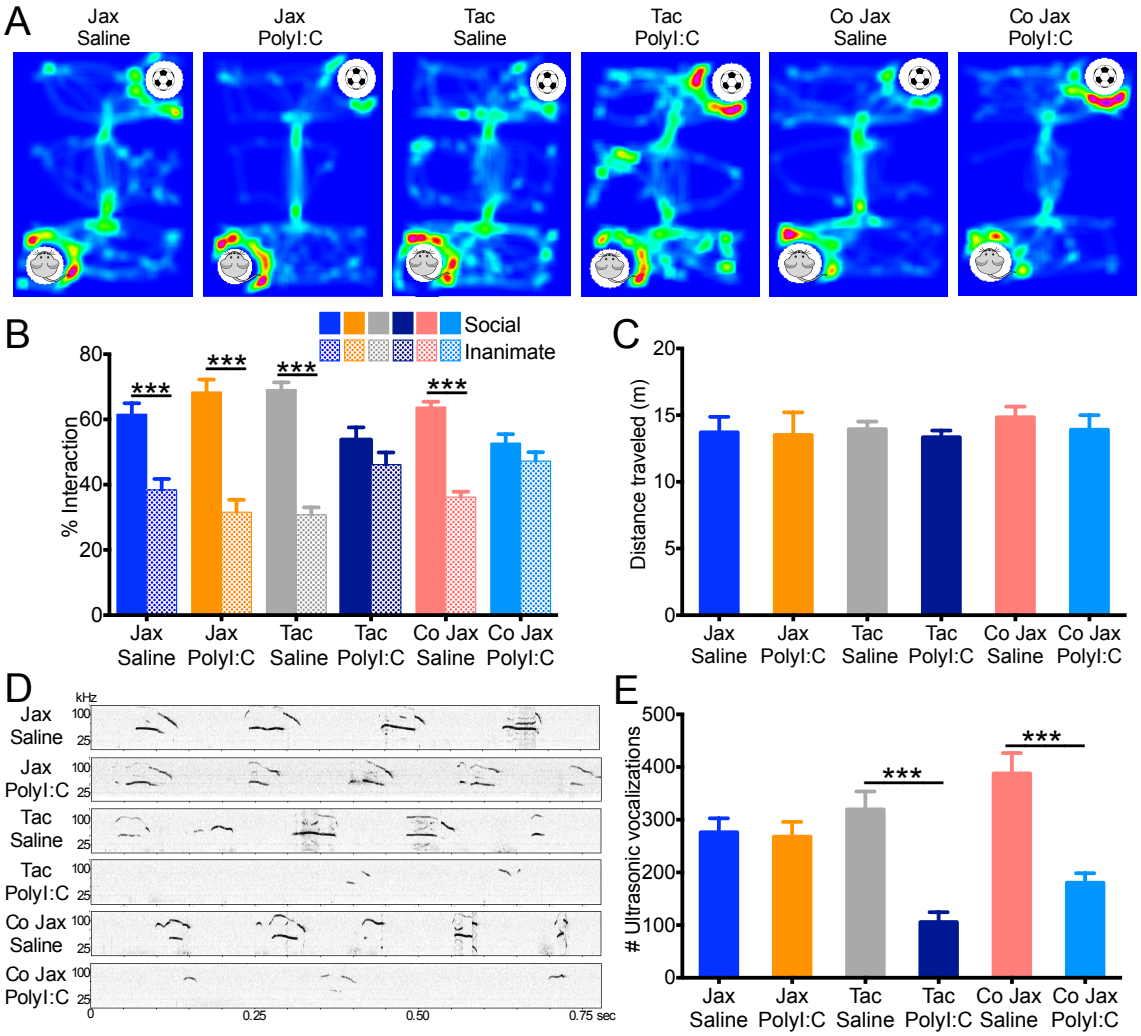

Figure 4.2. Microbiota transfer can confer susceptibility to the development of autism-related phenotypes in the MIA model. Jax mice were cohoused with Tac fecal microbiota (Co Jax) for two weeks, and then pregnant Co Jax and conventionally housed Jax and Tac mice were treated with either 20 mg/kg Poly(I:C) or saline on E11.5 and E12.5. (A-C) Social preference was evaluated by a three-chamber sociability test in adult MIA offspring (Jax Saline *n*=17, Jax Poly(I:C) *n*=12, Tac Saline *n*=30, Tac Poly(I:C) *n*=27, Co Jax Saline *n*=17, Co Jax Poly(I:C) *n*=13; 4-8 independent experiments). (A) Representative heat maps depicting time spent interacting with a novel mouse (bottom chamber) or a novel object (top chamber). (B) Percent interaction with the novel mouse (social) and object (inanimate). (C) Total distance traveled by MIA offspring during the three-chamber sociability test. (D-E) Communicative deficits in 10-day-old pups were evaluated through recording of ultrasonic vocalizations (USVs) (Jax Saline *n*=16, Jax Poly(I:C) *n*=12, Tac Saline *n*=17, Tac Poly(I:C) *n*=15, Co Jax Saline *n*=11, Co Jax Poly(I:C) *n*=11; 3-9 independent experiments). (D) Representative USV detection plots. (E) Total number of USVs. Error bars depict mean ± s.e.m. **P* < 0.05, ***P* < 0.01, ****P* < 0.001 calculated by (C & E) one-way and (B) two-way ANOVA with Tukey or Sidak post hoc tests.

Microbiota influence the development of autistic-like phenotypes through modulation of the immune response

The commensal bacteria SFB in the Taconic microbiome is known to promote induction of IL-17a inflammatory responses[193], which provides one plausible immune-based route through which the Taconic microbiome can influence neurodevelopment disease. Interestingly, recent studies demonstrate that IL-17a can modulate neurodevelopment, neural circuit function, and behavior[152-154, 195]. Therefore, we were particularly interested in exploring a potential role for microbiota-mediated regulation of IL-17a inflammatory responses in driving autism-related phenotypes.

To first validate that our microbiota transplantation methodology results in the transfer of SFB to Jackson mice, we evaluated the colonization of SFB in co-housed Jackson mice. Consistent with previous reports [193], we observed levels of SFB colonization in Jackson fecal transplantation mice (Co Jax mice) that were similar to those found in conventionally raised Taconic mice (Fig. 4.3 a). In contrast, we did not detect major changes in the relative abundance of Bacteroides, Prevotellaceae, Lactobacillus, or Bifidobacterium spp in Jax mice following co-housing (Fig. 4.4). Changes in microbiota composition in Jackson co-housed dams also promoted enhanced IL-17a secretion following Poly(I:C) injection (Fig. 4.3 b). These findings suggest that maternal microbiota landscape centrally impacts MIA-induced inflammatory cytokine production. Moreover, these results provide further rationale for testing a causal role for dysregulated gestational IL-17a production in driving the development of autistic phenotypes in offspring from Jackson dams that underwent microbiota transplantation. To this end, we first sought out to confirm a role for IL-17a in driving neurodevelopmental disorders in the MIA model. Consistent with a recently published study [152], we found that blockade of IL-17a in MIA mothers

prevented Taconic offspring from developing communicative deficits, abnormal social preference, and stereotyped/repetitive behaviors (Fig. 4.5).

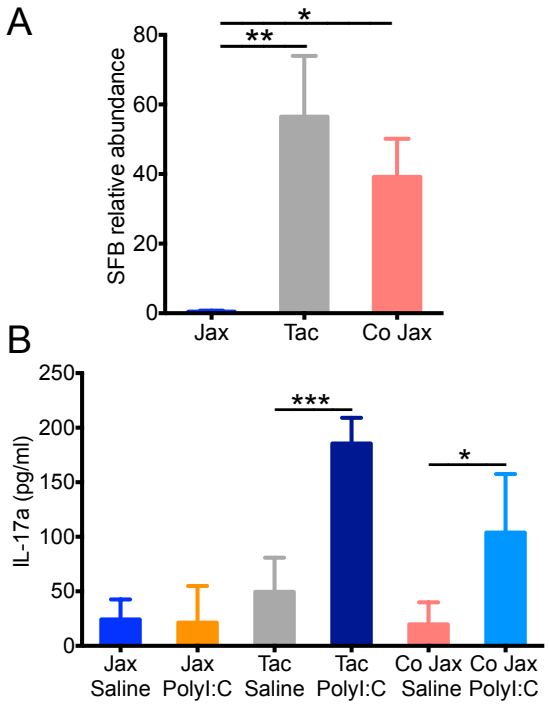

Figure 4.3. Microbiota landscape impacts MIA-induced inflammatory responses. (A) Jax mice were co-housed with fecal microbiota from Tac mice (Co Jax) for two weeks, and then the abundance of segmented filamentous bacteria (SFB) in fecal samples from conventionally housed (Jax *n*=9, Tac *n*=5) and Co Jax mice (*n*=9) was determined by quantitative PCR (qPCR). Representative data from three independent experiments. (B) Co Jax and conventionally housed Jax and Tac dams were treated with either 20 mg/kg Poly(I:C) or saline on E11.5 and E12.5 and then serum IL-17a levels were determined by ELISA 48 hrs after the last Poly(I:C) injection (*n*=4 for all groups; representative data from two independent experiments). Error bars depict mean ± s.e.m. **P* < 0.05, ***P* < 0.01, ****P* < 0.001 calculated by one-way (A) or two-way (B) ANOVA with Tukey post hoc tests.

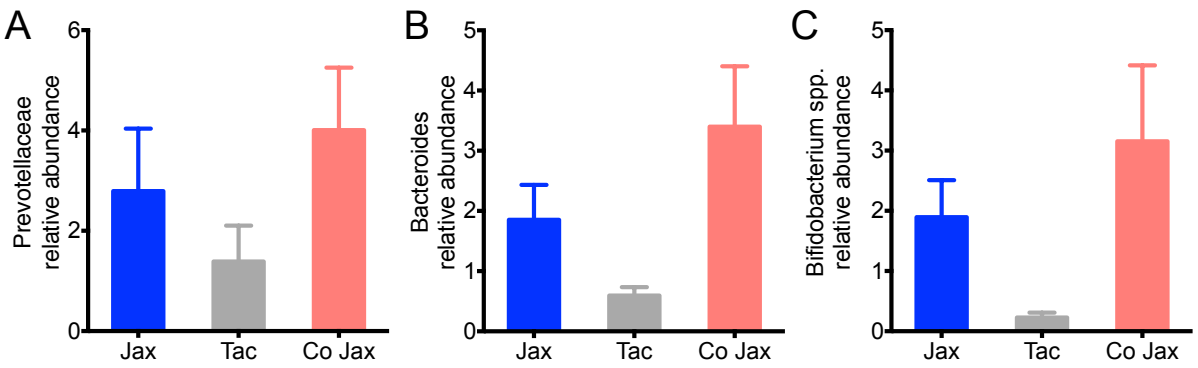

Figure 4.4. Vendor-specific and co-housing-associated differences in microbiota landscape. Jax mice were co-housed with fecal microbiota from Tac mice (Co Jax) for two weeks, and then the relative abundance of Prevotellaceae (A), Bacteroides (B), and Bifidobacterium spp. (C) in fecal samples from conventionally housed (Jax *n*=9, Tac *n*=5) and Co Jax mice (*n*=9) was determined by quantitative PCR (qPCR). Representative data from three independent experiments. Error bars depict mean ± s.e.m.

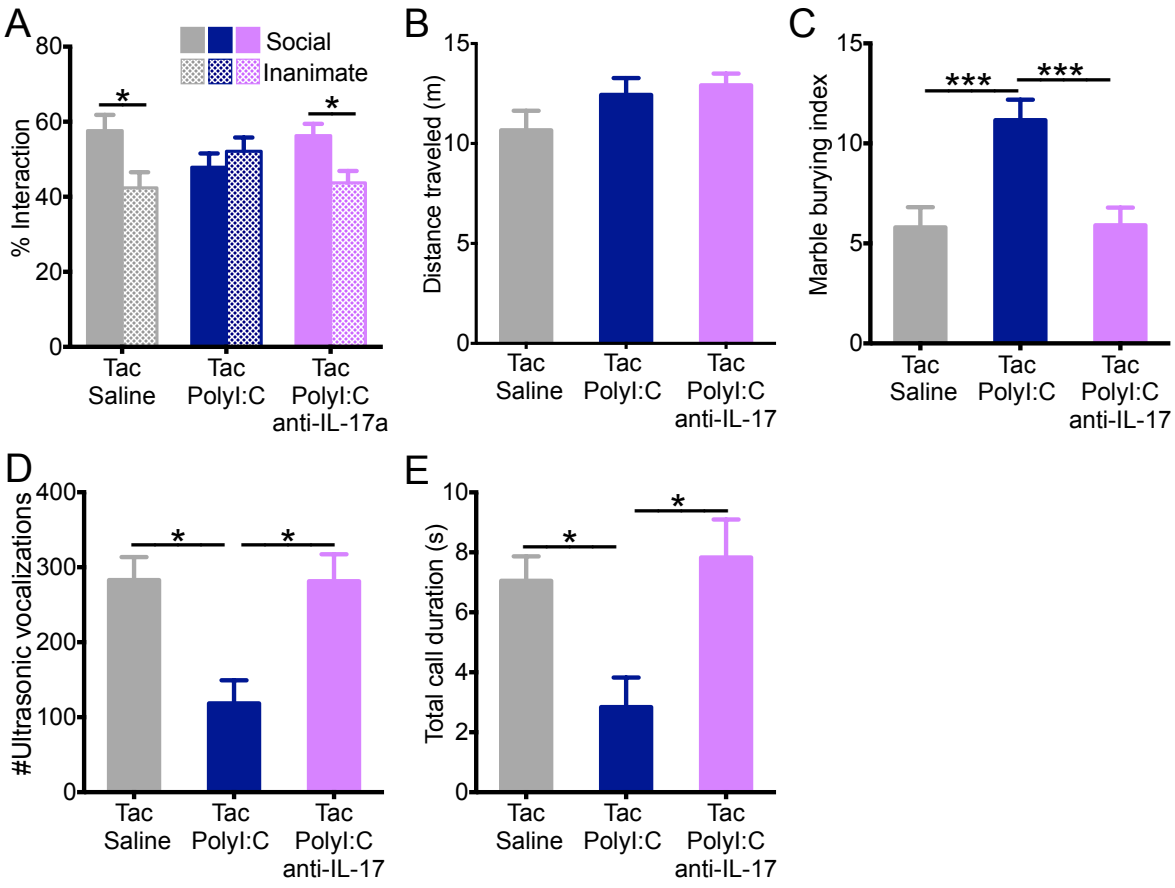

Figure 4.5. Gestational IL-17a promotes MIA-induced neurodevelopmental abnormalities in Taconic mice. Taconic (Tac) mice received either anti-IL-17a neutralizing antibody (500 µg/mouse) or sham treatment (saline) by intraperitoneal injection on E11.25 followed by treatment with 20 mg/kg Poly(I:C) or saline on E11.5 and E12.5. (A-C) Social preference was evaluated by a three-chamber sociability test in adult MIA offspring (Tac Saline *n*=14, Tac Poly(I:C) *n*=13, Tac Poly(I:C) anti-IL-17a *n*=21; 5-6 independent experiments). (A) Percent interaction with the novel mouse (social) and object (inanimate). (B) Total distance traveled by MIA offspring during the three-chamber sociability test. (C) Repetitive/stereotyped behavior in adult MIA offspring was assessed in the marble burying test (Tac Saline *n*=20, Tac Poly(I:C) *n*=22, Tac Poly(I:C) anti-IL-17a *n*=21; 5-6 independent experiments). (D-E) Communicative deficits in 10-day-old pups were evaluated through recording of ultrasonic vocalizations (USVs) (Tac Saline *n*=19, Tac Poly(I:C) *n*=7, Tac Poly(I:C) anti-IL-17a *n*=6; 3-5 independent experiments). (D) Number of USVs. (E) Total duration of vocalization. Error bars depict mean ± s.e.m. **P* < 0.05, ***P* < 0.01, ****P* < 0.001 calculated by two-way ANOVA with Sidak post hoc tests (A) or one-way ANOVA with Tukey post hoc test (B-E).

Next we investigated whether neutralization of IL-17a impacts the development of autism-related behaviors in Jackson mice that were previously co-housed with microbiota from Taconic mice. We found that inhibition of IL-17a signaling during gestation rescues social abnormalities in MIA offspring from Jackson dams that previously underwent fecal transplantation with Taconic microflora (Fig. 4.6 a-b). Importantly, the amelioration of social impairments with anti-IL-17a treatment was not due to enhanced arousal or activity, as distances traveled were similar between the experimental groups (Fig. 4.6 c). Neutralization of IL-17a during gestation in co-housed Jackson dams was also effective in restoring normal communicative behavior in MIA offspring (Fig. 4.6 d-f). In contrast, we observed substantial reductions in the number and duration of ultrasonic vocalizations in MIA offspring from cohoused Jackson dams that received sham treatment during gestation (Fig. 4.6 d-f).

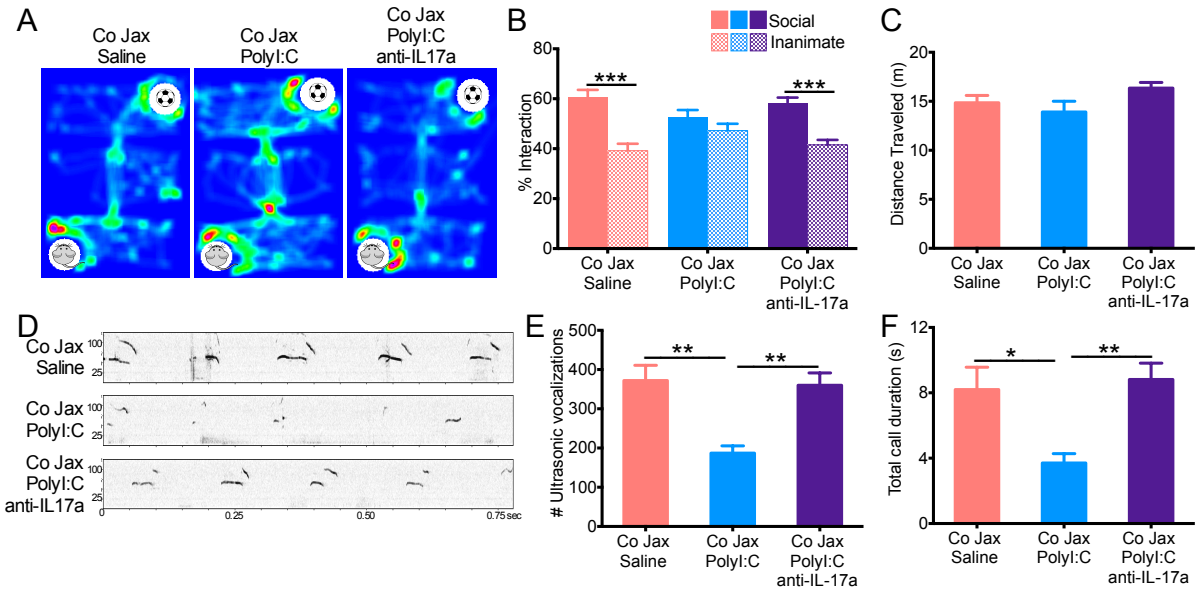

Figure 4.6. Critical roles for microbiota-mediated modulation of IL-17a in the MIA model of autism. Jax mice were cohoused with Tac fecal microbiota (Co Jax) for two weeks. Co Jax mice then received either anti-IL-17a neutralizing antibody (500 µg/mouse) or sham treatment (saline) by intraperitoneal injection on E11.25 followed by treatment with 20 mg/kg Poly(I:C) or saline on E11.5 and E12.5. (A-C) Social preference was evaluated by a three-chamber sociability test in adult MIA offspring (Co Jax Saline *n*=18, Co Jax Poly(I:C) *n*=13, Co Jax Poly(I:C) anti-IL-17a *n*=19; 6-7 independent experiments). (A) Representative heat maps depicting time spent interacting with a novel mouse (bottom chamber) or a novel object (top chamber). (B) Percent interaction with the novel mouse (social) and object (inanimate). (C) Total distance traveled by MIA offspring during the three-chamber sociability test. (D-F) Communicative deficits in 10-day-old pups were evaluated through recording of ultrasonic vocalizations (USVs) (Co Jax Saline *n*=10, Co Jax Poly(I:C) *n*=10, Co Jax Poly(I:C) anti-IL-17a *n*=14; 2-3 independent experiments). (D) Representative USV detection plots. (E) Number of USVs. (F) Total duration of vocalization. Error bars depict mean ± s.e.m. **P* < 0.05, ***P* < 0.01, ****P* < 0.001 calculated by one-way ANOVA with Tukey post hoc tests (C; E-F) or two-way ANOVA with Sidak post hoc tests (B).

Discussion

In summary, our findings implicate k*ey roles for microbiota-mediated regulation of immunity in a prenatal inflammation model of autism.* We find that differences in microbiome between vendors is sufficient to confer susceptibility to MIA induced ASD as mice from The Jackson Laboratories are protected against MIA induced ASD while mice from Taconic develop the core symptoms of ASD in response to MIA. Moreover, we find that susceptibility to MIA can be transferred through co-housing. Co-housing Jackson females with Taconic females, to allow for microbiome transfer, prior to MIA is sufficient to generate ASD associated behaviors the offspring of Jackson mice. We find that microbiota differences contribute to this effect through their regulation of inflammation as co-housing Jackson females with Taconic females increases the level of inflammation in the serum of Jackson mice post Poly(I:C). Moreover, our results identify IL-17a as a specific immune regulator that contributes to the effects of the microbiome on the development of ASD-related phenotypes in the MIA model. These findings suggest that targeting the maternal microbiome and/or immune system during pregnancy may offer therapeutic strategies to prevent some forms of neurodevelopmental disorders.

Chapter 5: Discussion and future perspectives

As with most big questions in science, answers are never simple and straightforward. Often times, answers to experimental hypothesis result in even bigger and more complicated questions. The goal of my graduate work was to study the role of the innate immune system in neurodevelopment and while work accomplished in the past five years have given us significant insights into the role of the innate immune system and inflammasome signaling in neurodevelopment, many unanswered questions still remain. In this next chapter I will discuss some of the questions we are poised to answer, and some of the preliminary data we have generated in order to begin to untangle the complicated role of the innate immune system in the CNS.

Is AIM2 inflammasome-induced cell death during development restricted to a particular cell type and a particular window of development?

Cell type

Our work published in *Nature* (chapter 2), indicates that genetically compromised CNS cells can activate the AIM2 inflammasome and undergo programmed cell death rather than be incorporated into the central nervous system. We show that inability to remove these cells results in altered CNS architecture and anxiety-associated behaviors in inflammasome knockout mice, Aim2, Caspase-1, and Gsdmd. We also demonstrate that this pathway is relevant in the nervous system by utilizing *Casp1*$^{fl/fl}$*Nestin*^{Cre} mice. We show that Caspase-1 deletion in Nestin-expressing cells recapitulates the behavioral abnormalities and excessive DNA damage accumulation seen in AIM2 inflammasome-deficient mice (Figure 2.14). However, a major outstanding question is which cell type/types are important for driving these phenotypes as our *Casp1*$^{fl/fl}$*Nestin*^{Cre} will have *Casp1* removed from multiple cell types, including astrocytes,

neurons, and oligodendrocyte lineage cells. We see that mixed CNS cells (neurons and glia) in culture are protected against DNA damage-induced cell death (figure 2.8) and we see this same protection in pure neuronal cultures (Figure 5.1).

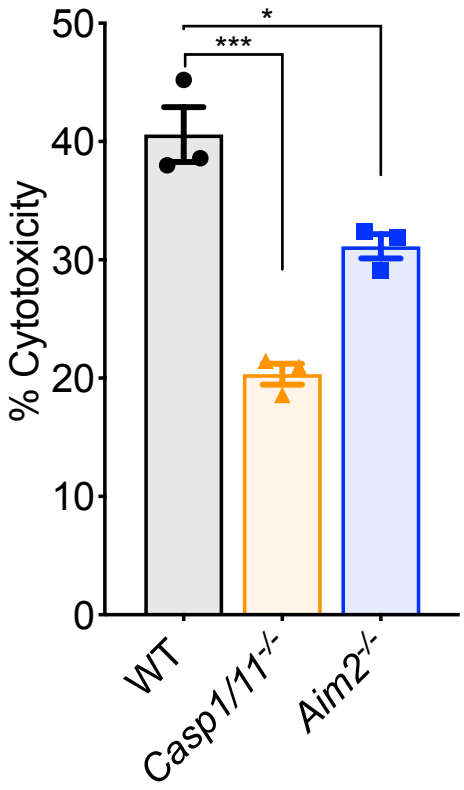

Figure 5.1 Activation of the AIM2 inflammasome in response to DNA damage coordinates cell death of neurons *in vitro*. Postnatal day 0 (p0) neuron cultures were primed with LPS for 4 hrs followed by overnight treatment with 10μM etoposide (WT *n*=3, *Ice*$^{-/-}$ *n*=3, *Aim2*$^{-/-}$ *n*=3. Cell death was measured by LDH release.

We have begun to attempt to answer this question at the timepoint in which we see high levels of ASC speck formation during development, p5. When we use markers to delineate cell types that are activating the inflammasome and thus have an ASC speck, we see that neurons are the main cell type (Figure 5.2). This is not unexpected, as our adult data indicates an increased number of Purkinje neurons in the adult brain (Figure 2.8, 2.11). Moreover, when we look to see which cell types are harboring DNA damage in the adult brain, we see that most of the CNS cells that have existing DNA damage, marked by γH2AX, are again neurons (Figure 5.3).

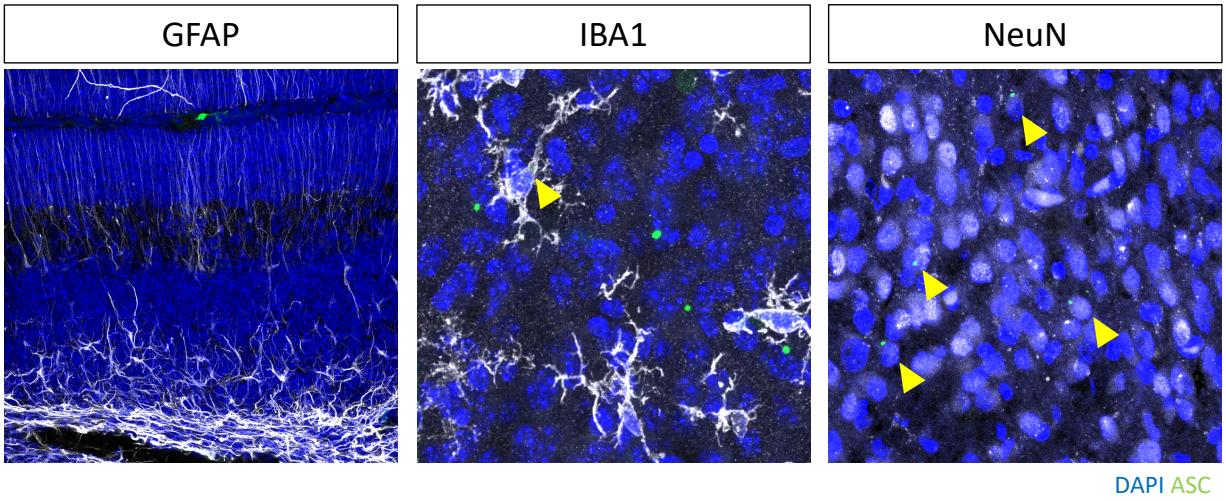

Figure 5.2 ASC specks form mainly in neurons at p5. Brains from p5 ASC reporter mice were analyzed for cell type harboring ASC specks (ASC, green) using confocal microscopy. Yellow arrows show co-localization of multiple NeuN+ neurons containing ASC specks, occasional IBA1+ microglia harboring ASC specks, and no GFAP+ astrocytes with ASC specks.

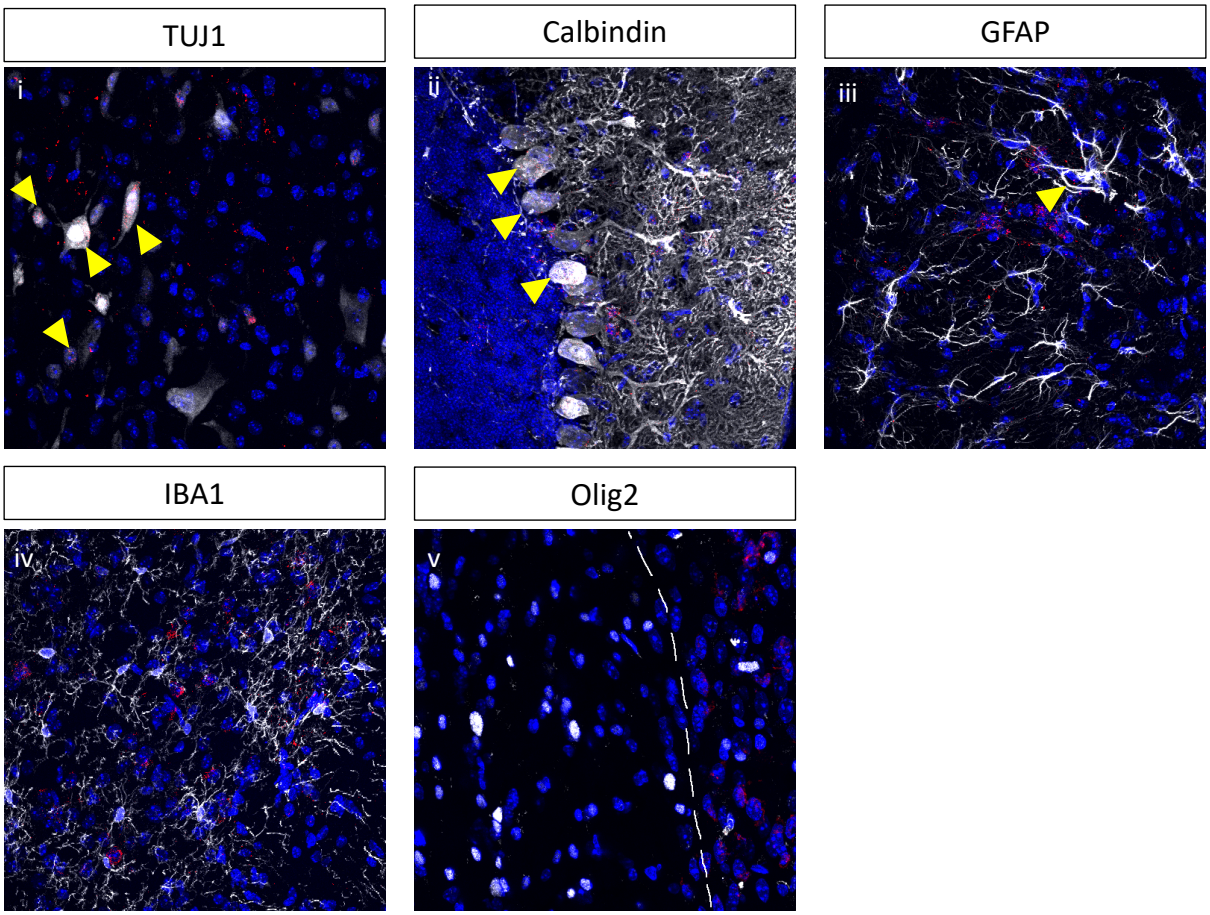

Figure 5.3 DNA damage accumulates in neurons in *Aim2*$^{-/-}$ mice. Brains from adult (8-12 week) *Aim2*$^{-/-}$ mice were analyzed for cell type harboring DNA damage (γH2AX, red) using confocal microscopy. Yellow arrows show co-localization of (i) multiple TUJ1+ neurons and (ii) Calbindin+ neurons harboring DNA damage, (iii) occasional GFAP+ astrocyte harboring DNA damage, (iv) IBA1+ microglia with no DNA damage, and (v) Olig+ Oligodendrocytes in the corpus callosum (dashed line) with no DNA damage.

Future planned studies will determine how disruption of neuron-specific DNA damage surveillance by AIM2 impacts CNS homeostasis. To test this, we will evaluate anxiety and motor behaviors, as wells as abnormal neuroanatomy in *Aim2*$^{fl/fl}$*Syn1*^{Cre}, *Aim2*$^{WT/WT}$*Syn1*^{Cre}, *Aim2*$^{fl/fl}$, and *Aim2*$^{-/-}$ mice. Following validation of our conditional targeting, we will conduct behavioral testing to evaluate motor dysfunction using the accelerating rotarod and anxiety-related phenotypes using both the open-field test and the elevated plus-maze. Likewise, we will assess potential differences in neuroanatomy by performing histological staining for DNA damage accumulation using two markers of DNA damage 53BP1 and γH2AX, astrogliosis using GFAP, and microglia activation using IBA1 and CD68. We will confirm any IHC findings with western blot and will also conduct comet assays as a secondary approach to measure DNA damage.

Neurons themselves are an extremely heterogeneous population, comprising of multiple types of excitatory, inhibitory, and interneurons. It is, therefore, possible that a particular subpopulation of neurons is utilizing this mechanism of cell death in response to DNA damage. We have begun to attempt to answer this question by first looking at numbers of an inhibitory interneuron population, Parvalbumin (PV) neurons. PV neurons are inhibitory neurons that are powerful regulators of E/I balance, something that is commonly disrupted in neurodevelopmental disorders. Indeed, there are many neurodevelopmental disorders that are thought to be driven by a disruption in E/I balance including schizophrenia and autism[196]. In preliminary studies, we have found an increase in the number of PV^+ neurons in the cerebellum of both *Aim2*$^{-/-}$ and *Casp1/11*$^{-/-}$ mice (Figure 5.4). These data indicate that PV^+ inhibitory neurons in the cerebellum are one subpopulation of neurons that might utilize inflammasome mediated cell death during development. More work will need to be done in order to see if other populations of neurons

undergo inflammasome mediated cell death including looking at other forms of both inhibitory and excitatory cells as well as confirming increased expression at the protein level.

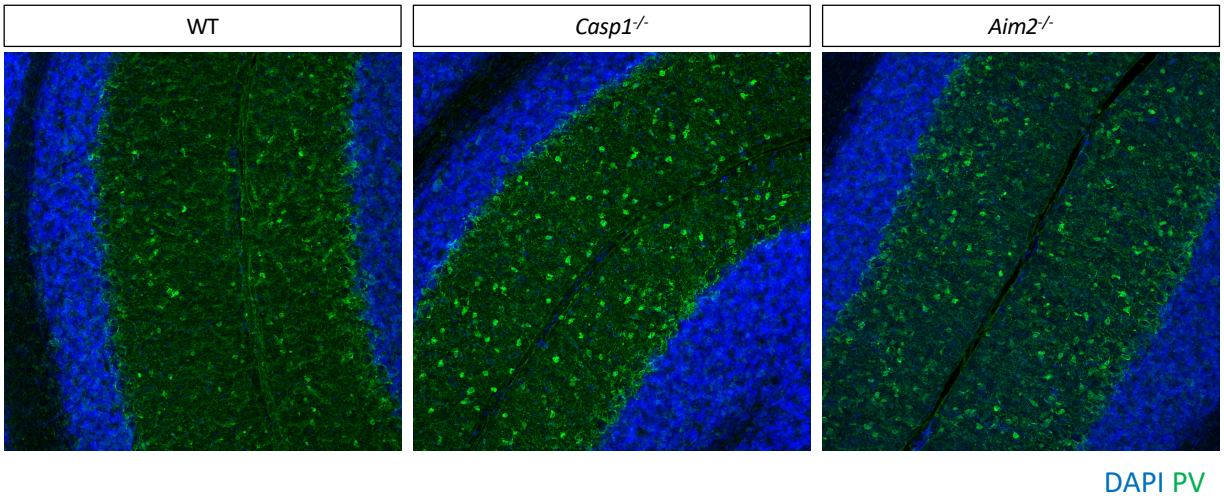

Figure 5.4 Increased number of PV^{+} neurons in AIM2 inflammasome deficient cerebellums. Cerebellums from adult (8-12 week) WT, *Casp1/11*$^{-/-}$ and *Aim2*$^{-/-}$ mice were analyzed for PV^{+} neurons (green) using confocal microscopy.

Finally, changes in one cell population within the CNS are likely to impact all CNS resident cells, making it difficult to discern what are the exact causes of the observed phenotypes; more likely, there are a multitude of factors that are contributing to altered behaviors. Even though we see DNA damage mostly accumulating in neurons, this does not mean that other cell types are not impacted. For example, we consistently observe high levels of astrogliosis in areas of the brain where we see high levels of DNA damage in neurons, such as the cerebellum (Figure 5.5). Whether or not the increase observed in astrocyte reactivity in our global knockouts will be seen in our *Aim2*$^{fl/fl}$*Syn1*^{Cre} mice and if it is contributing to any of the observed phenotypes remains unclear.

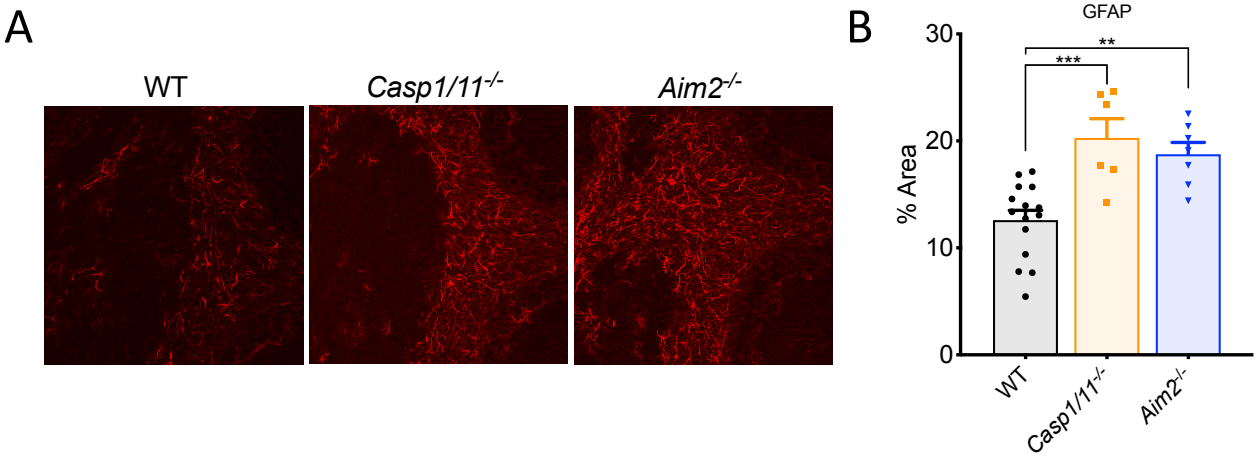

Figure 5.5 Increased astrogliosis in Aim2 inflammasome deficient cerebellums. Cerebellums from adult (8-12 week) WT, *Casp1*$^{-/-}$ and *Aim2*$^{-/-}$ mice were analyzed for astrogliosis(GFAP, red) using confocal microscopy (WT *n*=15, *Ice*$^{-/-}$ *n*=6, *Aim2*$^{-/-}$ *n*=7).

Timing during neurodevelopment

Although we see substantial inflammasome activation at p5 (Figure 2.3) it is unclear if this is the timepoint when the AIM2 inflammasome is most activated during neurodevelopment. As previously discussed in the introduction, the type of DNA damage and the downstream consequences of that damage change as neurodevelopment progresses[74]. For example, during periods of neurogenesis that are defined by high levels of proliferation, progenitor cells that experience dsDNA breaks are more likely to be eliminated via programmed cell death[90, 91] It is therefore possible that levels of inflammasome activation will be higher at earlier points of neurodevelopment. To get at this question we will clear the brains of ASC reporter mice at different points during neurodevelopment (e12.5, e14.5, e18.5, and p0) and image the whole brain using light-sheet microscopy. This technique will enable us to not only see levels of inflammasome activation at key timepoints during development, but will also provide insight into

the localization of inflammasome activation and if this also changes throughout development. If we anticipate inflammasome mediated cell death to be important during neurogenesis, for example, we should see high levels of ASC speck in progenitor pools in the dentate gyrus. Visualizing both ASC expression and localization at different timepoints during development will provide key insights into what types of damage the inflammasome might be responding to and how that will impact cell survival.

Is inflammasome activation important in the adult CNS?

Published studies from our lab (chapter 2) show an important role for inflammasome activation in response to DNA damage during neurodevelopment. However, whether or not inflammasome activation occurs in the adult CNS and how inflammasome activation contributes to CNS homeostasis in the mature brain remains less defined.

Does inflammasome activation occur in the adult CNS?

From our published work, we see a decrease in the amount of inflammasome transcript in the brain as the mouse ages (Figure 2.1). However, whether or not inflammasome proteins are being activated in the adult CNS remains unclear. Unpublished studies from our lab show that ASC specks are present in the adult CNS, indicating that the inflammasome is active during adulthood. (Figure 5.6).

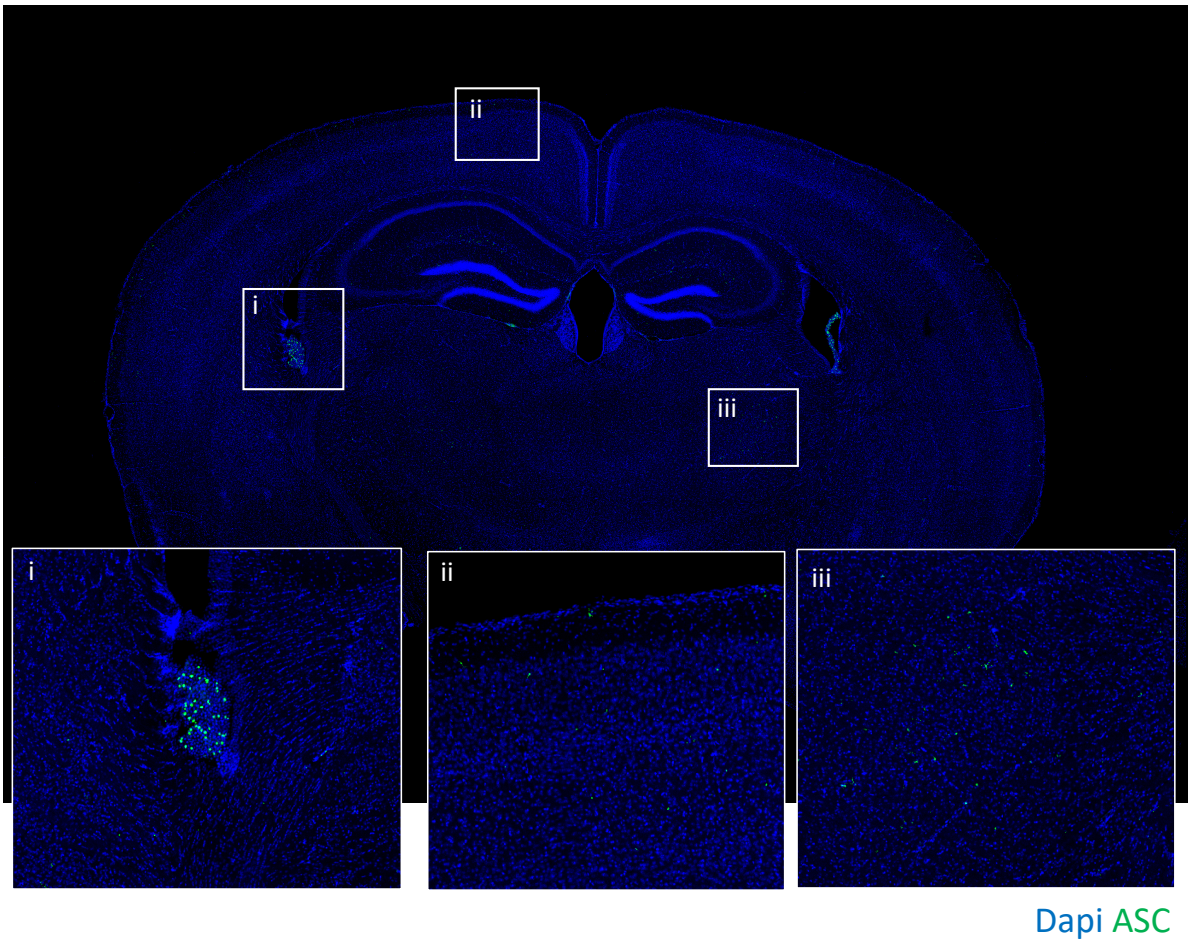

Figure 5.6 ASC specks are present in the adult CNS. Brains from adult (8-12wks) ASC reporter mice were analyzed for ASC specks (ASC, green) using confocal microscopy. ASC specks are seen throughout the adult CNS including in the (i) chroid plexus, (ii) cortex, and (iii) thalamus.

As discussed in the introduction, DNA damage occurs in the CNS throughout the life of the organism[74]. Recent data suggest that dsDNA breaks are induced when neurons fire and can, therefore, be increased during paradigms including environmental enrichment (EE)[197]. To see if inflammasome activation in the adult CNS is dynamic and can respond to DNA damage, as seen in development, we environmentally enriched mice and looked for levels of ASC speck formation in the hippocampus. We see that the inflammasome is activated in response to environmental enrichment in the adult CNS (Figure 5.7). These results indicate that the inflammasome is active in the adult CNS under homeostatic conditions.

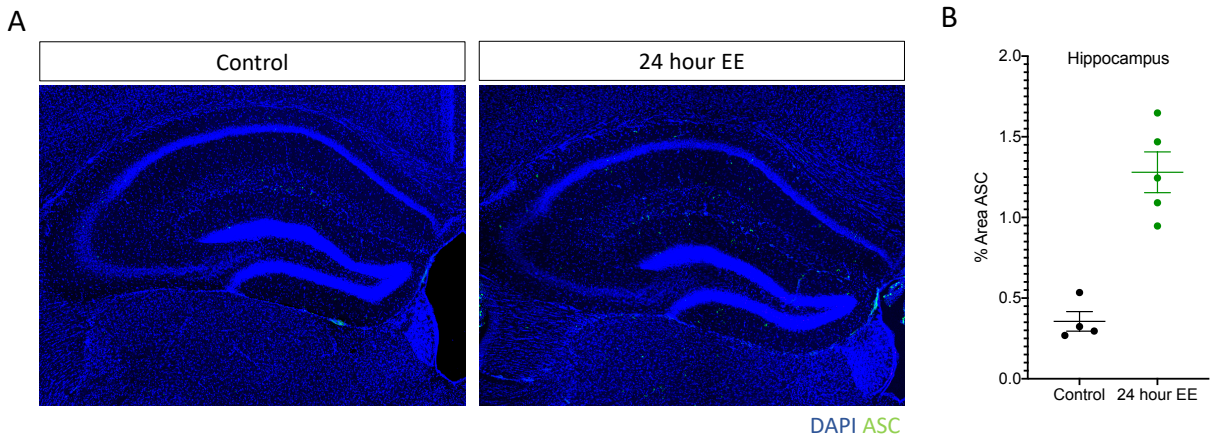

Figure 5.7 The inflammasome is activated in the hippocampus in response to EE. Adult (8-12wks) ASC reporter mice were either left in their home cage with no toys or environmentally enriched with toys for 24 hours. The hippocamous was then analyzed for ASC specks (ASC, green) using confocal microscopy. (A) Representative images showing increase ASC speck formation after EE. (B) Quantification of %Area of ASC expression in control and EE hippocampus.

What is the role of inflammasome activation in the adult CNS?

The amount of ASC specks that we observe in the adult CNS, along with the fact that CNS cells are long-lived, implies that cell death might not be the only consequence of inflammasome activation. Recent studies demonstrate that *Aim2* can function in the adult CNS to regulate neuronal morphology[37]. These studies show that mice lacking *Aim2* have an increase in dendritic complexity[37], yet how *Aim2* regulates dendritic morphology remains unclear. Current and future studies in the lab are aiming to assess if the inflammasome and Gasdermin-D pore formation could potentially provide a novel "pruning" mechanism for dendritic architecture in the adult CNS. We hypothesize that AIM2 inflammasome activation and subsequent Gasdermin-D pore formation in the neuronal cell membrane will promote elimination of the process. If our hypothesis is true, and the inflammasome functions locally in dendritic processes to alter neuronal morphology, we would expect to see inflammasome activation within dendritic processes of neurons. In preliminary experiments, we find that ASC specks are present in the dendritic spines of Purkinje cells (Figure 5.8) indicating that inflammasome activation within dendrites could result in dendritic Gasdermin-D pores.

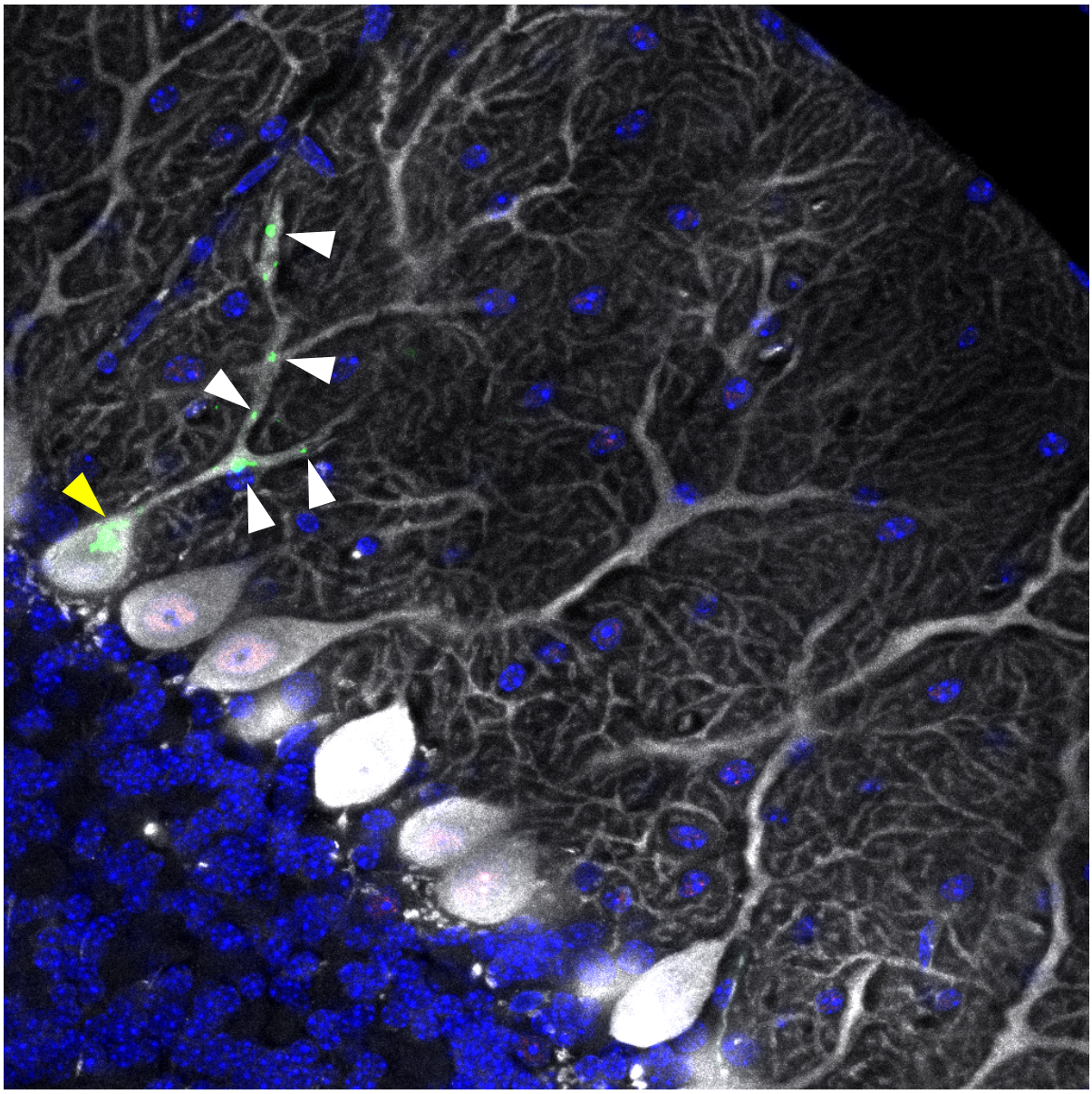

Dapi Calbindin ASC yH2AX

Figure 5.8 ASC specks are present in dendritic branches of Purkinje neurons
Adult (8-12wks) ASC reporter mice analyzed for localization of ASC specks (green) within dendritic branches of Purkinje neurons (Calbindin^{+}; grey). Arrows show that ASC specks are present in Purkinje neurons and localize to both dendritic processes (white arrows) and the soma (yellow arrow).

To investigate a role for the AIM2 inflammasome in neuronal process elimination we have begun to analyze dendritic and neurite branching in pure neuronal cultures from p0 WT, *Aim2*$^{-/-}$, *Casp1/11*$^{-/-}$, and *Gsdmd*$^{-/-}$ pups by utilizing IHC. Preliminary experiments with help from a new graduate student, Kristine Zengeler, have indicated that changes in dendritic complexity seen in *Aim2*$^{-/-}$ cells are inflammasome dependent, as *Casp1/11*$^{-/-}$ show similar trends towards an increase in dendrite length (Figure 5.9). These trends are also observed *in vivo* using a Golgi stain. Analysis done by Kristine Zengeler found that cortical neurons from both *Aim2*$^{-/-}$ and *Casp1/11*$^{-/-}$ mice show an increase in both the number of dendritic spines as well as an increase in the spine length (Figure 5.10). However, to see if these effects are indeed a result of Gasdermin-D pores, these experiments will need to be repeated and include *Gsdmd*$^{-/-}$ mice and cultured cells.

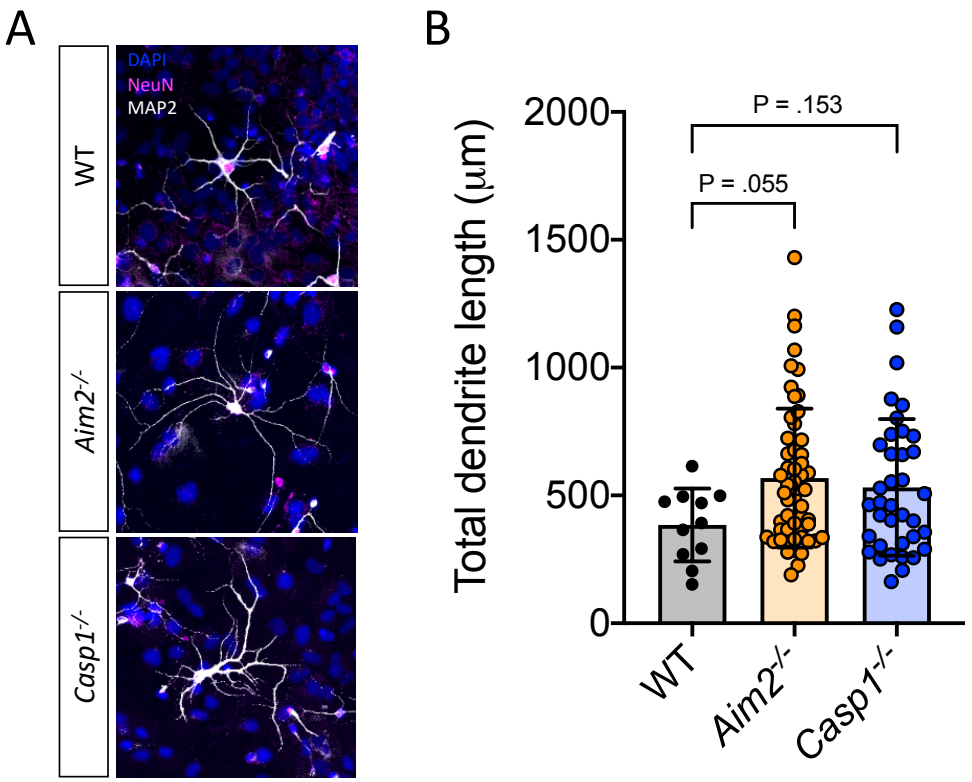

Figure 5.9 AIM2 Inflammasome deficient neurons have an increased total dendrite length *in vitro.* Neurons were cultured from p0 WT, *Aim2*$^{-/-}$, and *Casp1/11*$^{-/-}$ pups, allowed to grow for 2 weeks, and were then fixed to analyze neuronal morphology using confocal microscopy. (A) Representative images showing neuronal processes (MAP2) from fixed cultures. (B) Quantification of total dendritic length of cultured neurons.

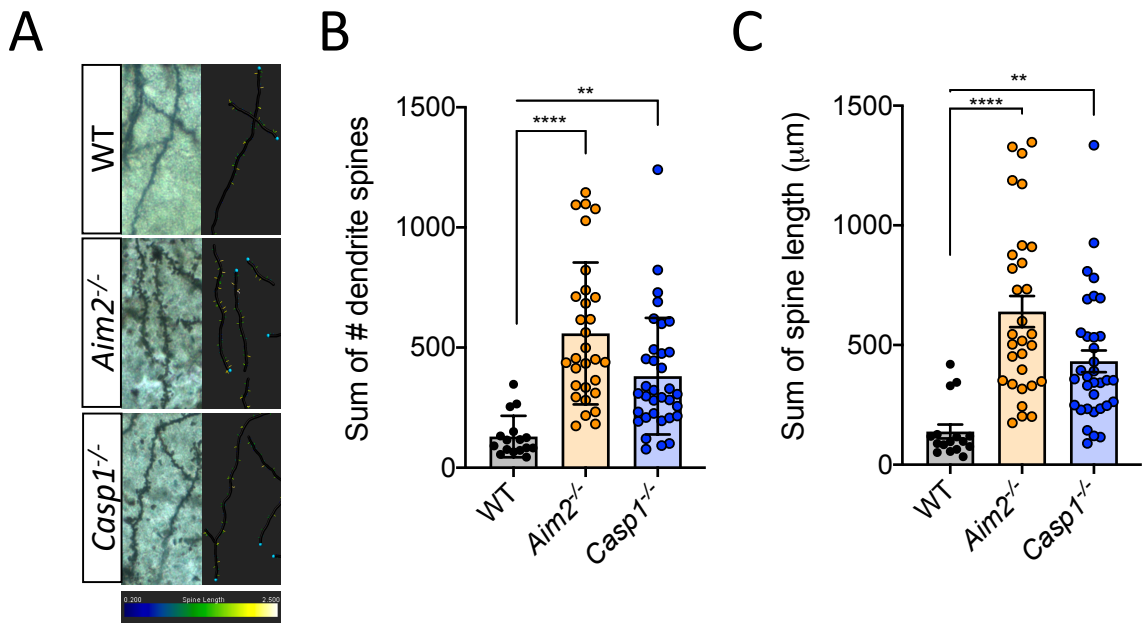

Figure 5.10 AIM2 Inflammasome deficient neurons have an altered dendritic spines *in vivo.* Golgi stain was performed on brains from adult WT, *Aim2*$^{-/-}$, and *Casp1/11*$^{-/-}$ mice. (A) representative image dendritic spines on cortical neurons. (B-C) Quantification of (B) total number of dendritic spines and (C) sum of dendritic spine length.

Future experiments will attempt to elucidate if these changes in neuronal morphology are intrinsic to the neuron or if they are result of the supporting glial cells. We will perform similar analyses as seen in figure 5.9 with both pure neuronal cultures and with cultures containing glia. This will enable us to determine if inflammasome-mediated process elimination is intrinsic to the neuron or if it requires other glia to aid in this removal process. If, for example, we do not see differences in axon or dendritic properties between genotypes in our pure neuronal cultures but do see differences in our mixed glia culture, we can assume that these process eliminations are glia dependent.

Lastly, we will attempt to uncover where the inflammasome is being activated in adult neurons. Visualization of ASC specks in the dendrite could be a result of local activation of the inflammasome or trafficked ASC specks from the soma into dendritic processes. In order to further assess the location of inflammasome activation in neurons, we will utilize cultured neurons from ASC-citrine reporter mice and perform live imaging. We will culture neurons from p0 ASC-citrine mice and inflammasome activation will be induced by inciting dsDNA breaks with etoposide (5 μM) or ionizing radiation (40Gy). Using live-cell imaging, we will attempt to visualize the formation of ASC specks in response to DNA damage. This will provide important insight as to what type of damage the inflammasome might be responding to in mature neurons.

In addition to nuclear DNA, mitochondrial DNA has also been shown to be susceptible to dsDNA breaks and deficits in mitochondrial DNA repair have been linked to neurological disorders[74, 88]. Synapses are packed with mitochondria who provide structural support and are essential for synaptic function[198]. Moreover, recent studies have demonstrated that deterioration of mitochondria function within synapses can lead to complement dependent synapse loss in AD[199]. Damaged mitochondria, however, can be harmful to neurons and therefore need to be

eliminated through processes such as mitophagy[198] or potentially through Gasdermin-D pores. In future studies, it will be important to use markers for mitochondria within our ASC reporter mice to interrogate if ASC specks are colocalizing with mitochondria and therefore responding to mitochondrial stress.

Preliminary studies indicate an important role for the inflammasome in sculpting the nervous system. We envision that this can happen through many potential scenarios (Figure 5.11). It is possible that damage generated in a neuron might activate the inflammasome and utilize a Gasdermin-D pore to excrete the damage to prevent death. These membrane pores could result in changes in osmotic pressure and the intrinsic severing of a process, or these pores might be repaired. A recently published study demonstrates that the formation of a Gasdermind-D pore does not guarantee the cell will die[200]. Instead, these pores were shown to be repaired by ESCRT proteins, which are known to be highly prevalent in neurons. Another possible mechanism in which the inflammasome could contribute to dendritic pruning is though release of cytosolic contents such as ATP, from Gasdermin-D pores to promote microglial recruitment. Released contents could provide an "eat-me signal" encouraging microglial-mediated process removal. Additionally, inflammasome-mediated cytokine production and signaling was found to be important for changes in morphology seen in *Aim2*$^{-/-}$ mice, raising the possibility that the inflammasome acts as a platform to generate cytokine mediators of neurite growth[37]. In summary, there are a variety of potential mechanisms in which inflammasomes could impact neuronal morphology, some of which are depicted in figure 5.11. Future experiments in the lab will aim to uncover which, if any, are contributing to altered dendritic morphology.

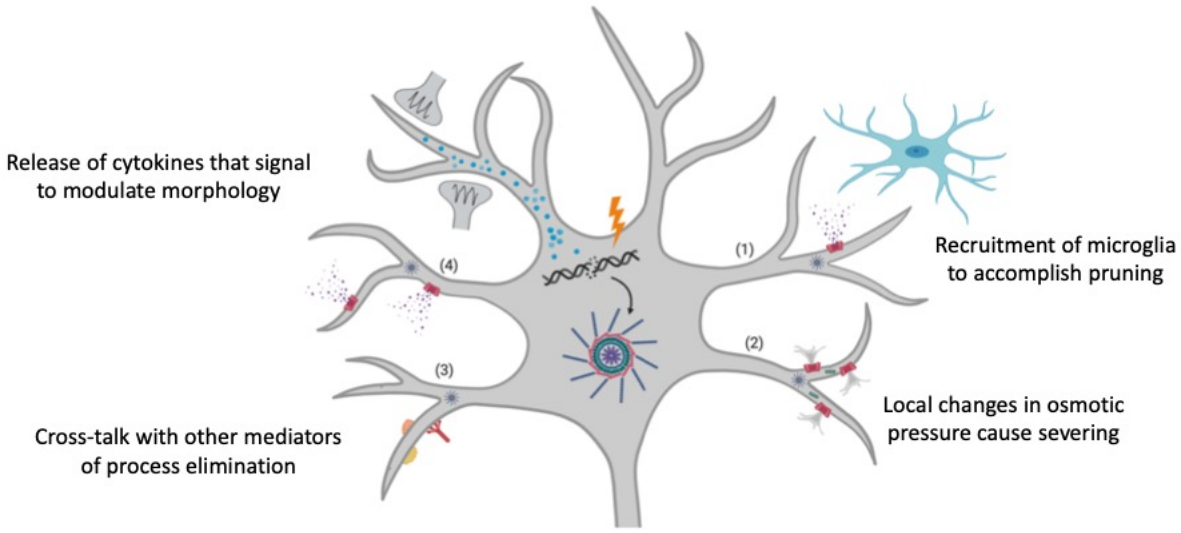

Figure 5.11. Potential mechanisms in which the inflammasome could modulate neuronal morphology. (1) Inflammasome mediated formation of Gasdermin-D pores and release of intracellular molecules, such as ATP, recruit microglia and provide and "eat-me" signal. (2) Inflammasome-mediated formation of Gasdermin-D pores disrupts local osmotic pressure leading to the lysis of process. Membrane repair via ESCRT machinery might facilitate damage control. (3) Inflammasomes signaling cross-talk with other synaptic pruning mediators, such the complement cascade and mitochondrial damage, promotes changes in dendritic morphology. (4) Inflammasome activation acts as a platform for cytokine production and release, resulting in changes to neuronal morphology.

Are there functional consequences of lacking inflammasome components in CNS cells?

Changes in dendritic morphology can greatly impact neuronal firing and circuitry, ultimately leading to altered behavior. Moreover, buildup of DNA damage in cells has been shown to promote cytokine production, metabolic distress, senescence, and cell death all of which can have adverse effects on neuronal function. To see if changes in dendritic morphology result in functional changes in neurons we performed patch clamp recordings of Purkinje neurons in the cerebellum with help from collaborators at Charles River. Preliminary recordings demonstrate that *Aim2*$^{-/-}$ neurons are receiving more spontaneous input than their WT controls (Figure 5.12). This data could be a result of a multitude of different things that have yet to be uncovered. One possibility is that an increase in the number of inhibitory cells in the cerebellum (Figure 6.3) could be increasing the number of synapses on a particular Purkinje neuron, therefore also increasing the number of dendritic spines.

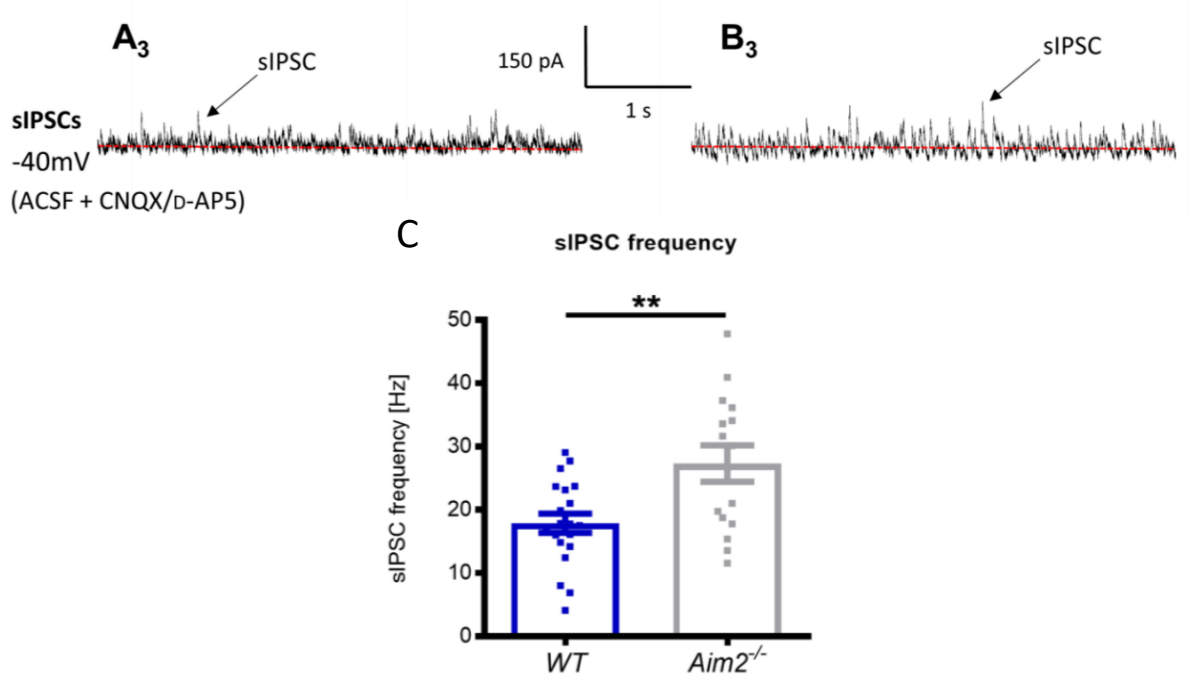

Figure 5.12 AIM2 Inflammasome deficient Purkinje neurons receive more spontaneous inhibitory inputs. Single cell recordings of purkinje cells from WT and *Aim2*$^{-/-}$ mice. (A-B) representative tracings of sPISCs from (A) WT and (B) *Aim2*$^{-/-}$ Purkinje cells. (C) Quantification of frequency of sIPSCs.

As previously stated, changes in neuronal firing can greatly impact behavior. Since we see altered electrophysiological states in Purkinje cells from *Aim2*$^{-/-}$ mice, we wanted to assay a relevant behavior to cerebellum signaling. We, therefore, ran inflammasome deficit mice on the accelerating rotarod to see if changes in Purkinje cell firing resulted in altered behavior. We see that inflammasome knockout mice perform worse on the accelerating rotarod than their WT controls (Figure 5.13).

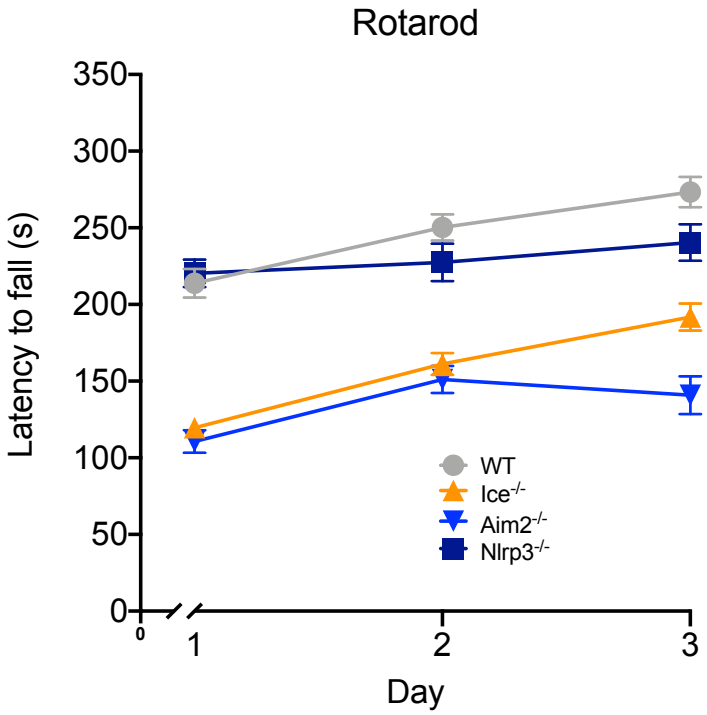

Figure 5.13 AIM2 Inflammasome deficient mice show altered performance on the accelerating rotarod. Adult WT, *Casp1*$^{-/-}$*, Aim2*$^{-/-}$*, and Nlrp3*$^{-/-}$ mice were tested on the accelerating rotarod for three consecutive days. Graph depicts latency to fall (s).

To further investigate how the AIM2 inflammasome impacts neuronal function we plan to culture neurons from p0 WT, *Aim2*$^{-/-}$, *Casp1/11*$^{-/-}$, and *Gsdmd*$^{-/-}$ pups and visualize both spontaneous and evoked firing using Ca^{2+} signaling. Next, we will investigate how removal or accumulation of dsDNA breaks affects neuronal function and firing. In order to determine how accumulation of DNA damage might impact the firing and function of neurons, we will induce DNA damage in cultured neurons from WT, *Aim2*$^{-/-}$, *Casp1/11*$^{-/-}$, and *Gsdmd*$^{-/-}$ p0 pups with ionizing radiation (40Gy). We will then measure spontaneous and evoked firing using Ca^{2+} signaling.

Cytokines in CNS development

As previously discussed in the introduction, cytokines can play an important role during neurodevelopment, both in the context of homeostasis and disease. Although there is clear evidence that immune dysfunction can have profound effects on neurodevelopment and downstream behaviors, less well understood are the sources and cellular targets of the cytokines that drive abnormal brain maturation and development of autistic-like behaviors. The diversity of cytokines, along with the many stages of neurodevelopment, makes discerning their role in neurodevelopment difficult. Just as in the immune system, the cytokine network in the developing brain is intricate and its functions within neurodevelopment likely depend upon the cell type, microenvironment of the brain region, time point, and converging signaling cascades.

Our preliminary results show that aberrant IL-1 signaling promotes ASD phenotypes; however, where the detrimental inflammatory signaling is occurring to drive these neurological and behavioral abnormalities remains to be conclusively determined. Future studies aimed to investigate if the detrimental IL-1 signaling is occurring in the mother or the fetus can be

accomplished by selectively knocking out IL-1R to disrupt IL-1 signaling in the mother or in the fetus. To accomplish this, two genetic crosses will be performed: (1) *Il1r*$^{-/-}$ females will be bred with wild-type males to produce IL-1R heterozygote offspring. (2) *Il1r*$^{+/-}$ females will be bred with *Il1r* $^{-/-}$ males to produce both *Il1r*$^{+/-}$ and *Il1r* $^{-/-}$ offspring. The pregnant females will be treated with Poly(I:C) or saline at E11.5 and E12.5 and their offspring will be evaluated for the three core ASD associated phenotypes. In the first cross, the heterozygote offspring will have partially rescued IL-1 inflammatory signaling while the mother will have none. Therefore, if IL-1R signaling is detrimental in the fetus, these mice will develop the core ASD associated phenotypes. In the second cross, the mother will have sufficient IL-1 signaling while the offspring will be either heterozygous or null for IL-1signaling. If the *Il1r*$^{+/-}$ offspring develop ASD-associated phenotypes and the *Il1r*$^{-/-}$ offspring do not, this would suggest that the detrimental IL-1 signaling occurs in the fetus. If, however, both genotypes are protected from abnormal neurological development, it can be inferred that detrimental IL-1 signaling is occurring in the mother.

Our knowledge of how the immune system functions within the CNS, particularly in neurodevelopment, is in its infancy. Expression patterns of innate immune components and cytokines (in addition to their receptors and signaling components) show remarkable regional and developmental specificity within the CNS. Moreover, disruption of immune signaling in fetal brain development can lead to both neurodevelopmental and neurogenerative disease. Uncovering the signaling pathways, timing, and consequences of these key immune mediators will give us insights into many neurologic disorders.

Chapter 6: Materials and methods

Mice

All mouse experiments were performed in accordance with the relevant guidelines and regulations of the University of Virginia and approved by the University of Virginia Animal Care and Use Committee. Mice were housed and behavior was conducted in specific pathogen-free conditions under standard 12 h light/dark cycle conditions in rooms equipped with control for temperature (21±1.5°C) and humidity (50±10%). Mice were randomly assigned into experimental groups matched for sex and age.

Vendor specific wild type mice

C57BL/6 mice were obtained from either The Jackson Laboratory (Jax) or Taconic Biosciences (Tac).

Genetic knockout models

Wild-type (WT) C57BL/6, *Aim2*$^{-/-}$[158], *Casp1/11*$^{-/-}$ (*Ice*$^{-/-}$)[201], *Nlrp3*$^{-/-}$[202], *Myd88*$^{-/-}$[203], *Il1r*$^{-/-}$[204], *Il18r*$^{-/-}$[205], R26-CAG-ASC-citrine[170], *Casp11*$^{-/-}$[206], *Casp1*$^{fl/fl}$[207], *Nestin*^{Cre}[208], and *Cx3cr1*^{Cre}[209] mice were obtained from The Jackson Laboratory. *Gsdmd*$^{-/-}$ mice were generously provided by Vishva Dixit[9].

Co-housing

Taconic bedding containing fecal samples was transferred to cages of 3-6 week-old Jackson mice 3 times per week for a total of two weeks. Mice were then mated and subjected to maternal immune activation (MIA), as described in detail below.

Maternal immune activation (MIA)

For more detailed methods paper describing the MIA protocol see **appendix 1**.

Mice were mated overnight and the presence of a vaginal plug was designated as embryonic day 0.5 (E0.5). Each pregnant dam was weighed and administered 20 mg/kg PolyI:C potassium salt (Sigma Aldrich) or saline by intraperitoneal (i.p.) injections on both E11.5 and E12.5. Pups were weaned from their mothers at post-natal day 21 (P21) and housed with same sex littermates with 2-5 mice per cage.

Cytokine blockade

Monoclonal anti-mouse IL-17A neutralizing antibody (clone 17F3; BioXCell, West Lebanon, NH) was administered via i.p. injections (500 µg/mouse) 6 hours prior to MIA-induction with PolyI:C administration.

IL-1β injections

Mice were mated overnight and the presence of a vaginal plug was designated as embryonic day 0.5 (E0.5). Each pregnant dam was weighed and administered 1.5 µg of recombinant IL-1β by intraperitoneal (i.p.) injections on both E11.5 and E12.5.

Behavioral testing

All behavioral testing was performed according to previously established behavioral methodologies. Behavioral experiments were carried out during daylight hours in a blinded fashion. All behavior was carried out using adult male mice (8-12 weeks old) except recordings of ultrasonic vocalizations which were conducted at postnatal day 10.

Elevated plus maze

Anxiety was assessed using an elevated plus maze. The elevated plus maze was comprised of two open arms (35 x 6 cm^2) and two closed arms (35 x 6 cm^2) with black plexiglass walls (20 cm in height) that extended from a common central platform (8 x 6 cm^2). The apparatus was constructed from polypropylene and Plexiglas (white floor, black walls) and elevated to a height of (121 cm) above floor level. Mice were individually placed on the center square, facing an open arm, and allowed to freely explore the apparatus for 5 min. Activity was measured by a computer-assisted TopScan optical animal activity system (version 3.0).

Open field testing

Spontaneous locomotor activity and anxiety was assessed in an open field test. The open field consists of a square arena (40 x 40 cm^2) with white Plexiglas walls and floor, evenly illuminated. All mice were individually placed in the upper left corner of the open field and left undisturbed to explore the arena over a 10 min session. Activity was measured by a computer-assisted TopScan optical animal activity system (version 3.0). Bouts into and time spent in a central square (15 x 15 cm^2) of the open field were automatically recorded as center bouts and center time, respectively. After the 10 min open field exploration, mice were returned to their home cage and number of urine stains and fecal pellets in the field were counted.

Sucrose preference

Depression-associated behaviors were assessed by measuring sucrose preference. Mice were given access to both untreated water and 2% sucrose water for 3 days. To prevent possible

effects of side-preference in drinking behavior, the position of the bottles in the cage was alternated every other day. No previous food or water deprivation was applied before the test.

Escape behavior

A modified tail suspension test was used to measure escape behavior. Mice were raised by their tails 30 cm into the air and assessed for escape behavior. Mice were monitored and time was measured until they became immobile.

Visual platform test

Visual performance was assessed using a visual escape platform test in the Morris Water Maze. Mice were placed in clear water with a visible white platform and performance was evaluated as time spent reaching the platform.

Ultrasonic vocalizations

On postnatal day 10, male pups were removed from their cages and habituated to the room away from their mother for 10 min. After the habituation period, mice were placed in a clean 1 L plastic flask. Ultrasonic vocalizations (USVs) were measured for 3 min using an UltraSoundGateGM16/CMPA microphone (AviSoft Bioacoustics) and recorded with SAS Prolab software (AviSoft Bioacoustics). USVs were measured between 25-125 kHz, and background recordings shorter than 0.02 ms were excluded.

Three-chamber social preference

Adult male mice were assessed for social preference using the three-chamber social approach test, which utilizes a three-chamber arena where chambers containing either a novel age- and

sex-matched mouse (male C57BL/6) or a novel object (plastic blue ball) in wire cups are separated by an empty center chamber. Experimental mice were habituated to the three-chamber arena with empty wire cages for two 5 min sessions. One day later, mice were placed in the empty center chamber without access to other test arenas for 5 min. Following this exploration period, the barriers were removed and mice were allowed to freely roam between the three chambers for 10 min and observed for interaction time with the targets in each chamber. Sessions were video recorded, and investigation time and distance traveled were tracked and analyzed using TopScan (version 3.0). The social preference index was calculated as the percentage of time investigating the novel mouse out of the total time investigating both the object and the mouse.

Marble burying

One week following the three-chamber social approach test, male mice were acclimated overnight to caging containing wood chip bedding. The following day, experimental mice were placed in a testing arena (arena size: 12”x7”x5”) that was filled with 2” of wood chip bedding. 20 glass marbles were arranged on the top of the bedding in 5 rows of 4 marbles equidistant from one another. After a 15 min exploration period, mice were carefully removed from the cages and a marble burying index score was calculated based on the following scale: 1 for marbles covered >50% by bedding, 0.5 for ~50% covered, or 0 for anything less.

Quantitative PCR

Genomic DNA was isolated from fecal pellets according to the manufacturer’s instructions (QIAamp DNA Stool Mini Kit, Qiagen). Quantitative PCR was performed as previously described using primers for SFB, Bacteroides, Prevotellaceae, Bifidobacterium spp., and total bacterial

16S rRNA genes[193, 210]. Relative quantity of SFB was calculated using the ΔC_t method and was normalized to the amount of total bacterial rRNA in each sample.

ELISA

Blood was collected by submandibular venipuncture from dams 48 hrs following the last injection with either 20 mg/kg PolyI:C or saline. Blood was allowed to clot for 60 min at room temperature. Serum was collected after centrifugation and IL-17a serum cytokine levels were measured by ELISA according to manufacturer's instructions (eBioscience).

Immunofluorescence

Mice were perfused with 4% paraformaldehyde (PFA) in phosphate buffered saline (PBS). The brains were removed and fixed in 4% PFA in PBS overnight at 4°C. After dehydration in 30% sucrose, 30 µm sagittal sections were obtained using a Leica CM1950 cryostat (Leica). Sections were permeabilized with blocking solution containing 0.4% Triton X-100, 2% donkey serum, and 1% bovine serum albumin (BSA) in PBS for 1 h at room temperature and then incubated with primary antibodies overnight at 4°C. Primary antibodies were diluted as follows: anti-GFAP (Invitrogen, 13-0300, 1:500), anti-calbindin (Sigma, C9848, 1:1,000), anti-γH2AX (abcam, ab11174, 1:1,000), anti-53bp1 (abcam, ab21083, 1:1,000). The following day, sections were incubated with fluorescently conjugated secondary antibodies (Invitrogen) for 2 h at room temperature and mounted in ProLong Gold antifade reagent (Invitrogen). Images of stained brain sections were acquired using a confocal microscope (Leica TCS SP8) and analyzed using ImageJ software. ASC visualization was accomplished using 488 nm detectors. 2-3 sections from each individual mouse were analyzed and averages were used for data analysis.

TUNEL assay

Cell death was measured *in vivo* using a TUNEL assay (Roche, 11 684 795 910) according to manufacturer's instructions. Briefly, P5 brains were perfused with PBS followed by 4% PFA and then drop fixed in 4% PFA for 24 hrs. After dehydration in 30% sucrose, 30 μm sagittal sections were obtained using a Leica CM1950 cryostat (Leica). Sections were permeabilized with blocking solution containing 0.4% Triton X-100, 2% donkey serum, and 1% BSA in PBS for 1 h at room temperature and then incubated with primary antibodies overnight at 4°C and secondary antibodies the following day for 2 h at room temperature. Sections were mounted and allowed to dry on a slide before 50 μL of the TUNEL reaction mixture was added to each section. Slides were then incubated in a humidified atmosphere for 60 min at +37°C in the dark. Slides were then rinsed 3x with 1x PBS and then analyzed under a fluorescence microscope using a 488 nm laser. 2-3 sections from each individual mouse were analyzed and averages were used for data analysis.

Comet assay

The comet assay was performed using the Oxiselect Comet Assay Kit (Cell-Biolabs Inc.) according to the manufacturer's instructions with minor modifications. Slides were coated in low melting agarose the night before the assay and left to dry overnight. Cells were added to the top of agarose-coated slides followed by immediate placement of a cover slip to ensure an even and flat distribution of cells on the slide.

Mixed neuron/glia culture

Mixed CNS culture was performed according to a previously established protocol with minor modifications[211]. All cell culture plates were pre-coated with Poly-D-Lysine before seeding. P0

pups were euthanized and the brain was placed into cold Neuron-Glia dissection buffer. After removal of the meninges, the cortex was detached and placed in a 50 mL conical with cold Neuron-Glia dissection buffer. The cortices were triturated into a single cell suspension using serological pipette and 3 x 10^5 cells were plated per well in a 24-well plate. Cells were cultured for 10-14 days before treatment, with media changes every 2-3 days.

dsDNA stimulations

After 10-14 days in culture, cells were stimulated +/- lipopolysaccharide (LPS) (0.5 μg/mL) in stimulation media containing Iscove's Modified Dulbecco's Medium (Gibco), 1% Penicillin/Strepomycin, 10% fetal bovine serum, 1% L-Glutamine, and 50 μM 2-beta-mercaptoethanol for 4 h at 37°C. After 4 h, cells were given additional stimuli to induce/mimic dsDNA breaks.

Etoposide (abcam, ab120227): A 100 mM stock was prepared in DMSO according to the manufacturer's instructions and diluted to a final concentration of 20 μM or 100 μM in stimulation media. Cells were treated with +/- etoposide and incubated overnight at 37°C and supernatants were collected the following morning for additional assays.

Ionizing radiation: Cells were exposed to 40 Gy for 20 min and incubated overnight at 37°C. Supernatants were collected the following morning for additional assays. P5 mice were exposed to 14 Gy ionizing radiation and then returned to their home cage for 6 h. After 6 h, brain tissue was harvested for immunofluorescence and TUNEL staining.

PolydA:dT: Mixed glia cells were transfected with +/- polydA:dT using lipofectamine 2000 reagent (Invitrogen, 11668-030) according to the manufacturer's instructions and incubated overnight at 37°C. Supernatants were collected the following morning for additional assays.

Cytotoxicity

LDH release was measured using the CytoTox96 Non-Radioactive Cytotoxicity Assay (Promega, G1780) according to the manufacturer's instructions. Maximum LDH release control for each plate was generated using Lysis Solution.

RNA *in situ* hybridization (ISH)

Brains from P5 pups were formalin fixed for 48 h, embedded in paraffin, and cut into 5 µm sections. In situ hybridization was carried out according to the manufacturer's instructions (Affymetrix, QVT0012). Probes recognizing *Aim2* RNA (NM_001013779) were multiplexed with probes recognizing RNA expressed in neurons (*Rbfox3*, NM_001039167), microglia (*Aif1*, NM_019467), and astrocytes (*Gfap*, NM_010277). Ubiquitin (*Ubc*, NM_019639) was used as a positive control.

Statistical analysis

All statistical analyses were performed using GraphPad Prism. Statistical significance was calculated by Student's *t*-test, one-way analysis of variance (ANOVA) with Tukey's *post hoc* tests or two-way ANOVA with Tukey's *post hoc* tests. *P*-values <0.05 were considered significant. Asterisks denote *P* values as follows: $*P < 0.05$, $**P < 0.01$, $***P < 0.001$.

Appendix 1: Modeling autism-related disorders in mice with maternal immune activation (MIA)

Materials

Maternal immune activation (MIA) induction

1. Prepare 10 mg/ml stock of Polyinosinic-polycytidylic acid potassium salt (PolyI:C) (Millipore Sigma P9582) using salt weight in sterile PBS. For one vial of PolyI:C dissolve powder (50 mg) in 5 mL sterile PBS (*See* **Note 1**).

Ultrasonic vocalization recording

1. Microphone capable of recording ultrasonic vocalizations (USVs) between 2 kHz-200 kHz needed (*See* **Note 2**).
2. Software that can detect and analyze USVs (*See* **Note 3**).
3. Glass or plastic container that is capable of fitting microphone and mouse pup (approximately the size of a 500 mL beaker).

Social preference test

1. Arena for three chamber social preference testing (*See* **Note 4).**
2. Containment cage (*See* **Note 5**).
3. Object that the mouse has not previously encountered (plastic toy).
4. Software and cameras capable of tracking and analyzing movement of experimental mice (*See* **Note 6**).

Marble burying test

1. Teklad Laboratory Grade Sani-chip bedding.
2. 20 marbles (1.5 cm diameter).

Fecal transplantation

1. QIAamp DNA Stool Mini Kit for extraction of genomic DNA from fecal samples (Catalog number 51504).

2. Segmented Filamentous Bacteria (SFB) forward and reverse primers for confirmation of Taconic microbiome transfer.
    a. Forward: 5’ GAC GCT GAG GCA TGA GAG CAT 3’
    b. Reverse: 5’ GAC GGC ACG GAT TGT TAT TCA 3’
3. Universal (UNI) forward and reverse primers for total bacteria.
    a. Forward: 5’ ACT CCT ACG GGA GGC AGC AGT 3’
    b. Reverse: 5’ ATT ACC GCG GCT GCT GCG 3’
4. Quantitative real time PCR thermocycler.

Methods

Maternal immune activation

Studies from our lab and others have identified that appropriate gestational inflammatory conditions, such as induction of IL-17a-mediated inflammation, need to be present during pregnancy to consistently promote the development of autism-related phenotypes in MIA offspring [152-154]. Mice from Taconic Biosciences, due to their propensity to generate robust levels of IL-17a in response to immune triggers, produce the most consistent results in the MIA model of neurodevelopmental disease. It should be noted that mice from other vendors can also be used to study MIA-induced neurodevelopmental disorders; however, fecal transplantation with Taconic microbiota or troubleshooting with different dosages of PolyI:C may be required to generate consistent results (*See* **Note 7**).

1. In order to ensure that maternal immune activation occurs at the correct embryonic time points, mice are mated overnight and females are checked twice daily, once in the

morning and once in the evening, for the presence of vaginal plugs (Fig. A.1). The presence of a plug denotes embryonic day 0.5 (E0.5).

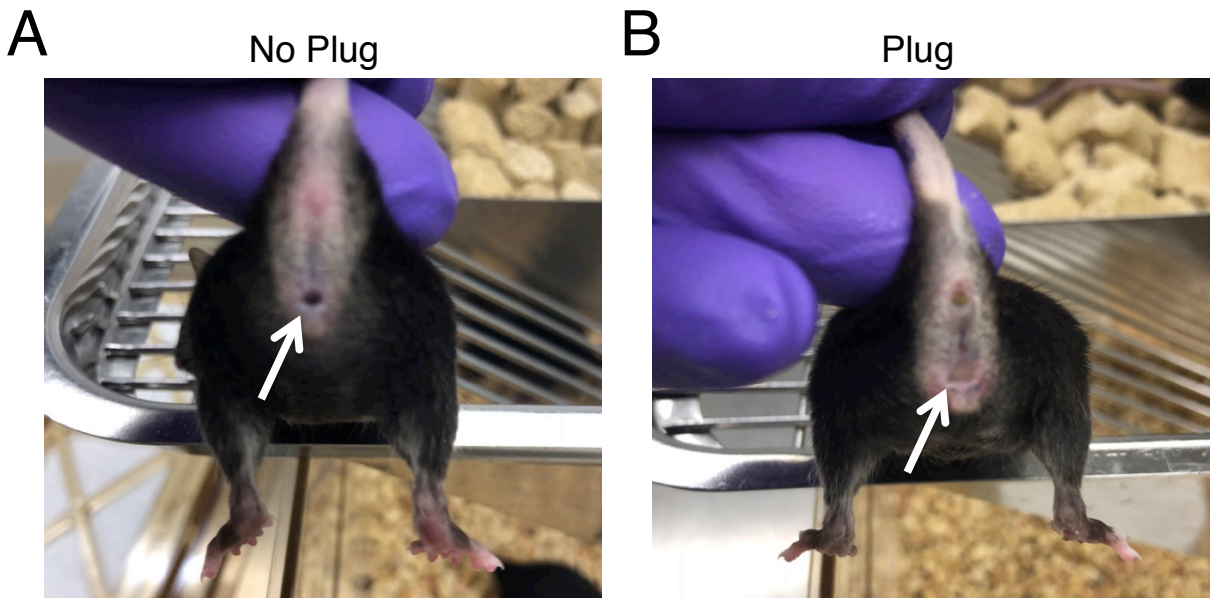

Figure A1. Calculating date of conception with vaginal plug identification. (A) White arrow indicates no plug. (B) White arrow indicates plug. Presence of a vaginal plug can be used to mark embryonic day 0.5 (E0.5).

2. Mice are then left undisturbed until E11.5 when pregnant female mice are weighed and treated with 20 mg/kg PolyI:C or PBS by intraperitoneal (ip) injection (*See* **Note 8**).
3. Females are then subjected to a second dose of PolyI:C (20 mg/kg; i.p.) or PBS on E12.5 (*See* **Note 9**).
4. Each dam is returned to its cage and left undisturbed until the birth of its litter. All pups remain with the mother until weaning (typically between postnatal day 21 (P21) and P24),

at which time mice can be group housed at 2-5 mice per cage with same-sex littermates (*See* **Note 10**).

Behavior

In order to ensure reproducible results in behavioral testing, it is important to conduct all behavioral tests under controlled and consistent conditions. The same animal handler should conduct all behavioral tests at the same time of day. It is important to eliminate extraneous noises and to habituate the mice to the room for a least one hour before behavioral tests are conducted. Behavioral equipment should be thoroughly cleaned with 70% ethanol between each experimental mouse to eliminate any urine, feces, or odors. Multiple litters should also be tested to confirm that the behaviors are robust and reproducible. Behavioral abnormalities in the PolyI:C MIA model are typically only observed in male offspring and are absent in their female littermates [212, 213]. This sex bias is also observed in human populations where there is a strong bias towards males in both autism and schizophrenia [214, 215].

Ultrasonic vocalization recording

1. On postnatal days 9-11, bring cages containing both mothers and litters to the testing room and allow mice to habituate for 1 h (*See* **Note 11**).
2. After mice are habituated, remove all male pups from the nest (away from the mother) and put them into a cup with bedding from their cage for 10 min without recording.
3. After the habituation period, individually place mice in a clean holding dish and record mouse pup USVs for 3 min using a microphone capable of recording USVs (e.g., UltraSoundGate GM16/CMPA microphone; AviSoft Bioacoustics) and recording software that can analyze USV data (e.g., SAS Prolab software; AviSoft Bioacoustics) (*See* **Note**

12). Record USVs that are measured between 25-125 kHz, and exclude background recordings that are shorter than 0.02 ms.

Social Preference Test

1. Mice can be assessed in the social preference test once they are 8 weeks old. One day prior to testing, experimental mice need to be individually habituated to the three-chamber arena containing empty object containment cages, for two 5 min sessions in a 3-4 h period (*See* **Note 13**).
2. On the following day, assess social behavior by first placing each mouse in the center chamber without access to either the top or bottom chambers, which contain an unfamiliar C57BL/6 age-matched male mouse in one chamber and an inanimate object (plastic toy) in the other chamber under object containment cages (*See* **Note 14**).
3. After the 5 min exploration period in the center chamber, remove the barriers to the adjacent chambers, enabling the mouse to explore the top and bottom arenas freely.
4. Allow the mouse to explore all chambers for an additional 10 min while tracking interaction time as time spent sniffing or approaching ~ 2 cm from the containment cage.
5. After 10 min, experimental and novel mice should be gently removed and returned to home cages, and then all surfaces of the arena, containment cages, and plastic toy should be thoroughly cleaned with 70% ethanol.
6. Social preference index data can be calculated and plotted as the percentage of time spent investigating the social target (novel mouse) out of the total exploration time of both objects (novel mouse + novel object) (*See* **Note 15**).

Marble burying test

1. One week following the social preference test, acclimate male mice overnight to autoclaved woodchip bedding (*See* **Note 16**).
2. The following morning, place mice in a clean cage filled with ~2 in of fresh, autoclaved woodchip bedding containing 20 glass marbles laid out in four rows of five marbles equidistant from one another.
3. After a 15 min exploration period, gently remove mice from the testing cages and record the number of marbles buried using the marble burying index: marbles covered >50% by bedding are given a score of 1, ~50% covered are given a score of 0.5, and marbles covered <50% are given a score of 0 [152].

Notes

1. Store PolyI:C stock in small (~200 µL) aliquots at -20°C and avoid freeze-thaw cycles.
2. USVs were recorded using an UltraSoundGateGM16/CMPA microphone (AviSoft Bioacoustics, Glienicke, Germany).
3. USVs were measured and analyzed with SAS Prolab software (AviSoft Bioacoustics, Glienicke, Germany). When troubleshooting USVs, it is important to confirm counts by hand.
4. Total arena area 24 x 16 x 9 inches. Dimensions of chambers 8 x 16 x 9 inches.
5. Containment cages for the sociability test should enable objects to be clearly seen and smelled, while limiting fighting and mounting.
6. Social preference data presented in was tracked and analyzed using TopScan version 3.00.
7. Fecal microbiota from Taconic mice can be transferred into mice from The Jackson Laboratory or other vendors by exposing mice to feces from Taconic mice for at least two

weeks. A small scoop (enough to fill a 50 mL beaker) of Taconic bedding containing feces from sex-matched mice is mixed into cages housing Jackson mice for two weeks, with fresh fecal samples being added every 3 days. SFB transfer can be confirmed by collecting fecal pellets before and after cohousing and assaying for the presence of total bacteria (total 16S rRNA) and SFB by qPCR. Mice can then be mated and subjected to MIA using the same protocol as described in the Methods section. We have confirmed that this experimental strategy is effective in inducing MIA-associated ASD-like phenotypes in Jackson C57BL/6 mice that previously underwent fecal transplantation with microbiota from Taconic C57BL/6 mice. We have not, however, attempted these fecal transfer experiments in mice from other vendors and thus further troubleshooting may be required when using mice from vendors other than Jackson and Taconic.

8. Pregnant dams injected with PolyI:C should not show overt signs of sickness behavior such as dramatic weight loss or immobility, although they will exhibit reduced weight gain and sometimes minor weight loss for the first few days following PolyI:C injection.
9. This two-injection MIA protocol (PolyI:C on days E11.5 and E12.5) differs slightly from others in the field, that only rely on a single PolyI:C injection on E12.5. However, through exhaustive troubleshooting that involved various injection regimens, we have found that an injection on both E11.5 and E12.5 produces the most consistent results.
10. Mice should not be singly housed because this can affect behavior. Studies show that singly housed mice often develop depressive-like behaviors, which can ultimately affect performance in behavioral testing.
11. Due to differences in USV trends observed between labs, where some labs observe an increase in vocalizations from MIA offspring [152-154] while others detect less [129, 147, 213], it is

helpful to first measure USVs over multiple days (postnatal days 7-14) to detect where the most robust differences are observed.

12. The microphone should hang ~ 2 in above the bottom of the container.
13. Since experimental mice can climb up the containment cages during the test, it helps to have an object on top to prevent the mouse from climbing on top of the containment cage.
14. Before performing social preference testing and while the experimental mice are acclimating to the room, habituate novel mice 2 times (5 min each) under the containment cages.
15. It is important to also track distance traveled during both the habituation and social preference tests to ensure that any observed differences in social preference are not due to overall lack of activity or alertness.
16. If mice are already housed in woodchip bedding, this step is not necessary. The same cages can be used for mice from the same litter; however, it is important to change the woodchip bedding between each mouse regardless of if they are littermates

Chapter 8: Literature Cited

1. Louveau A, Harris TH and Kipnis J. Revisiting the Mechanisms of CNS Immune Privilege. *Trends Immunol*. 2015;36:569-577.

2. Stevens B, Allen Nj Fau - Vazquez LE, Vazquez Le Fau - Howell GR, Howell Gr Fau - Christopherson KS, Christopherson Ks Fau - Nouri N, Nouri N Fau - Micheva KD, Micheva Kd Fau - Mehalow AK, Mehalow Ak Fau - Huberman AD, Huberman Ad Fau - Stafford B, Stafford B Fau - Sher A, Sher A Fau - Litke AM, Litke Am Fau - Lambris JD, Lambris Jd Fau - Smith SJ, Smith Sj Fau - John SWM, John Sw Fau - Barres BA and Barres BA. The classical complement cascade mediates CNS synapse elimination.
3. Lampron A, Elali A and Rivest S. Innate immunity in the CNS: redefining the relationship between the CNS and Its environment. *Neuron*. 2013;78:214-32.
4. Walsh JG, Muruve DA and Power C. Inflammasomes in the CNS. *Nat Rev Neurosci*. 2014;15:84-97.
5. Lukens JR, Gross JM and Kanneganti TD. IL-1 family cytokines trigger sterile inflammatory disease. *Front Immunol*. 2012;3:315.
6. Broz P, von Moltke J, Jones JW, Vance RE and Monack DM. Differential requirement for Caspase-1 autoproteolysis in pathogen-induced cell death and cytokine processing. *Cell Host Microbe*. 2010;8:471-83.
7. Guey B, Bodnar M, Manié SN, Tardivel A and Petrilli V. Caspase-1 autoproteolysis is differentially required for NLRP1b and NLRP3 inflammasome function. *Proc Natl Acad Sci U S A*. 2014;111:17254-9.
8. Van Opdenbosch N, Gurung P, Vande Walle L, Fossoul A, Kanneganti TD and Lamkanfi M. Activation of the NLRP1b inflammasome independently of ASC-mediated caspase-1 autoproteolysis and speck formation. *Nat Commun*. 2014;5:3209.
9. Kayagaki N, Stowe IB, Lee BL, O'Rourke K, Anderson K, Warming S, Cuellar T, Haley B, Roose-Girma M, Phung QT, Liu PS, Lill JR, Li H, Wu J, Kummerfeld S, Zhang J, Lee WP, Snipas SJ, Salvesen GS, Morris LX, Fitzgerald L, Zhang Y, Bertram EM, Goodnow CC and Dixit VM. Caspase-11 cleaves gasdermin D for non-canonical inflammasome signalling. *Nature*. 2015;526:666-71.
10. Sborgi L, Rühl S, Mulvihill EA-O, Pipercevic J, Heilig R, Stahlberg HA-O, Farady CJ, Müller DJ, Broz P and Hiller SA-O. GSDMD membrane pore formation constitutes the mechanism of pyroptotic cell death.
11. Sims JE and Smith DE. The IL-1 family: regulators of immunity. *Nat Rev Immunol*. 2010;10:89-102.
12. Allan SM, Tyrrell PJ and Rothwell NJ. Interleukin-1 and neuronal injury. *Nat Rev Immunol*. 2005;5:629-40.
13. Martinon F, Burns K and Tschopp J. The inflammasome: a molecular platform triggering activation of inflammatory caspases and processing of proIL-beta. *Mol Cell*. 2002;10:417-26.
14. Boyden ED and Dietrich WF. Nalp1b controls mouse macrophage susceptibility to anthrax lethal toxin. *Nat Genet*. 2006;38:240-4.
15. Turk BE. Manipulation of host signalling pathways by anthrax toxins. *Biochem J*. 2007;402:405-17.
16. Liao KC and Mogridge J. Activation of the Nlrp1b inflammasome by reduction of cytosolic ATP. *Infect Immun*. 2013;81:570-9.
17. Geldhoff M, Mook-Kanamori BB, Brouwer MC, Valls Seron M, Baas F, van der Ende A and van de Beek D. Genetic variation in inflammasome genes is associated with outcome in bacterial meningitis. *Immunogenetics*. 2013;65:9-16.
18. Pontillo A, Catamo E, Arosio B, Mari D and Crovella S. NALP1/NLRP1 genetic variants are associated with Alzheimer disease. *Alzheimer Dis Assoc Disord*. 2012;26:277-81.

19. Zhao Y, Yang J, Shi J, Gong YN, Lu Q, Xu H, Liu L and Shao F. The NLRC4 inflammasome receptors for bacterial flagellin and type III secretion apparatus. *Nature*. 2011;477:596-600.
20. Kofoed EM and Vance RE. Innate immune recognition of bacterial ligands by NAIPs determines inflammasome specificity. *Nature*. 2011;477:592-5.
21. Gutierrez O, Pipaon C and Fernandez-Luna JL. Ipaf is upregulated by tumor necrosis factor-alpha in human leukemia cells. *FEBS Lett*. 2004;568:79-82.
22. Poyet JL, Srinivasula SM, Tnani M, Razmara M, Fernandes-Alnemri T and Alnemri ES. Identification of Ipaf, a human caspase-1-activating protein related to Apaf-1. *J Biol Chem*. 2001;276:28309-13.
23. Miao EA, Alpuche-Aranda Cm Fau - Dors M, Dors M Fau - Clark AE, Clark Ae Fau - Bader MW, Bader Mw Fau - Miller SI, Miller Si Fau - Aderem A and Aderem A. Cytoplasmic flagellin activates caspase-1 and secretion of interleukin 1beta via Ipaf.
24. Franchi L, Kamada N, Nakamura Y, Burberry A, Kuffa P, Suzuki S, Shaw MH, Kim YG and Núñez G. NLRC4-driven production of IL-1β discriminates between pathogenic and commensal bacteria and promotes host intestinal defense. *Nat Immunol*. 2012;13:449-56.
25. Canna SW, de Jesus AA, Gouni S, Brooks SR, Marrero B, Liu Y, DiMattia MA, Zaal KJ, Sanchez GA, Kim H, Chapelle D, Plass N, Huang Y, Villarino AV, Biancotto A, Fleisher TA, Duncan JA, O'Shea JJ, Benseler S, Grom A, Deng Z, Laxer RM and Goldbach-Mansky R. An activating NLRC4 inflammasome mutation causes autoinflammation with recurrent macrophage activation syndrome. *Nat Genet*. 2014;46:1140-6.
26. Romberg N, Al Moussawi K, Nelson-Williams C, Stiegler AL, Loring E, Choi M, Overton J, Meffre E, Khokha MK, Huttner AJ, West B, Podoltsev NA, Boggon TJ, Kazmierczak BI and Lifton RP. Mutation of NLRC4 causes a syndrome of enterocolitis and autoinflammation. *Nat Genet*. 2014;46:1135-1139.
27. Duncan JA, Gao X, Huang MT, O'Connor BP, Thomas CE, Willingham SB, Bergstralh DT, Jarvis GA, Sparling PF and Ting JP. Neisseria gonorrhoeae activates the proteinase cathepsin B to mediate the signaling activities of the NLRP3 and ASC-containing inflammasome. *J Immunol*. 2009;182:6460-9.
28. Ichinohe T, Lee HK, Ogura Y, Flavell R and Iwasaki A. Inflammasome recognition of influenza virus is essential for adaptive immune responses. *J Exp Med*. 2009;206:79-87.
29. Halle A, Hornung V, Petzold GC, Stewart CR, Monks BG, Reinheckel T, Fitzgerald KA, Latz E, Moore KJ and Golenbock DT. The NALP3 inflammasome is involved in the innate immune response to amyloid-beta. *Nat Immunol*. 2008;9:857-65.
30. Martinon F, Pétrilli V, Mayor A, Tardivel A and Tschopp J. Gout-associated uric acid crystals activate the NALP3 inflammasome. *Nature*. 2006;440:237-41.
31. Hornung V, Bauernfeind F, Halle A, Samstad EO, Kono H, Rock KL, Fitzgerald KA and Latz E. Silica crystals and aluminum salts activate the NALP3 inflammasome through phagosomal destabilization. *Nat Immunol*. 2008;9:847-56.
32. Zhang X, Zhang JH, Chen XY, Hu QH, Wang MX, Jin R, Zhang QY, Wang W, Wang R, Kang LL, Li JS, Li M, Pan Y, Huang JJ and Kong LD. Reactive oxygen species-induced TXNIP drives fructose-mediated hepatic inflammation and lipid accumulation through NLRP3 inflammasome activation. *Antioxid Redox Signal*. 2015;22:848-70.
33. Zhou R, Tardivel A, Thorens B, Choi I and Tschopp J. Thioredoxin-interacting protein links oxidative stress to inflammasome activation. *Nat Immunol*. 2010;11:136-40.

34. Muñoz-Planillo R, Kuffa P, Martínez-Colón G, Smith BL, Rajendiran TM and Núñez G. K^+ efflux is the common trigger of NLRP3 inflammasome activation by bacterial toxins and particulate matter. *Immunity*. 2013;38:1142-53.
35. Halle A, Hornung V Fau - Petzold GC, Petzold Gc Fau - Stewart CR, Stewart Cr Fau - Monks BG, Monks Bg Fau - Reinheckel T, Reinheckel T Fau - Fitzgerald KA, Fitzgerald Ka Fau - Latz E, Latz E Fau - Moore KJ, Moore Kj Fau - Golenbock DT and Golenbock DT. The NALP3 inflammasome is involved in the innate immune response to amyloid-beta.
36. Codolo G, Plotegher N, Pozzobon T, Brucale M, Tessari I, Bubacco L and de Bernard M. Triggering of inflammasome by aggregated α-synuclein, an inflammatory response in synucleinopathies. *PLoS One*. 2013;8:e55375.
37. Wu PJ, Liu HY, Huang TN and Hsueh YP. AIM 2 inflammasomes regulate neuronal morphology and influence anxiety and memory in mice. *Sci Rep*. 2016;6:32405.
38. Gadani SP, Walsh JT, Lukens JR and Kipnis J. Dealing with Danger in the CNS: The Response of the Immune System to Injury. *Neuron*. 2015;87:47-62.
39. Adamczak S, Dale G, de Rivero Vaccari JP, Bullock MR, Dietrich WD and Keane RW. Inflammasome proteins in cerebrospinal fluid of brain-injured patients as biomarkers of functional outcome: clinical article. *J Neurosurg*. 2012;117:1119-25.
40. Wallisch JS, Simon DW, Bayır H, Bell MJ, Kochanek PM and Clark RSB. Cerebrospinal Fluid NLRP3 is Increased After Severe Traumatic Brain Injury in Infants and Children. *Neurocrit Care*. 2017;27:44-50.
41. Irrera N, Pizzino G, Calò M, Pallio G, Mannino F, Famà F, Arcoraci V, Fodale V, David A, Francesca C, Minutoli L, Mazzon E, Bramanti P, Squadrito F, Altavilla D and Bitto A. Lack of the Nlrp3 Inflammasome Improves Mice Recovery Following Traumatic Brain Injury. *Front Pharmacol*. 2017;8:459.
42. Liu HD, Li W, Chen ZR, Hu YC, Zhang DD, Shen W, Zhou ML, Zhu L and Hang CH. Expression of the NLRP3 inflammasome in cerebral cortex after traumatic brain injury in a rat model. *Neurochem Res*. 2013;38:2072-83.
43. de Rivero Vaccari JP, Lotocki G, Marcillo AE, Dietrich WD and Keane RW. A molecular platform in neurons regulates inflammation after spinal cord injury. *J Neurosci*. 2008;28:3404-14.
44. Barrington J, Lemarchand E and Allan SM. A brain in flame; do inflammasomes and pyroptosis influence stroke pathology? *Brain Pathol*. 2017;27:205-212.
45. Mamik MK and Power C. Inflammasomes in neurological diseases: emerging pathogenic and therapeutic concepts. *Brain*. 2017;140:2273-2285.
46. Inoue M and Shinohara ML. NLRP3 Inflammasome and MS/EAE. *Autoimmune Dis*. 2013;2013:859145.
47. Voet S, Mc Guire C, Hagemeyer N, Martens A, Schroeder A, Wieghofer P, Daems C, Staszewski O, Vande Walle L, Jordao MJC, Sze M, Vikkula HK, Demeestere D, Van Imschoot G, Scott CL, Hoste E, Gonçalves A, Guilliams M, Lippens S, Libert C, Vandenbroucke RE, Kim KW, Jung S, Callaerts-Vegh Z, Callaerts P, de Wit J, Lamkanfi M, Prinz M and van Loo G. A20 critically controls microglia activation and inhibits inflammasome-dependent neuroinflammation. *Nat Commun*. 2018;9:2036.
48. Inoue M, Williams KL, Gunn MD and Shinohara ML. NLRP3 inflammasome induces chemotactic immune cell migration to the CNS in experimental autoimmune encephalomyelitis. *Proc Natl Acad Sci U S A*. 2012;109:10480-5.

49. Gris D, Ye Z, Iocca HA, Wen H, Craven RR, Gris P, Huang M, Schneider M, Miller SD and Ting JP. NLRP3 plays a critical role in the development of experimental autoimmune encephalomyelitis by mediating Th1 and Th17 responses. *J Immunol*. 2010;185:974-81.
50. Jha S, Srivastava SY, Brickey WJ, Iocca H, Toews A, Morrison JP, Chen VS, Gris D, Matsushima GK and Ting JP. The inflammasome sensor, NLRP3, regulates CNS inflammation and demyelination via caspase-1 and interleukin-18. *J Neurosci*. 2010;30:15811-20.
51. De Strooper B and Karran E. The Cellular Phase of Alzheimer's Disease.
52. Sala Frigerio C and De Strooper B. Alzheimer's Disease Mechanisms and Emerging Roads to Novel Therapeutics.
53. Sarlus H and Heneka MT. Microglia in Alzheimer's disease.
54. Griffin WS, Stanley LC, Ling C, White L, MacLeod V, Perrot LJ, White CL and Araoz C. Brain interleukin 1 and S-100 immunoreactivity are elevated in Down syndrome and Alzheimer disease. *Proc Natl Acad Sci U S A*. 1989;86:7611-5.
55. Simard AR, Soulet D Fau - Gowing G, Gowing G Fau - Julien J-P, Julien Jp Fau - Rivest S and Rivest S. Bone marrow-derived microglia play a critical role in restricting senile plaque formation in Alzheimer's disease.
56. Saresella M, La Rosa F, Piancone F, Zoppis M, Marventano I, Calabrese E, Rainone V, Nemni R, Mancuso R and Clerici M. The NLRP3 and NLRP1 inflammasomes are activated in Alzheimer's disease.
57. Stancu IC, Cremers N, Vanrusselt H, Couturier J, Vanoosthuyse A, Kessels S, Lodder C, Brône B, Huaux F, Octave JN, Terwel D and Dewachter I. Aggregated Tau activates NLRP3-ASC inflammasome exacerbating exogenously seeded and non-exogenously seeded Tau pathology in vivo. *Acta Neuropathol*. 2019;137:599-617.
58. Heneka MT, McManus RM and Latz E. Inflammasome signalling in brain function and neurodegenerative disease. *Nat Rev Neurosci*. 2018;19:610-621.
59. Dempsey C, Rubio Araiz A, Bryson KJ, Finucane O, Larkin C, Mills EL, Robertson AAB, Cooper MA, O'Neill LAJ and Lynch MA. Inhibiting the NLRP3 inflammasome with MCC950 promotes non-phlogistic clearance of amyloid-β and cognitive function in APP/PS1 mice.
60. Venegas C, Kumar S, Franklin BS, Dierkes T, Brinkschulte R, Tejera D, Vieira-Saecker A, Schwartz S, Santarelli F, Kummer MP, Griep A, Gelpi E, Beilharz M, Riedel D, Golenbock DT, Geyer M, Walter J, Latz E and Heneka MT. Microglia-derived ASC specks cross-seed amyloid-β in Alzheimer's disease.
61. Wu PJ, Hung Yf Fau - Liu H-Y, Liu Hy Fau - Hsueh Y-P and Hsueh YP. Deletion of the Inflammasome Sensor Aim2 Mitigates Aβ Deposition and Microglial Activation but Increases Inflammatory Cytokine Expression in an Alzheimer Disease Mouse Model.
62. Tan MS, Tan L, Jiang T, Zhu XC, Wang HF, Jia CD and Yu JT. Amyloid-β induces NLRP1-dependent neuronal pyroptosis in models of Alzheimer's disease.
63. Przedborski S. The two-century journey of Parkinson disease research.
64. Zhou Y, Lu M, Du RH, Qiao C, Jiang CY, Zhang KZ, Ding JH and Hu G. MicroRNA-7 targets Nod-like receptor protein 3 inflammasome to modulate neuroinflammation in the pathogenesis of Parkinson's disease.
65. Mogi M, Harada M Fau - Kondo T, Kondo T Fau - Riederer P, Riederer P Fau - Inagaki H, Inagaki H Fau - Minami M, Minami M Fau - Nagatsu T and Nagatsu T. Interleukin-1 beta, interleukin-6, epidermal growth factor and transforming growth factor-alpha are elevated in the brain from parkinsonian patients.

66. Ferrari CC, Pott Godoy Mc Fau - Tarelli R, Tarelli R Fau - Chertoff M, Chertoff M Fau - Depino AM, Depino Am Fau - Pitossi FJ and Pitossi FJ. Progressive neurodegeneration and motor disabilities induced by chronic expression of IL-1beta in the substantia nigra.
67. Mao Z, Liu C, Ji S, Yang Q, Ye H, Han H and Xue Z. The NLRP3 Inflammasome is Involved in the Pathogenesis of Parkinson's Disease in Rats.
68. Wang W, Nguyen LT, Burlak C, Chegini F, Guo F, Chataway T, Ju S, Fisher OS, Miller DW, Datta D, Wu F, Wu CX, Landeru A, Wells JA, Cookson MR, Boxer MB, Thomas CJ, Gai WP, Ringe D, Petsko GA and Hoang QQ. Caspase-1 causes truncation and aggregation of the Parkinson's disease-associated protein α-synuclein.
69. Azevedo FA, Carvalho Lr Fau - Grinberg LT, Grinberg Lt Fau - Farfel JM, Farfel Jm Fau - Ferretti REL, Ferretti Re Fau - Leite REP, Leite Re Fau - Jacob Filho W, Jacob Filho W Fau - Lent R, Lent R Fau - Herculano-Houzel S and Herculano-Houzel S. Equal numbers of neuronal and nonneuronal cells make the human brain an isometrically scaled-up primate brain.
70. von Bartheld CS, Bahney J and Herculano-Houzel S. The search for true numbers of neurons and glial cells in the human brain: A review of 150 years of cell counting.
71. Lindahl T and Barnes DE. Repair of endogenous DNA damage. *Cold Spring Harb Symp Quant Biol*. 2000;65:127-33.
72. Subba Rao K. Mechanisms of disease: DNA repair defects and neurological disease. *Nat Clin Pract Neurol*. 2007;3:162-72.
73. Madabhushi R, Pan L and Tsai LH. DNA damage and its links to neurodegeneration. *Neuron*. 2014;83:266-82.
74. McKinnon PJ. Maintaining genome stability in the nervous system. *Nat Neurosci*. 2013;16:1523-9.
75. Barzilai A, Biton S and Shiloh Y. The role of the DNA damage response in neuronal development, organization and maintenance. *DNA Repair (Amst)*. 2008;7:1010-27.
76. Abner CW and McKinnon PJ. The DNA double-strand break response in the nervous system. *DNA Repair (Amst)*. 2004;3:1141-7.
77. Takashima H, Boerkoel CF, John J, Saifi GM, Salih MA, Armstrong D, Mao Y, Quiocho FA, Roa BB, Nakagawa M, Stockton DW and Lupski JR. Mutation of TDP1, encoding a topoisomerase I-dependent DNA damage repair enzyme, in spinocerebellar ataxia with axonal neuropathy. *Nat Genet*. 2002;32:267-72.
78. Haugen AC, Di Prospero NA, Parker JS, Fannin RD, Chou J, Meyer JN, Halweg C, Collins JB, Durr A, Fischbeck K and Van Houten B. Altered gene expression and DNA damage in peripheral blood cells from Friedreich's ataxia patients: cellular model of pathology. *PLoS Genet*. 2010;6:e1000812.
79. El-Khamisy SF, Saifi GM, Weinfeld M, Johansson F, Helleday T, Lupski JR and Caldecott KW. Defective DNA single-strand break repair in spinocerebellar ataxia with axonal neuropathy-1. *Nature*. 2005;434:108-13.
80. O'Driscoll M and Jeggo PA. The role of the DNA damage response pathways in brain development and microcephaly: insight from human disorders. *DNA Repair (Amst)*. 2008;7:1039-50.
81. Barzilai A. DNA damage, neuronal and glial cell death and neurodegeneration. *Apoptosis*. 2010;15:1371-81.
82. Shiwaku H and Okazawa H. Impaired DNA damage repair as a common feature of neurodegenerative diseases and psychiatric disorders. *Curr Mol Med*. 2015;15:119-28.

83. Jackson SP and Bartek J. The DNA-damage response in human biology and disease. *Nature*. 2009;461:1071-8.
84. Lee Y, Shull ER, Frappart PO, Katyal S, Enriquez-Rios V, Zhao J, Russell HR, Brown EJ and McKinnon PJ. ATR maintains select progenitors during nervous system development. *EMBO J*. 2012;31:1177-89.
85. Shull ER, Lee Y, Nakane H, Stracker TH, Zhao J, Russell HR, Petrini JH and McKinnon PJ. Differential DNA damage signaling accounts for distinct neural apoptotic responses in ATLD and NBS. *Genes Dev*. 2009;23:171-80.
86. Shiloh Y and Ziv Y. The ATM protein kinase: regulating the cellular response to genotoxic stress, and more. *Nat Rev Mol Cell Biol*. 2013;14:197-210.
87. Cimprich KA and Cortez D. ATR: an essential regulator of genome integrity. *Nat Rev Mol Cell Biol*. 2008;9:616-27.
88. McKinnon PJ. Genome integrity and disease prevention in the nervous system. *Genes Dev*. 2017;31:1180-1194.
89. Kumagai A, Lee J, Yoo HY and Dunphy WG. TopBP1 activates the ATR-ATRIP complex. *Cell*. 2006;124:943-55.
90. Lee Y, Katyal S, Downing SM, Zhao J, Russell HR and McKinnon PJ. Neurogenesis requires TopBP1 to prevent catastrophic replicative DNA damage in early progenitors. *Nat Neurosci*. 2012;15:819-26.
91. Orii KE, Lee Y, Kondo N and McKinnon PJ. Selective utilization of nonhomologous end-joining and homologous recombination DNA repair pathways during nervous system development. *Proc Natl Acad Sci U S A*. 2006;103:10017-22.
92. Yang Z, Li M, Hu X, Xiang B, Deng W, Wang Q, Wang Y, Zhao L, Ma X, Sham PC, Northoff G and Li T. Rare damaging variants in DNA repair and cell cycle pathways are associated with hippocampal and cognitive dysfunction: a combined genetic imaging study in first-episode treatment-naive patients with schizophrenia. *Transl Psychiatry*. 2017;7:e1028.
93. Ionita-Laza I, Xu B, Makarov V, Buxbaum JD, Roos JL, Gogos JA and Karayiorgou M. Scan statistic-based analysis of exome sequencing data identifies FAN1 at 15q13.3 as a susceptibility gene for schizophrenia and autism. *Proc Natl Acad Sci U S A*. 2014;111:343-8.
94. Stewart GS, Maser RS, Stankovic T, Bressan DA, Kaplan MI, Jaspers NG, Raams A, Byrd PJ, Petrini JH and Taylor AM. The DNA double-strand break repair gene hMRE11 is mutated in individuals with an ataxia-telangiectasia-like disorder. *Cell*. 1999;99:577-87.
95. Carney JP, Maser RS, Olivares H, Davis EM, Le Beau M, Yates JR, Hays L, Morgan WF and Petrini JH. The hMre11/hRad50 protein complex and Nijmegen breakage syndrome: linkage of double-strand break repair to the cellular DNA damage response. *Cell*. 1998;93:477-86.
96. O'Driscoll M, Dobyns WB, van Hagen JM and Jeggo PA. Cellular and clinical impact of haploinsufficiency for genes involved in ATR signaling. *Am J Hum Genet*. 2007;81:77-86.
97. O'Driscoll M, Ruiz-Perez VL, Woods CG, Jeggo PA and Goodship JA. A splicing mutation affecting expression of ataxia-telangiectasia and Rad3-related protein (ATR) results in Seckel syndrome. *Nat Genet*. 2003;33:497-501.
98. Borsini A, Zunszain PA, Thuret S and Pariante CM. The role of inflammatory cytokines as key modulators of neurogenesis.
99. Carpentier PA and Palmer TD. Immune influence on adult neural stem cell regulation and function.
100. Deverman BE and Patterson PH. Cytokines and CNS development. *Neuron*. 2009;64:61-78.

101. Nolan AM, Nolan Ym Fau - O'Keeffe GW and O'Keeffe GW. IL-1β inhibits axonal growth of developing sympathetic neurons.
102. Boato F, Hechler D Fau - Rosenberger K, Rosenberger K Fau - Lüdecke D, Lüdecke D Fau - Peters EM, Peters Em Fau - Nitsch R, Nitsch R Fau - Hendrix S and Hendrix S. Interleukin-1 beta and neurotrophin-3 synergistically promote neurite growth in vitro.
103. Ma L Fau - Li X-W, Li Xw Fau - Zhang S-J, Zhang Sj Fau - Yang F, Yang F Fau - Zhu G-M, Zhu Gm Fau - Yuan X-B, Yuan Xb Fau - Jiang W and Jiang W. Interleukin-1 beta guides the migration of cortical neurons.
104. Gilmore JH, Fredrik Jarskog L, Vadlamudi S and Lauder JM. Prenatal infection and risk for schizophrenia: IL-1beta, IL-6, and TNFalpha inhibit cortical neuron dendrite development. *Neuropsychopharmacology*. 2004;29:1221-9.
105. Kanner L. Autistic disturbances of affective contact. *Acta Paedopsychiatr*. 1968;35:100-36.
106. King BH, Navot N, Bernier R and Webb SJ. Update on diagnostic classification in autism. *Curr Opin Psychiatry*. 2014;27:105-9.
107. Folstein S and Rutter M. Infantile autism: a genetic study of 21 twin pairs. *J Child Psychol Psychiatry*. 1977;18:297-321.
108. Persico AM and Bourgeron T. Searching for ways out of the autism maze: genetic, epigenetic and environmental clues. *Trends Neurosci*. 2006;29:349-58.
109. Durand CM, Betancur C, Boeckers TM, Bockmann J, Chaste P, Fauchereau F, Nygren G, Rastam M, Gillberg IC, Anckarsäter H, Sponheim E, Goubran-Botros H, Delorme R, Chabane N, Mouren-Simeoni MC, de Mas P, Bieth E, Rogé B, Héron D, Burglen L, Gillberg C, Leboyer M and Bourgeron T. Mutations in the gene encoding the synaptic scaffolding protein SHANK3 are associated with autism spectrum disorders. *Nat Genet*. 2007;39:25-7.
110. Fatemi SH. The role of Reelin in pathology of autism. *Mol Psychiatry*. 2002;7:919-20.
111. Fatemi SH, Snow AV, Stary JM, Araghi-Niknam M, Reutiman TJ, Lee S, Brooks AI and Pearce DA. Reelin signaling is impaired in autism. *Biol Psychiatry*. 2005;57:777-87.
112. Lammert DB and Howell BW. RELN Mutations in Autism Spectrum Disorder. *Front Cell Neurosci*. 2016;10:84.
113. Giovanoli S, Weber-Stadlbauer U, Schedlowski M, Meyer U and Engler H. Prenatal immune activation causes hippocampal synaptic deficits in the absence of overt microglia anomalies. *Brain Behav Immun*. 2016;55:25-38.
114. Giovanoli S, Weber L and Meyer U. Single and combined effects of prenatal immune activation and peripubertal stress on parvalbumin and reelin expression in the hippocampal formation. *Brain Behav Immun*. 2014;40:48-54.
115. Estes ML and McAllister AK. Immune mediators in the brain and peripheral tissues in autism spectrum disorder. *Nat Rev Neurosci*. 2015;16:469-86.
116. Golan HM, Lev V, Hallak M, Sorokin Y and Huleihel M. Specific neurodevelopmental damage in mice offspring following maternal inflammation during pregnancy. *Neuropharmacology*. 2005;48:903-17.
117. O'Roak BJ, Deriziotis P, Lee C, Vives L, Schwartz JJ, Girirajan S, Karakoc E, Mackenzie AP, Ng SB, Baker C, Rieder MJ, Nickerson DA, Bernier R, Fisher SE, Shendure J and Eichler EE. Exome sequencing in sporadic autism spectrum disorders identifies severe de novo mutations. *Nat Genet*. 2011;43:585-9.
118. Sanders SJ, Murtha MT, Gupta AR, Murdoch JD, Raubeson MJ, Willsey AJ, Ercan-Sencicek AG, DiLullo NM, Parikshak NN, Stein JL, Walker MF, Ober GT, Teran NA, Song Y, El-Fishawy P, Murtha RC, Choi M, Overton JD, Bjornson RD, Carriero NJ, Meyer KA, Bilguvar

K, Mane SM, Sestan N, Lifton RP, Günel M, Roeder K, Geschwind DH, Devlin B and State MW. De novo mutations revealed by whole-exome sequencing are strongly associated with autism. *Nature*. 2012;485:237-41.
119. Atladóttir HO, Thorsen P, Østergaard L, Schendel DE, Lemcke S, Abdallah M and Parner ET. Maternal infection requiring hospitalization during pregnancy and autism spectrum disorders. *J Autism Dev Disord*. 2010;40:1423-30.
120. Buffington SA, Di Prisco GV, Auchtung TA, Ajami NJ, Petrosino JF and Costa-Mattioli M. Microbial Reconstitution Reverses Maternal Diet-Induced Social and Synaptic Deficits in Offspring. *Cell*. 2016;165:1762-75.
121. Croen LA, Najjar DV, Fireman B and Grether JK. Maternal and paternal age and risk of autism spectrum disorders. *Arch Pediatr Adolesc Med*. 2007;161:334-40.
122. Schwartzer JJ, Careaga M, Coburn MA, Rose DR, Hughes HK and Ashwood P. Behavioral impact of maternal allergic-asthma in two genetically distinct mouse strains. *Brain Behav Immun*. 2016.
123. Chess S. Autism in children with congenital rubella. *J Autism Child Schizophr*. 1971;1:33-47.
124. Chess S. Follow-up report on autism in congenital rubella. *J Autism Child Schizophr*. 1977;7:69-81.
125. Chess S, Fernandez P and Korn S. Behavioral consequences of congenital rubella. *J Pediatr*. 1978;93:699-703.
126. Shi L, Fatemi SH, Sidwell RW and Patterson PH. Maternal influenza infection causes marked behavioral and pharmacological changes in the offspring. *J Neurosci*. 2003;23:297-302.
127. Zuckerman L, Rehavi M, Nachman R and Weiner I. Immune activation during pregnancy in rats leads to a postpubertal emergence of disrupted latent inhibition, dopaminergic hyperfunction, and altered limbic morphology in the offspring: a novel neurodevelopmental model of schizophrenia. *Neuropsychopharmacology*. 2003;28:1778-89.
128. Zuckerman L and Weiner I. Maternal immune activation leads to behavioral and pharmacological changes in the adult offspring. *J Psychiatr Res*. 2005;39:311-23.
129. Malkova NV, Yu CZ, Hsiao EY, Moore MJ and Patterson PH. Maternal immune activation yields offspring displaying mouse versions of the three core symptoms of autism. *Brain Behav Immun*. 2012;26:607-16.
130. Bauman MD, Iosif AM, Smith SE, Bregere C, Amaral DG and Patterson PH. Activation of the maternal immune system during pregnancy alters behavioral development of rhesus monkey offspring. *Biol Psychiatry*. 2014;75:332-41.
131. Kirsten TB, Lippi LL, Bevilacqua E and Bernardi MM. LPS exposure increases maternal corticosterone levels, causes placental injury and increases IL-1B levels in adult rat offspring: relevance to autism. *PLoS One*. 2013;8:e82244.
132. Bauman ML and Kemper TL. Neuroanatomic observations of the brain in autism: a review and future directions. *Int J Dev Neurosci*. 2005;23:183-7.
133. Coiro P, Padmashri R, Suresh A, Spartz E, Pendyala G, Chou S, Jung Y, Meays B, Roy S, Gautam N, Alnouti Y, Li M and Dunaevsky A. Impaired synaptic development in a maternal immune activation mouse model of neurodevelopmental disorders. *Brain Behav Immun*. 2015;50:249-58.
134. Elmer BM, Estes ML, Barrow SL and McAllister AK. MHCI requires MEF2 transcription factors to negatively regulate synapse density during development and in disease. *J Neurosci*. 2013;33:13791-804.

135. Glynn MW, Elmer BM, Garay PA, Liu XB, Needleman LA, El-Sabeawy F and McAllister AK. MHCI negatively regulates synapse density during the establishment of cortical connections. *Nat Neurosci*. 2011;14:442-51.
136. Aylward EH, Minshew NJ, Goldstein G, Honeycutt NA, Augustine AM, Yates KO, Barta PE and Pearlson GD. MRI volumes of amygdala and hippocampus in non-mentally retarded autistic adolescents and adults. *Neurology*. 1999;53:2145-50.
137. Fatemi SH, Aldinger KA, Ashwood P, Bauman ML, Blaha CD, Blatt GJ, Chauhan A, Chauhan V, Dager SR, Dickson PE, Estes AM, Goldowitz D, Heck DH, Kemper TL, King BH, Martin LA, Millen KJ, Mittleman G, Mosconi MW, Persico AM, Sweeney JA, Webb SJ and Welsh JP. Consensus paper: pathological role of the cerebellum in autism. *Cerebellum*. 2012;11:777-807.
138. Wu WL, Hsiao EY, Yan Z, Mazmanian SK and Patterson PH. The placental interleukin-6 signaling controls fetal brain development and behavior. *Brain Behav Immun*. 2017;62:11-23.
139. Reith RM, McKenna J, Wu H, Hashmi SS, Cho SH, Dash PK and Gambello MJ. Loss of Tsc2 in Purkinje cells is associated with autistic-like behavior in a mouse model of tuberous sclerosis complex. *Neurobiol Dis*. 2013;51:93-103.
140. Takano T. Role of Microglia in Autism: Recent Advances. *Dev Neurosci*. 2015;37:195-202.
141. Morgan JT, Chana G, Pardo CA, Achim C, Semendeferi K, Buckwalter J, Courchesne E and Everall IP. Microglial activation and increased microglial density observed in the dorsolateral prefrontal cortex in autism. *Biol Psychiatry*. 2010;68:368-76.
142. Ratnayake U, Quinn TA, Castillo-Melendez M, Dickinson H and Walker DW. Behaviour and hippocampus-specific changes in spiny mouse neonates after treatment of the mother with the viral-mimetic Poly I:C at mid-pregnancy. *Brain Behav Immun*. 2012;26:1288-99.
143. Garay PA, Hsiao EY, Patterson PH and McAllister AK. Maternal immune activation causes age- and region-specific changes in brain cytokines in offspring throughout development. *Brain Behav Immun*. 2013;31:54-68.
144. Lumeng CN. Inflammatory links between obesity and metabolic disease. . 2011;*121*:2111-2117.
145. Rodríguez-Hernández H. Obesity and inflammation: epidemiology, risk factors, and markers of inflammation. 2013.
146. Bruce-Keller AJ, Fernandez-Kim SO, Townsend RL, Kruger C, Carmouche R, Newman S, Salbaum JM and Berthoud HR. Maternal obese-type gut microbiota differentially impact cognition, anxiety and compulsive behavior in male and female offspring in mice. *PLoS One*. 2017;12:e0175577.
147. Hsiao EY, McBride SW, Hsien S, Sharon G, Hyde ER, McCue T, Codelli JA, Chow J, Reisman SE, Petrosino JF, Patterson PH and Mazmanian SK. Microbiota modulate behavioral and physiological abnormalities associated with neurodevelopmental disorders. *Cell*. 2013;155:1451-63.
148. Parracho HM, Bingham MO, Gibson GR and McCartney AL. Differences between the gut microflora of children with autistic spectrum disorders and that of healthy children. *J Med Microbiol*. 2005;54:987-91.
149. Keil A, Daniels JL, Forssen U, Hultman C, Cnattingius S, Söderberg KC, Feychting M and Sparen P. Parental autoimmune diseases associated with autism spectrum disorders in offspring. *Epidemiology*. 2010;21:805-8.
150. Smith SE, Li J, Garbett K, Mirnics K and Patterson PH. Maternal immune activation alters fetal brain development through interleukin-6. *J Neurosci*. 2007;27:10695-702.

151. Hsiao EY and Patterson PH. Activation of the maternal immune system induces endocrine changes in the placenta via IL-6. *Brain Behav Immun*. 2011;25:604-15.
152. Choi GB, Yim YS, Wong H, Kim S, Kim H, Kim SV, Hoeffer CA, Littman DR and Huh JR. The maternal interleukin-17a pathway in mice promotes autism-like phenotypes in offspring. *Science*. 2016;351:933-9.
153. Shin Yim Y, Park A, Berrios J, Lafourcade M, Pascual LM, Soares N, Yeon Kim J, Kim S, Kim H, Waisman A, Littman DR, Wickersham IR, Harnett MT, Huh JR and Choi GB. Reversing behavioural abnormalities in mice exposed to maternal inflammation. *Nature*. 2017;549:482-487.
154. Kim S, Kim H, Yim YS, Ha S, Atarashi K, Tan TG, Longman RS, Honda K, Littman DR, Choi GB and Huh JR. Maternal gut bacteria promote neurodevelopmental abnormalities in mouse offspring. *Nature*. 2017;549:528-532.
155. Lammert CR, Frost EL, Bolte AC, Paysour MJ, Shaw ME, Bellinger CE, Weigel TK, Zunder ER and Lukens JR. Cutting Edge: Critical Roles for Microbiota-Mediated Regulation of the Immune System in a Prenatal Immune Activation Model of Autism. *J Immunol*. 2018;201:845-850.
156. Fernandes-Alnemri T, Yu JW, Datta P, Wu J and Alnemri ES. AIM2 activates the inflammasome and cell death in response to cytoplasmic DNA. *Nature*. 2009;458:509-13.
157. Hornung V, Ablasser A, Charrel-Dennis M, Bauernfeind F, Horvath G, Caffrey DR, Latz E and Fitzgerald KA. AIM2 recognizes cytosolic dsDNA and forms a caspase-1-activating inflammasome with ASC. *Nature*. 2009;458:514-8.
158. Rathinam VA, Jiang Z, Waggoner SN, Sharma S, Cole LE, Waggoner L, Vanaja SK, Monks BG, Ganesan S, Latz E, Hornung V, Vogel SN, Szomolanyi-Tsuda E and Fitzgerald KA. The AIM2 inflammasome is essential for host defense against cytosolic bacteria and DNA viruses. *Nat Immunol*. 2010;11:395-402.
159. Guo H, Callaway JB and Ting JP. Inflammasomes: mechanism of action, role in disease, and therapeutics. *Nat Med*. 2015;21:677-87.
160. Lammert CR, Frost EL, Bellinger CE, Bolte AC, McKee CA, Hurt ME, Paysour MJ, Ennerfelt HE and Lukens JR. AIM2 inflammasome surveillance of DNA damage shapes neurodevelopment. *Nature*. 2020;580:647-652.
161. Rathinam VA and Fitzgerald KA. Inflammasome Complexes: Emerging Mechanisms and Effector Functions. *Cell*. 2016;165:792-800.
162. Cox DJ, Field RH, Williams DG, Baran M, Bowie AG, Cunningham C and Dunne A. DNA sensors are expressed in astrocytes and microglia in vitro and are upregulated during gliosis in neurodegenerative disease. *Glia*. 2015;63:812-25.
163. Felderhoff-Mueser U, Schmidt OI, Oberholzer A, Buhrer C and Stahel PF. IL-18: a key player in neuroinflammation and neurodegeneration? *Trends Neurosci*. 2005;28:487-93.
164. Dantzer R, O'Connor JC, Freund GG, Johnson RW and Kelley KW. From inflammation to sickness and depression: when the immune system subjugates the brain. *Nat Rev Neurosci*. 2008;9:46-56.
165. Garber C, Vasek MJ, Vollmer LL, Sun T, Jiang X and Klein RS. Astrocytes decrease adult neurogenesis during virus-induced memory dysfunction via IL-1. *Nat Immunol*. 2018;19:151-161.
166. Yamaguchi Y and Miura M. Programmed cell death in neurodevelopment. *Dev Cell*. 2015;32:478-90.

167. Kuan CY, Yang DD, Samanta Roy DR, Davis RJ, Rakic P and Flavell RA. The Jnk1 and Jnk2 protein kinases are required for regional specific apoptosis during early brain development. *Neuron*. 1999;22:667-76.
168. Cecconi F, Alvarez-Bolado G, Meyer BI, Roth KA and Gruss P. Apaf1 (CED-4 homolog) regulates programmed cell death in mammalian development. *Cell*. 1998;94:727-37.
169. Yoshida H, Kong YY, Yoshida R, Elia AJ, Hakem A, Hakem R, Penninger JM and Mak TW. Apaf1 is required for mitochondrial pathways of apoptosis and brain development. *Cell*. 1998;94:739-50.
170. Tzeng TC, Schattgen S, Monks B, Wang D, Cerny A, Latz E, Fitzgerald K and Golenbock DT. A Fluorescent Reporter Mouse for Inflammasome Assembly Demonstrates an Important Role for Cell-Bound and Free ASC Specks during In Vivo Infection. *Cell Rep*. 2016;16:571-582.
171. Herzog KH, Chong MJ, Kapsetaki M, Morgan JI and McKinnon PJ. Requirement for Atm in ionizing radiation-induced cell death in the developing central nervous system. *Science*. 1998;280:1089-91.
172. Schumacher B, Garinis GA and Hoeijmakers JH. Age to survive: DNA damage and aging. *Trends Genet*. 2008;24:77-85.
173. Hoeijmakers JH. DNA damage, aging, and cancer. *N Engl J Med*. 2009;361:1475-85.
174. Hu B, Jin C, Li HB, Tong J, Ouyang X, Cetinbas NM, Zhu S, Strowig T, Lam FC, Zhao C, Henao-Mejia J, Yilmaz O, Fitzgerald KA, Eisenbarth SC, Elinav E and Flavell RA. The DNA-sensing AIM2 inflammasome controls radiation-induced cell death and tissue injury. *Science*. 2016;354:765-768.
175. Denes A, Coutts G, Lenart N, Cruickshank SM, Pelegrin P, Skinner J, Rothwell N, Allan SM and Brough D. AIM2 and NLRC4 inflammasomes contribute with ASC to acute brain injury independently of NLRP3. *Proc Natl Acad Sci U S A*. 2015;112:4050-5.
176. Adamczak SE, de Rivero Vaccari JP, Dale G, Brand FJ, 3rd, Nonner D, Bullock MR, Dahl GP, Dietrich WD and Keane RW. Pyroptotic neuronal cell death mediated by the AIM2 inflammasome. *J Cereb Blood Flow Metab*. 2014;34:621-9.
177. Vanden Berghe T, Linkermann A, Jouan-Lanhouet S, Walczak H and Vandenabeele P. Regulated necrosis: the expanding network of non-apoptotic cell death pathways. *Nat Rev Mol Cell Biol*. 2014;15:135-47.
178. Filiano AJ, Gadani SP and Kipnis J. How and why do T cells and their derived cytokines affect the injured and healthy brain? *Nat Rev Neurosci*. 2017;18:375-384.
179. Hammond TR, Robinton D and Stevens B. Microglia and the Brain: Complementary Partners in Development and Disease. *Annu Rev Cell Dev Biol*. 2018;34:523-544.
180. Lukens JR and Kanneganti TD. Beyond canonical inflammasomes: emerging pathways in IL-1-mediated autoinflammatory disease. *Semin Immunopathol*. 2014;36:595-609.
181. Orjalo AV, Bhaumik D, Gengler BK, Scott GK and Campisi J. Cell surface-bound IL-1alpha is an upstream regulator of the senescence-associated IL-6/IL-8 cytokine network. *Proc Natl Acad Sci U S A*. 2009;106:17031-6.
182. Lukens JR, Barr MJ, Chaplin DD, Chi H and Kanneganti TD. Inflammasome-derived IL-1β regulates the production of GM-CSF by CD4(+) T cells and γδ T cells. *J Immunol*. 2012;188:3107-15.
183. Garlanda C, Dinarello CA and Mantovani A. The interleukin-1 family: back to the future. *Immunity*. 2013;39:1003-18.

184. de la Mano A, Gato A, Alonso MI, Carnicero E, Martín C and Moro JA. Role of interleukin-1beta in the control of neuroepithelial proliferation and differentiation of the spinal cord during development. *Cytokine*. 2007;37:128-37.
185. Girard S, Tremblay L, Lepage M and Sébire G. IL-1 receptor antagonist protects against placental and neurodevelopmental defects induced by maternal inflammation. *J Immunol*. 2010;184:3997-4005.
186. Molloy CA, Morrow AL, Meinzen-Derr J, Schleifer K, Dienger K, Manning-Courtney P, Altaye M and Wills-Karp M. Elevated cytokine levels in children with autism spectrum disorder. *J Neuroimmunol*. 2006;172:198-205.
187. Li X, Chauhan A, Sheikh AM, Patil S, Chauhan V, Li XM, Ji L, Brown T and Malik M. Elevated immune response in the brain of autistic patients. *J Neuroimmunol*. 2009;207:111-6.
188. Ashwood P, Krakowiak P, Hertz-Picciotto I, Hansen R, Pessah I and Van de Water J. Elevated plasma cytokines in autism spectrum disorders provide evidence of immune dysfunction and are associated with impaired behavioral outcome. *Brain Behav Immun*. 2011;25:40-5.
189. Estes ML and McAllister AK. Maternal immune activation: Implications for neuropsychiatric disorders. *Science*. 2016;353:772-7.
190. Finegold SM, Dowd SE, Gontcharova V, Liu C, Henley KE, Wolcott RD, Youn E, Summanen PH, Granpeesheh D, Dixon D, Liu M, Molitoris DR and Green JA, 3rd. Pyrosequencing study of fecal microflora of autistic and control children. *Anaerobe*. 2010;16:444-53.
191. Buie T, Campbell DB, Fuchs GJ, 3rd, Furuta GT, Levy J, Vandewater J, Whitaker AH, Atkins D, Bauman ML, Beaudet AL, Carr EG, Gershon MD, Hyman SL, Jirapinyo P, Jyonouchi H, Kooros K, Kushak R, Levitt P, Levy SE, Lewis JD, Murray KF, Natowicz MR, Sabra A, Wershil BK, Weston SC, Zeltzer L and Winter H. Evaluation, diagnosis, and treatment of gastrointestinal disorders in individuals with ASDs: a consensus report. *Pediatrics*. 2010;125 Suppl 1:S1-18.
192. Fung TC, Olson CA and Hsiao EY. Interactions between the microbiota, immune and nervous systems in health and disease. *Nat Neurosci*. 2017;20:145-155.
193. Ivanov, II, Atarashi K, Manel N, Brodie EL, Shima T, Karaoz U, Wei D, Goldfarb KC, Santee CA, Lynch SV, Tanoue T, Imaoka A, Itoh K, Takeda K, Umesaki Y, Honda K and Littman DR. Induction of intestinal Th17 cells by segmented filamentous bacteria. *Cell*. 2009;139:485-98.
194. Sivan A, Corrales L, Hubert N, Williams JB, Aquino-Michaels K, Earley ZM, Benyamin FW, Lei YM, Jabri B, Alegre ML, Chang EB and Gajewski TF. Commensal Bifidobacterium promotes antitumor immunity and facilitates anti-PD-L1 efficacy. *Science*. 2015;350:1084-9.
195. Chen C, Itakura E, Nelson GM, Sheng M, Laurent P, Fenk LA, Butcher RA, Hegde RS and de Bono M. IL-17 is a neuromodulator of Caenorhabditis elegans sensory responses. *Nature*. 2017;542:43-48.
196. Ferguson BR and Gao WJ. PV Interneurons: Critical Regulators of E/I Balance for Prefrontal Cortex-Dependent Behavior and Psychiatric Disorders. *Front Neural Circuits*. 2018;12:37.
197. Suberbielle E, Sanchez Pe Fau - Kravitz AV, Kravitz Av Fau - Wang X, Wang X Fau - Ho K, Ho K Fau - Eilertson K, Eilertson K Fau - Devidze N, Devidze N Fau - Kreitzer AC, Kreitzer Ac Fau - Mucke L and Mucke L. Physiologic brain activity causes DNA double-strand breaks in neurons, with exacerbation by amyloid-β.

198. Devine MJ and Kittler JT. Mitochondria at the neuronal presynapse in health and disease. *Nat Rev Neurosci*. 2018;19:63-80.
199. Györffy BA, Tóth V, Török G, Gulyássy P, Kovács R, Vadászi H, Micsonai A, Tóth ME, Sántha M, Homolya L, Drahos L, Juhász G, Kékesi KA and Kardos JA-O. Synaptic mitochondrial dysfunction and septin accumulation are linked to complement-mediated synapse loss in an Alzheimer's disease animal model. LID - 10.1007/s00018-020-03468-0 [doi].
200. Rühl S, Shkarina K, Demarco B, Heilig R, Santos JC and Broz P. ESCRT-dependent membrane repair negatively regulates pyroptosis downstream of GSDMD activation. *Science*. 2018;362:956-960.
201. Kuida K, Lippke JA, Ku G, Harding MW, Livingston DJ, Su MS and Flavell RA. Altered cytokine export and apoptosis in mice deficient in interleukin-1 beta converting enzyme. *Science*. 1995;267:2000-3.
202. Kovarova M, Hesker PR, Jania L, Nguyen M, Snouwaert JN, Xiang Z, Lommatzsch SE, Huang MT, Ting JP and Koller BH. NLRP1-dependent pyroptosis leads to acute lung injury and morbidity in mice. *J Immunol*. 2012;189:2006-16.
203. Hou B, Reizis B and DeFranco AL. Toll-like receptors activate innate and adaptive immunity by using dendritic cell-intrinsic and -extrinsic mechanisms. *Immunity*. 2008;29:272-82.
204. Glaccum MB, Stocking KL, Charrier K, Smith JL, Willis CR, Maliszewski C, Livingston DJ, Peschon JJ and Morrissey PJ. Phenotypic and functional characterization of mice that lack the type I receptor for IL-1. *J Immunol*. 1997;159:3364-71.
205. Hoshino K, Tsutsui H, Kawai T, Takeda K, Nakanishi K, Takeda Y and Akira S. Cutting edge: generation of IL-18 receptor-deficient mice: evidence for IL-1 receptor-related protein as an essential IL-18 binding receptor. *J Immunol*. 1999;162:5041-4.
206. Wang S, Miura M, Jung YK, Zhu H, Li E and Yuan J. Murine caspase-11, an ICE-interacting protease, is essential for the activation of ICE. *Cell*. 1998;92:501-9.
207. Case CL, Kohler LJ, Lima JB, Strowig T, de Zoete MR, Flavell RA, Zamboni DS and Roy CR. Caspase-11 stimulates rapid flagellin-independent pyroptosis in response to Legionella pneumophila. *Proc Natl Acad Sci U S A*. 2013;110:1851-6.
208. Tronche F, Kellendonk C, Kretz O, Gass P, Anlag K, Orban PC, Bock R, Klein R and Schutz G. Disruption of the glucocorticoid receptor gene in the nervous system results in reduced anxiety. *Nat Genet*. 1999;23:99-103.
209. Yona S, Kim KW, Wolf Y, Mildner A, Varol D, Breker M, Strauss-Ayali D, Viukov S, Guilliams M, Misharin A, Hume DA, Perlman H, Malissen B, Zelzer E and Jung S. Fate mapping reveals origins and dynamics of monocytes and tissue macrophages under homeostasis. *Immunity*. 2013;38:79-91.
210. Hu S, Peng L, Kwak YT, Tekippe EM, Pasare C, Malter JS, Hooper LV and Zaki MH. The DNA Sensor AIM2 Maintains Intestinal Homeostasis via Regulation of Epithelial Antimicrobial Host Defense. *Cell Rep*. 2015;13:1922-36.
211. Chen SH, Oyarzabal EA and Hong JS. Preparation of rodent primary cultures for neuron-glia, mixed glia, enriched microglia, and reconstituted cultures with microglia. *Methods Mol Biol*. 2013;1041:231-40.
212. Zhang Y, Cazakoff BN, Thai CA and Howland JG. Prenatal exposure to a viral mimetic alters behavioural flexibility in male, but not female, rats. *Neuropharmacology*. 2012;62:1299-307.

213. Schaafsma SM, Gagnidze K, Reyes A, Norstedt N, Mansson K, Francis K and Pfaff DW. Sex-specific gene-environment interactions underlying ASD-like behaviors. *Proc Natl Acad Sci U S A*. 2017;114:1383-1388.
214. Werling DM and Geschwind DH. Sex differences in autism spectrum disorders. *Curr Opin Neurol*. 2013;26:146-53.
215. Abel KM, Drake R and Goldstein JM. Sex differences in schizophrenia. *Int Rev Psychiatry*. 2010;22:417-28.